

518  
ORNL-4128 - END

15  
1  
Contract No. W-7405-eng-26 - 27ACV

Neutron Physics Division

3 REPRESENTATIVE RESULTS IN GRAPHICAL FORM FROM COMPUTER PRODUCTION  
RUNS OF THE LOW-ENERGY INTRANUCLEAR-CASCADE CALCULATION 6

6 Hugo W. Bertini, Barbara L. Bishop, and Miriam P. Guthrie 9

---

NOTE:

This work partially supported by  
NATIONAL AERONAUTICS AND SPACE ADMINISTRATION  
Under Order R-104(1) 27ACV

---

27 NASA ORDER #

9 AUGUST 1967 10

1 OAK RIDGE NATIONAL LABORATORY  
Oak Ridge, Tennessee 3  
operated by  
UNION CARBIDE CORPORATION  
for the  
U. S. ATOMIC ENERGY COMMISSION

TABLE OF CONTENTS

	<u>Page No.</u>
Abstract -----	1
Introduction -----	1
Description -----	2
Comments -----	3

REPRESENTATIVE RESULTS IN GRAPHICAL FORM FROM COMPUTER PRODUCTION  
RUNS OF THE LOW-ENERGY INTRANUCLEAR-CASCADE CALCULATION

Hugo W. Bertini, Barbara L. Bishop, and Miriam P. Guthrie

ABSTRACT

This report contains an extensive set of graphs which are meant to illustrate the mass and energy dependence of results that were selected from the output of computer production runs of a low-energy intranuclear-cascade calculation. The nuclear reactions considered are those resulting from the interaction of neutrons and protons with energies from 50 to 400 MeV and  $\pi^+$  and  $\pi^-$  with energies from 50 to 300 MeV with nuclei ranging from carbon to uranium. Plausibility arguments are given in an attempt to explain some of the results.

INTRODUCTION

The low-energy intranuclear-cascade calculation and its associated evaporation program, which are described elsewhere,<sup>1</sup> were used to generate an extensive set of data. Calculations were made on the nuclear interactions of protons, neutrons,  $\pi^+$ , and  $\pi^-$  with energies ranging from 25 to 400 MeV (25 to 300 MeV for pions) on nuclei with mass numbers from 12 to 238. A detailed description of the reactions that were calculated and the nature of the available data are given in ref. 2.\* Although calculations were made at energies as low as 25 MeV, the data presented in this report begin at 50 MeV.

Samples of the available data which the authors felt would be generally useful and interesting were selected, and these data are

<sup>1</sup>Hugo W. Bertini, Phys. Rev. 131, 1801 (1963); Phys. Rev. 138, AB2 (1965); for greater detail, see Monte Carlo Calculations on Intranuclear Cascades, ORNL-3383 (April 23, 1963), and Effect of Error on Results of a Low-Energy Intranuclear Cascade Calculation, ORNL-3786 (June 1966).

<sup>2</sup>Hugo W. Bertini, Results from Low-Energy Intranuclear-Cascade Calculation, ORNL TM-1225 (September 10, 1965).

\*These data can be obtained from the Oak Ridge Radiation Shielding Information Center where they are available on microfilm or on magnetic tape in a form that is suitable for listing on an IBM printer.

presented here in graphical form. Their mass and energy dependence are thereby readily ascertained. A user could, of course, determine these dependences for himself but he would be swamped with data from the computer, and it is a tedious task to sort out the particular pieces of information of interest, especially when dealing with data that have been put on microfilm.

This report, together with that of Alsmiller et al.,<sup>3</sup> provides an excellent summary of the computed data.

#### DESCRIPTION

The production of pions in any of the nuclear interactions was not taken into account because a large part of the energy range under consideration is below the effective production threshold. Therefore, the emitted particles for either incident protons or incident neutrons can only be protons and neutrons, whereas for incident charged pions\* they can be protons, neutrons,  $\pi^+$ ,  $\pi^0$ , and  $\pi^-$ .

The data pertaining to incident neutrons and emitted neutrons were given first preference. Some data pertaining to emitted protons for incident neutrons and to emitted protons and pions for incident protons or pions are also included.

To facilitate comparison, we attempted to keep the scales the same for the graphs that contain similar cross-section data. Tick marks were placed on the borders of each graph to aid in their reading. The calculated points were connected by straight lines merely to guide the eye. One should keep in mind that the calculation is a statistical one, and all of the results are expected to have statistical variations.

In the brief index that follows, the figure numbers in parentheses refer to graphs for incident pions. Those that are not in parentheses apply to incident nucleons. The parenthetical expressions in the titles

---

<sup>3</sup>R. G. Alsmiller, Jr., M. Leimdorfer, and J. Barish, Analytical Representation of Nonelastic Cross Sections and Particle-Emission Spectra from Nucleon-Nucleus Collisions in the Energy Range 25 to 400 MeV, ORNL-4046 (April 1967).

\*Pions can be emitted in a charged state different from that of the incident pion because charge-exchange reactions are included in the calculation.

refer to emitted particles when incident pions are used; otherwise, the titles apply to both incident nucleons and pions.

- Figs. 1, 2 (42, 43) Total Nonelastic Cross Sections.
- Figs. 3-6 (44-47) Average Number of Emitted Cascade Neutrons and Protons (Neutrons and Pions).
- Figs. 7-10 (48-51) Average Number of Evaporation Nucleons.
- Figs. 11-14 (52-55) Average Energy of Cascade and Evaporation Nucleons (Neutrons, Protons, and  $\pi^-$ )
- Figs. 15-22 (56-63) Differential Cross Sections for the Emission of Cascade Nucleons (Neutrons and  $\pi^-$ ) into Various Angular Intervals.
- Figs. 23-30 (64-71) Average Energy of Cascade Nucleons (Neutrons and  $\pi^-$ ) Emitted into Various Angular Intervals.
- Fig. 31 (72) Average Excitation Energy Following the Cascade Reaction.
- Figs. 32-35 (73-76) Excitation Energy Distributions Following the Cascade Reaction for Aluminum and Lead Targets.
- Figs. 36-41 (77-82) Radiochemical Cross Sections vs Mass Number for Aluminum, Copper, and Lead Targets.

#### COMMENTS

It is not readily apparent why some of the data have the values or the dependences that are illustrated. In this section plausibility arguments are given to explain some of these results.

The first result that we should discuss is illustrated in Fig. 1. Here the total nonelastic cross section for 400-MeV neutrons is slightly greater than that for 200-MeV neutrons over the bulk of the mass range. The higher mass nuclei have an excess of neutrons; therefore, for incident neutrons the free-particle n-n cross section has a greater effect on the nuclear nonelastic cross section than the n-p cross section does. The free-particle n-n (or p-p) cross section is higher at 430 MeV than it is at 230 MeV,\* whereas the reverse is true for the n-p cross section, so

---

\*The free-particle cross sections are evaluated at 430 and 230 MeV to include the effect of the attractive nuclear potential - about 30 MeV. The p-p cross section starts to increase rapidly at about 400 MeV.

the net effect is a slight increase in the total nuclear nonelastic cross section. The reverse of this is expected for incident protons, illustrated in Fig. 2.

The next result which requires an explanation is the factor-of-two difference in the number of cascade neutrons emitted compared to the number of cascade protons for incident neutrons. These data are illustrated in Figs. 3 and 4. If the free-particle cross sections were equal and if the neutron and proton densities inside the nucleus were the same, then the probability of an incident neutron interacting with a neutron or proton on the first collision would be the same. After the first collision, there would be two neutrons in the second generation if the first interaction were with a neutron. There would be one neutron and one proton if the interaction were with a proton. Under these circumstances, the average number of neutrons in the second generation is three times higher than the number of protons. This ratio is reduced in subsequent generations, but the particles escape before many generations can develop. Differences in cross sections and in the numbers of neutrons and protons inside the nucleus complicate the argument, but the main effect is apparent in the results. In Figs. 5 and 6 the same type of data is illustrated for incident protons, but the effect is manifest only in the light elements where the number of neutrons and protons in the nucleus is the same. The neutron excess in the heavier nuclei apparently wipes out the effect completely.

In Fig. 8 there is a peculiar discontinuity in the number of evaporation protons for a copper target ( $A = 65$ ). This comes from our use of the  $A = 65$ ,  $Z = 29$  isotope as our target, which is slightly to the right of the valley of stability, indicating a degree of proton deficiency. Our evaporation program is apparently quite sensitive to this in the midrange mass region, for when we use the  $A = 63$  isotope the number of evaporation protons is increased to the point where the discontinuities are eliminated.

A steep drop to zero at the end of the mass range for the average energy of evaporation protons using 50-MeV incident protons is illustrated in Fig. 14. There were no evaporation protons emitted for the  $A = 238$  case. The average number of evaporation protons is very small for the

$A = 183$  and  $A = 207$  cases (see Fig. 8), but not zero, so a reasonable average energy is obtained for these targets.

In Fig. 32, illustrating the excitation energy distribution for 50-MeV neutrons on lead, the value of the distribution is zero for the energy interval between 48 and 54 MeV and a peak between 54 and 60 MeV is exhibited. The peak should actually be a spike at 57 MeV because it represents the excitation energy when a 50-MeV neutron with a 7-MeV binding energy\* is absorbed without subsequent cascade particle emission. One has the maximum possible excitation energy when this occurs. The next highest possible excitation energy is given by the situation where the incident particle is absorbed and one nucleon is emitted with the smallest possible kinetic energy, i.e., the cutoff energy for the cascade calculation. The excitation energy is then the incident energy minus the cutoff energy (6.7 MeV for lead and 1.6 MeV for aluminum). Therefore, there cannot be an excitation energy between 48 and 54 MeV for the case of the lead target.

Figures 40 and 41 illustrate peaks in the mass distribution of the radiochemical cross sections for 50- and 100-MeV neutrons and protons on lead. These result from the rather high probability of absorption of the incident particle with the subsequent emission of particles (mostly neutrons) by evaporation only.

The pion-nucleon resonance at 200-MeV accounts for the fact that the total nonelastic cross sections for 150-MeV pions are larger than those with either 50- or 300-MeV incident energy. The curves are illustrated in Figs. 42 and 43.

The factor-of-two difference in the cascade neutron multiplicities between the  $\pi^-$  and  $\pi^+$  interactions (Figs. 44 and 45) is due to the large difference in the  $\pi^-+n$  and  $\pi^++n$  cross sections in this energy region. One assumes that

$$\sigma(\pi^-+n) = \sigma(\pi^++p)$$

---

\*The nucleons are assumed to have a 7-MeV binding energy in all the nuclei.

and

$$\sigma(\pi^+ + n) = \sigma(\pi^- + p)$$

from charge symmetry.

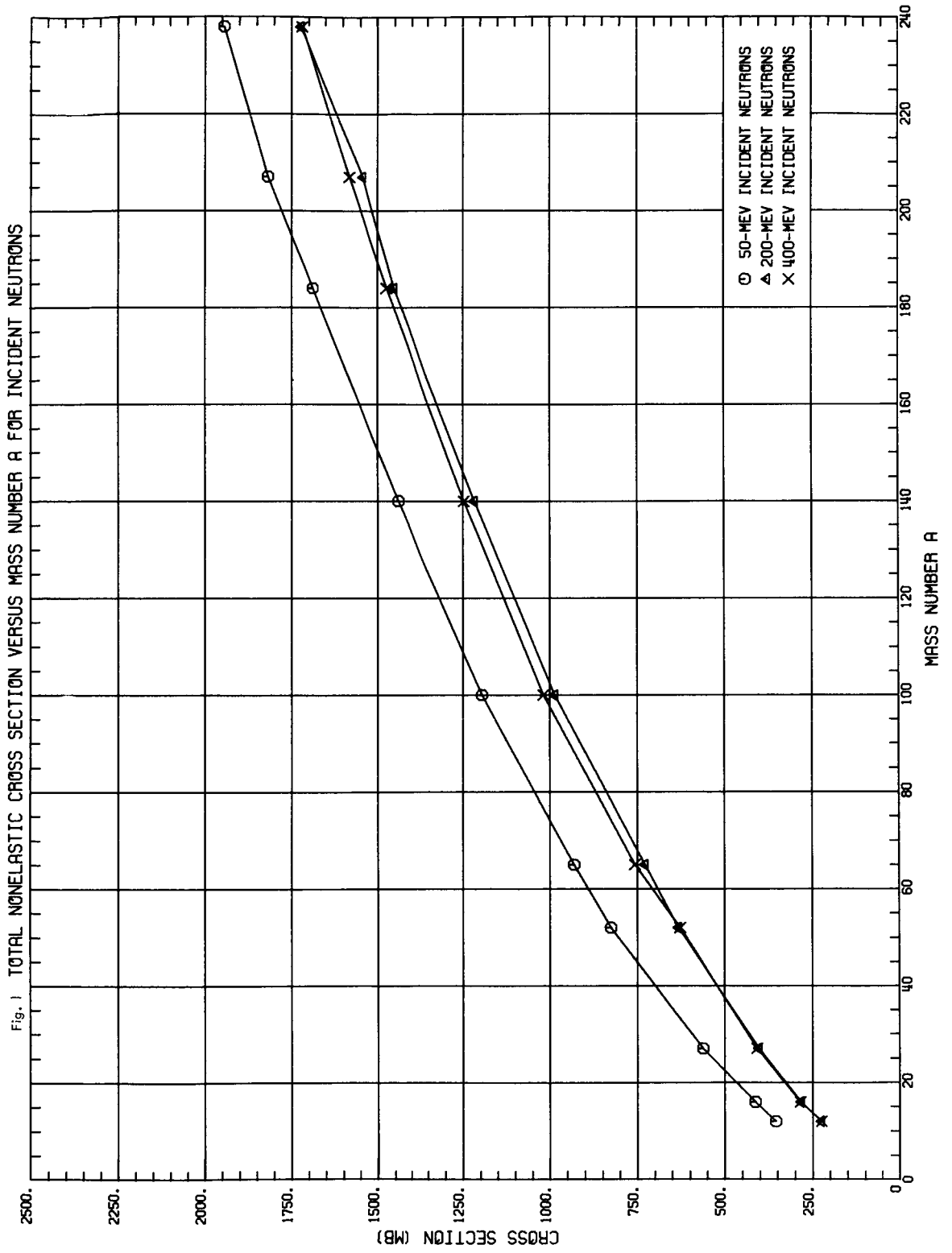
Pion absorption accounts for the high average cascade-neutron energy, particularly for 50-MeV incident  $\pi^-$ , illustrated in Fig. 52. When a pion is absorbed, its kinetic energy plus its rest mass energy ( $\sim 140$  MeV) is given up to the nucleons in the nucleus.

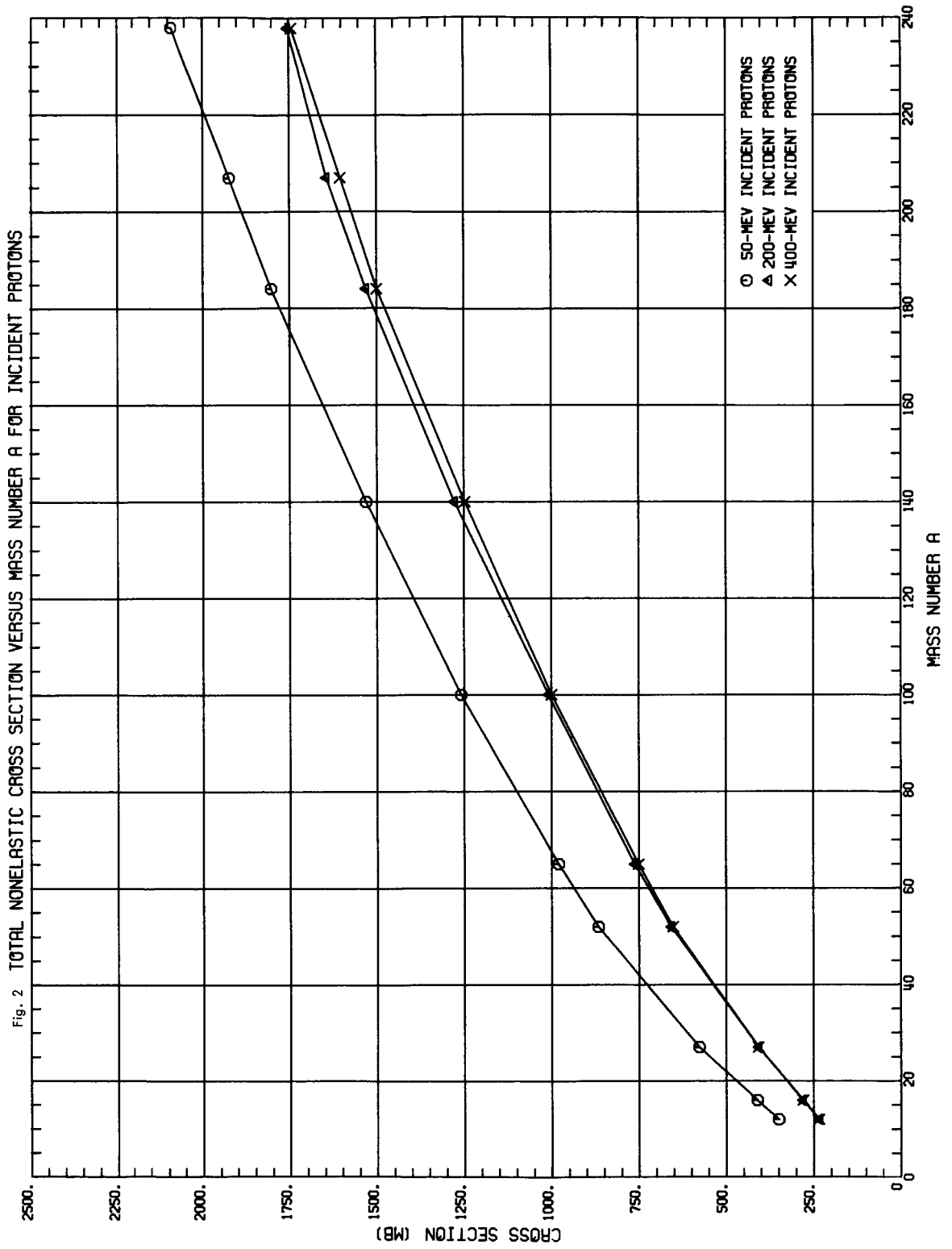
Absorption is also a contributing factor in the rather high magnitudes of the average evaporation neutron energies from the light elements, illustrated in Fig. 54, which result from the increased average excitation energy caused by absorption. The mass dependence of the average evaporation neutron energy for incident pions is the same as that for incident nucleons (Fig. 13), as would be expected.

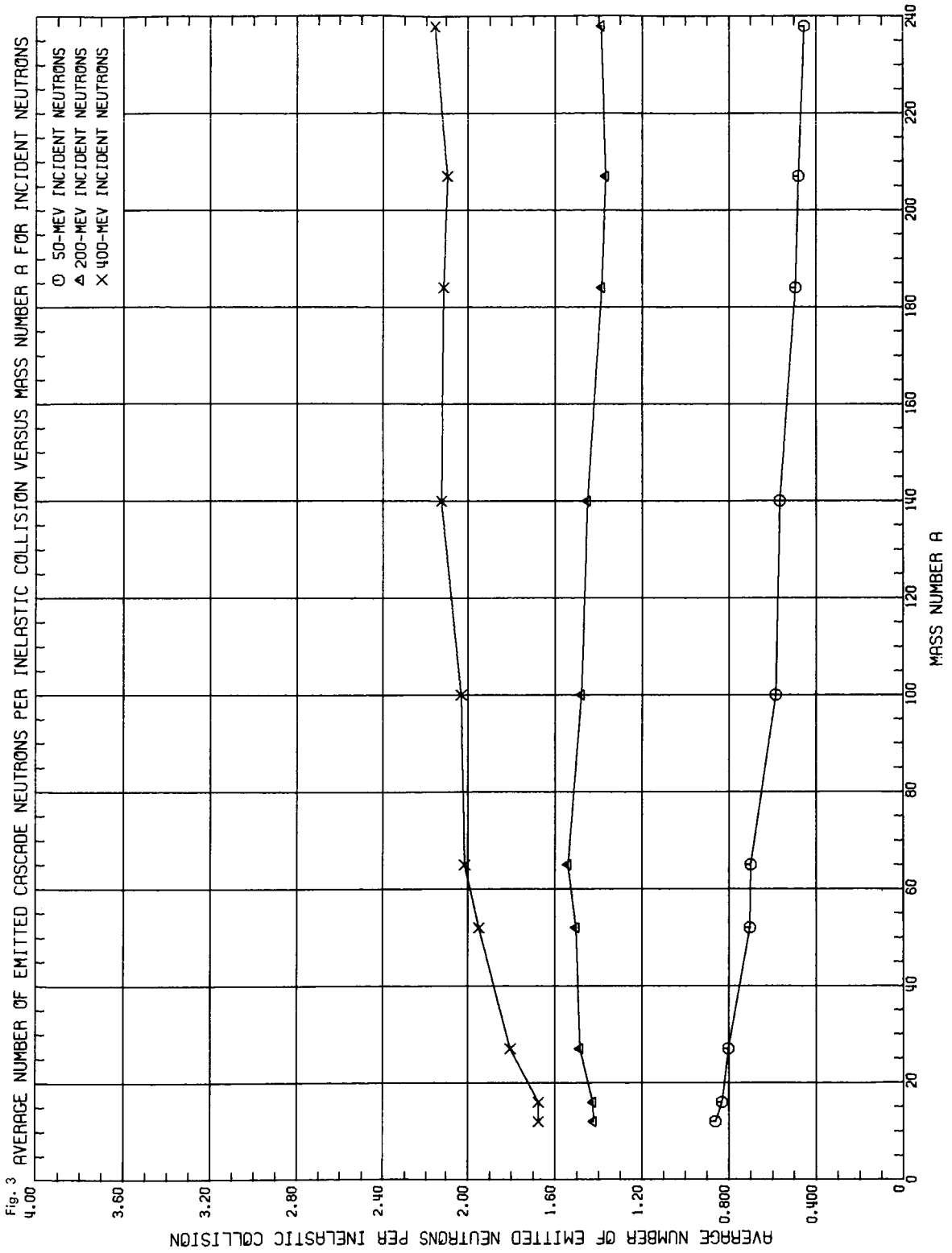
As shown in Figs. 81 and 82, there are many peaks in the cross sections, but the prominent one at mass number 190 for 50-MeV  $\pi^-$  and  $\pi^+$  on lead is caused by the rather high probability of absorption without emission of cascade nucleons. The others result from complicated relationships between all of the quantities associated with the cascade-evaporation process, and no attempt at an explanation will be made.



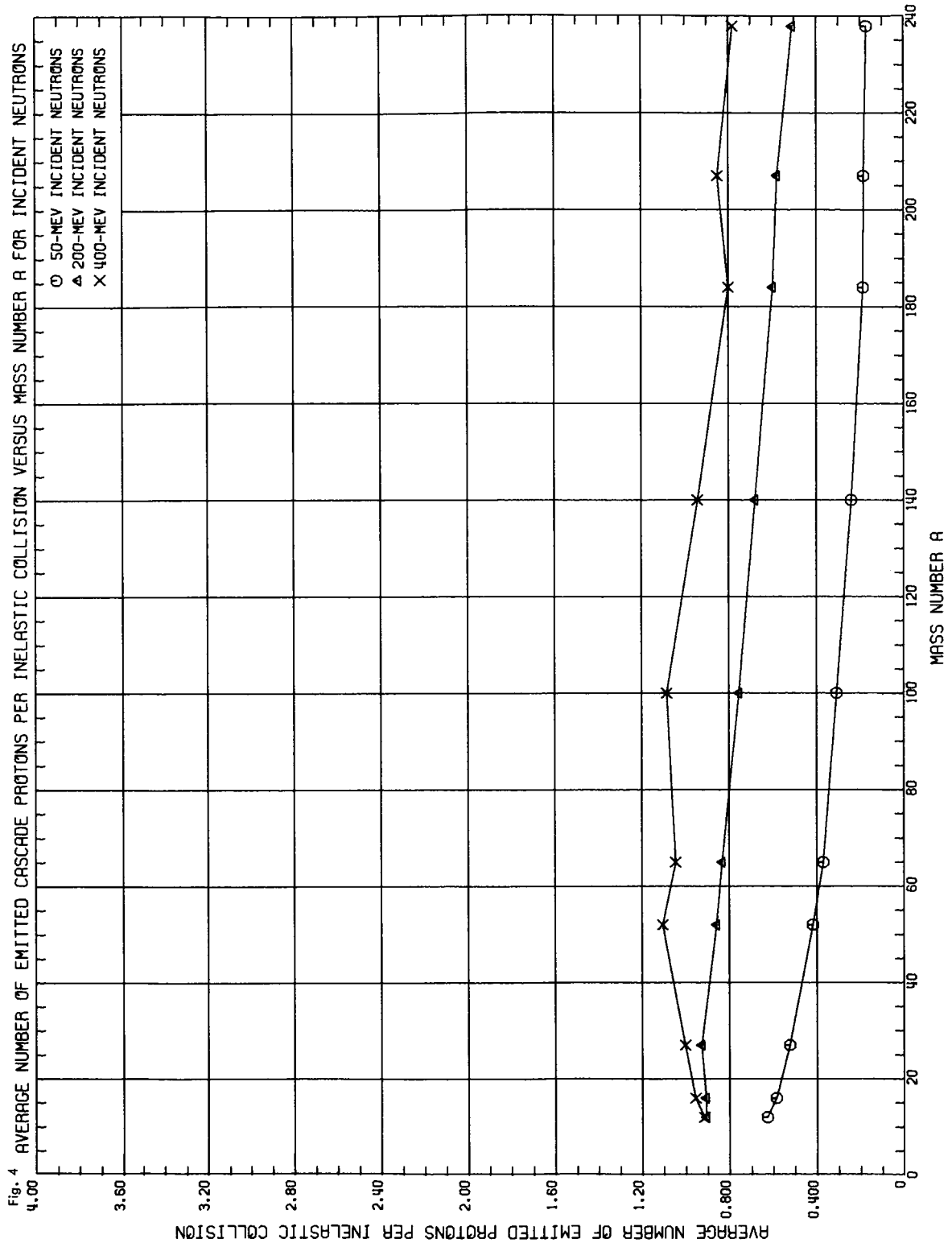
ORNL DWG 67-5531



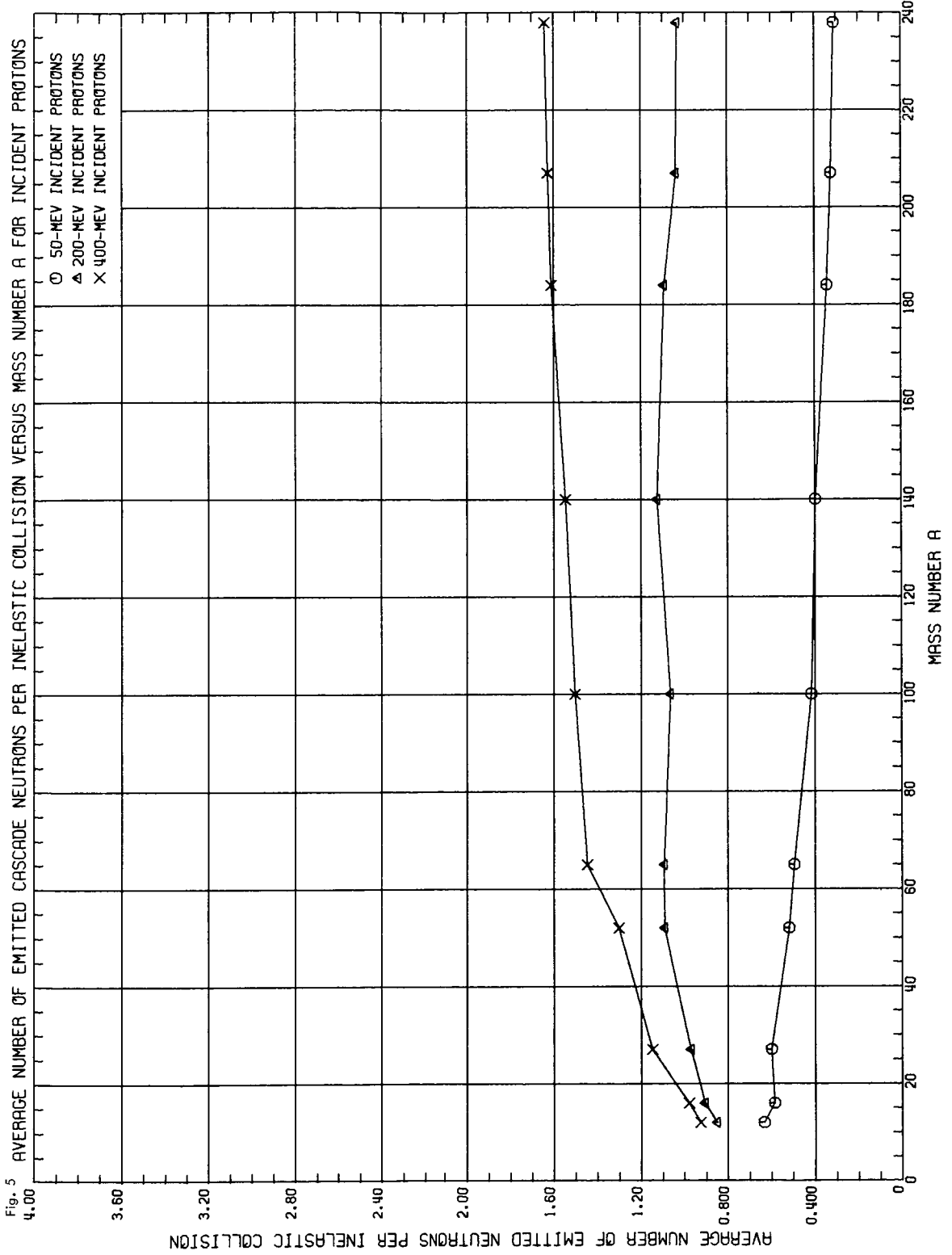




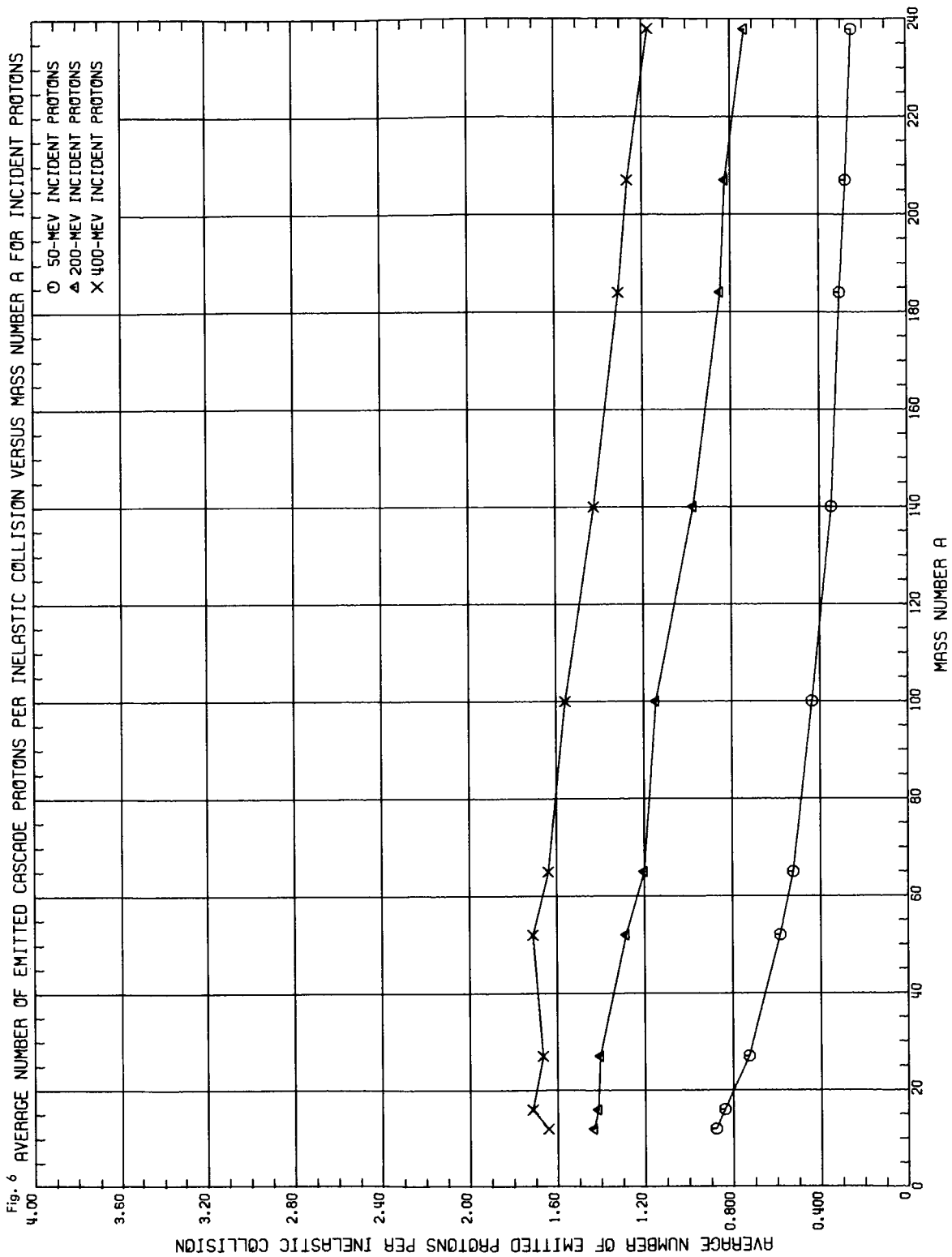
ORNL DWG 67-5534



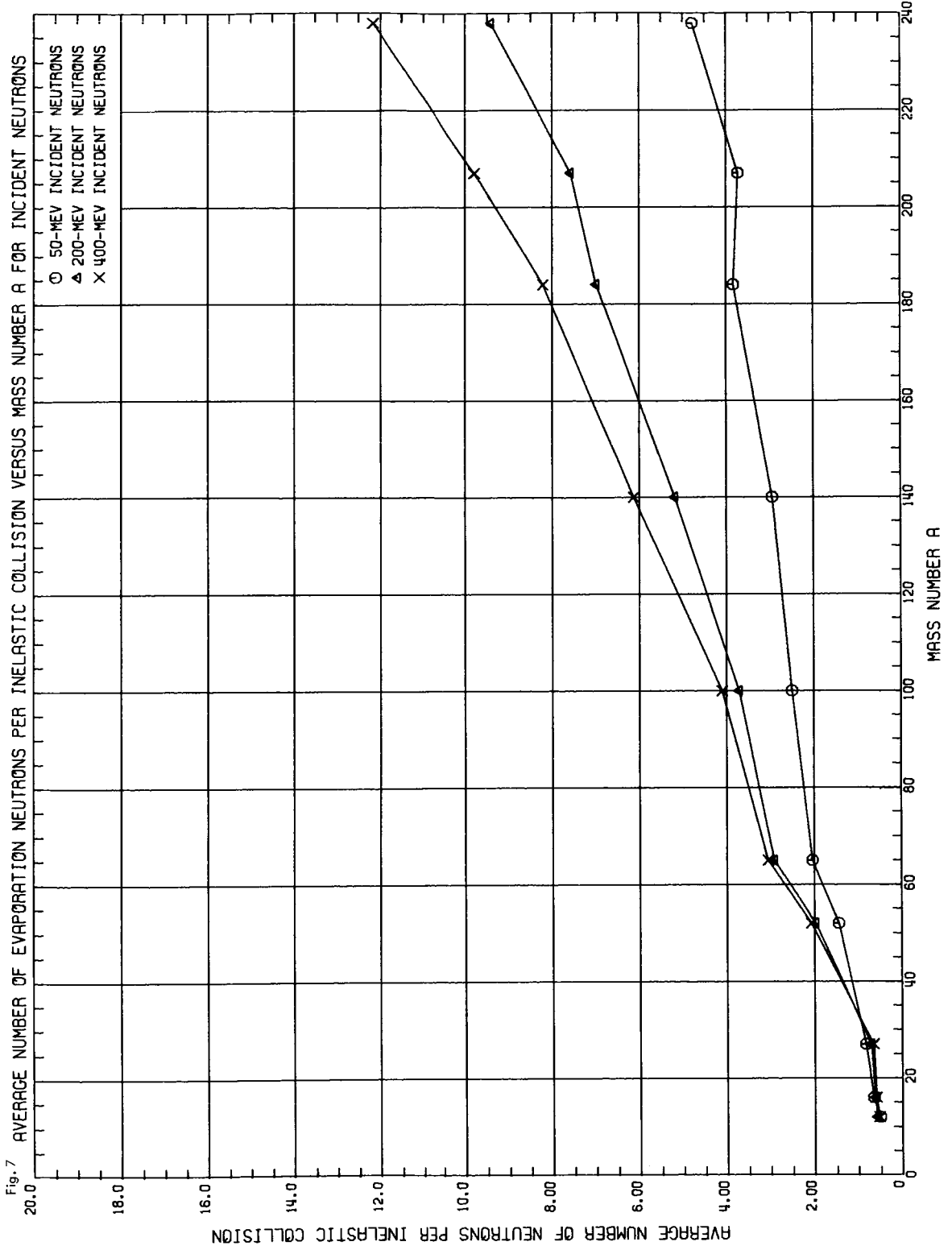
ORNL DWG 67-5535



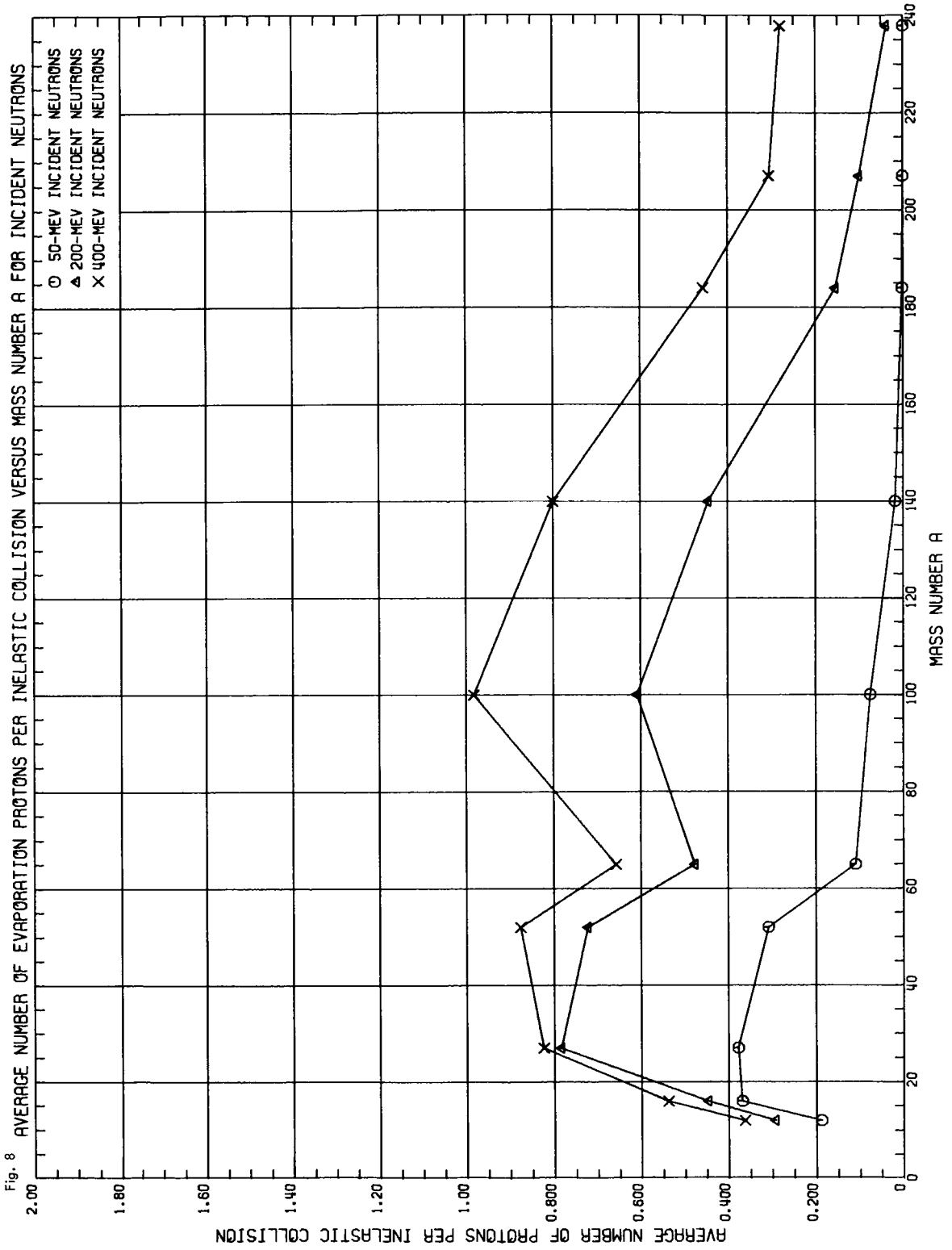
ORNL DWG 67-5536



ORNL DWG 67-5537

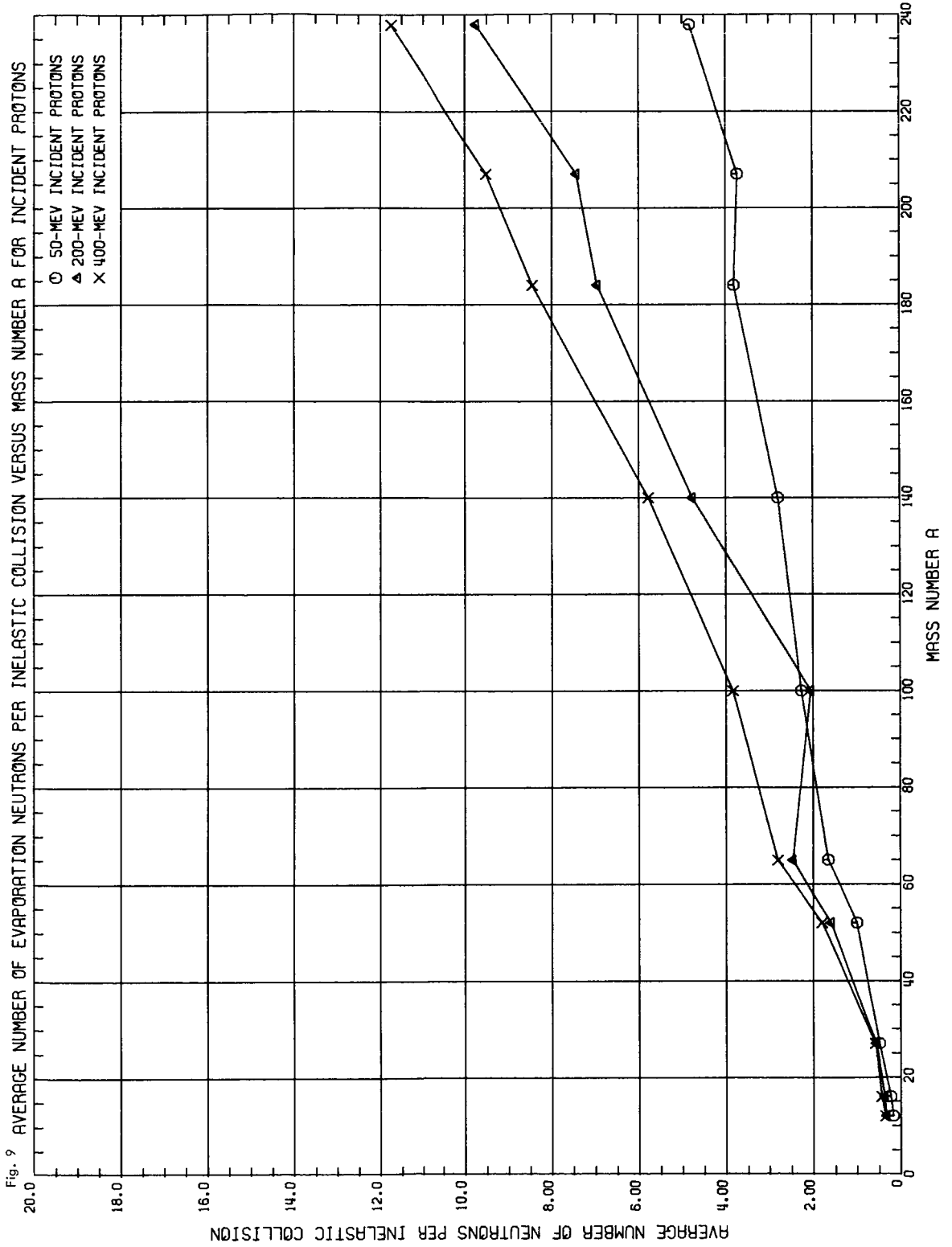


ORNL DWG 67-5538

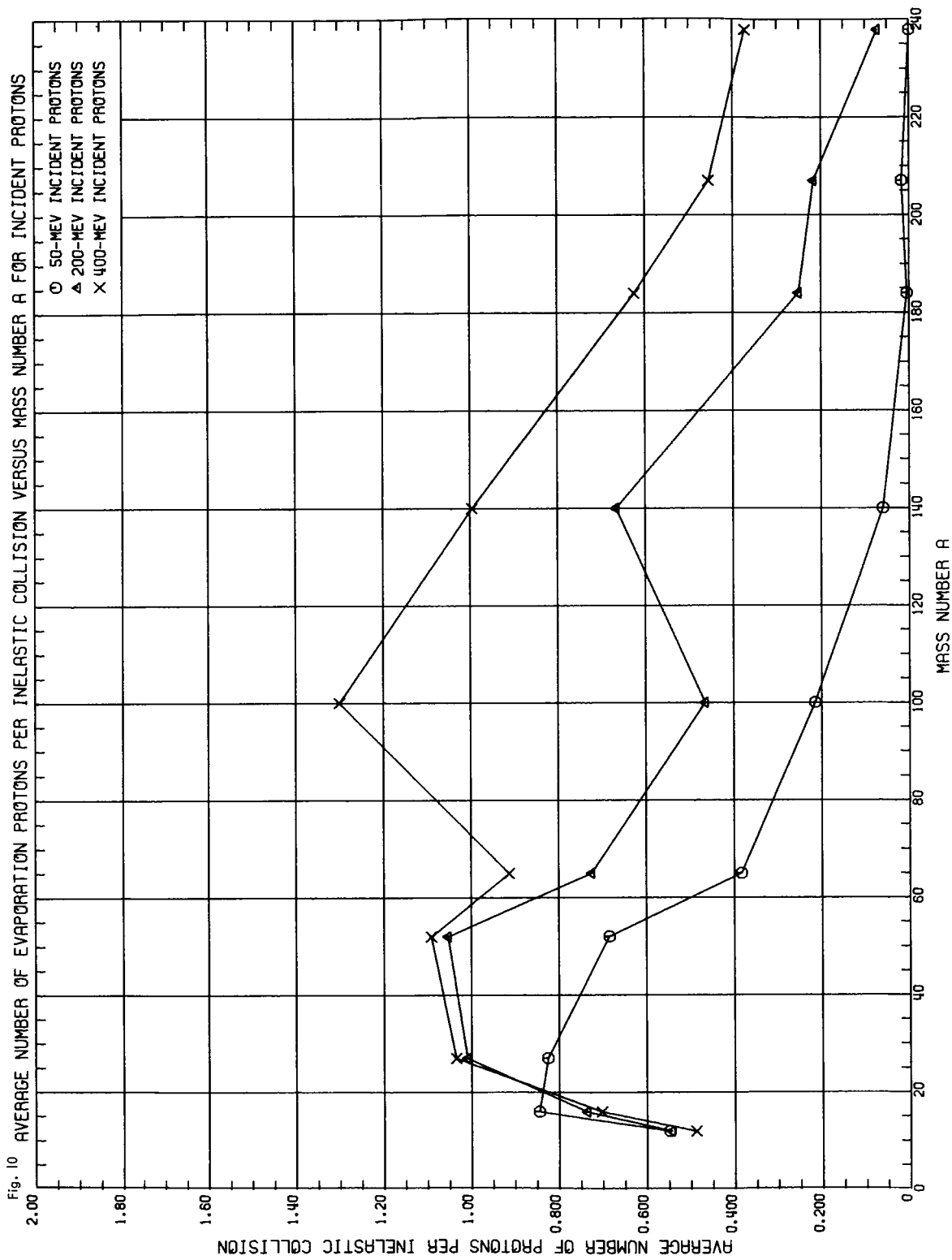




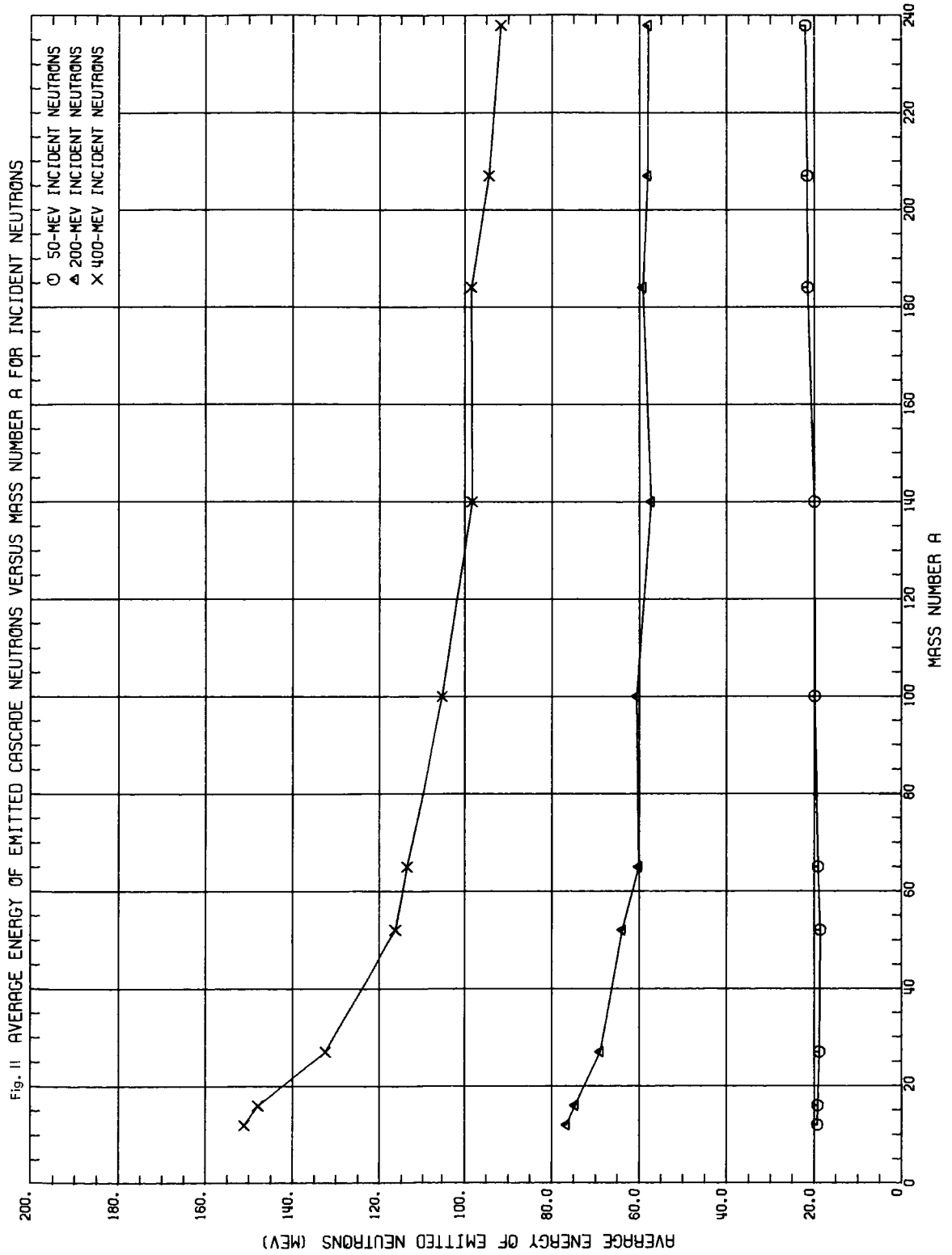
ORNL DWG 67-5539



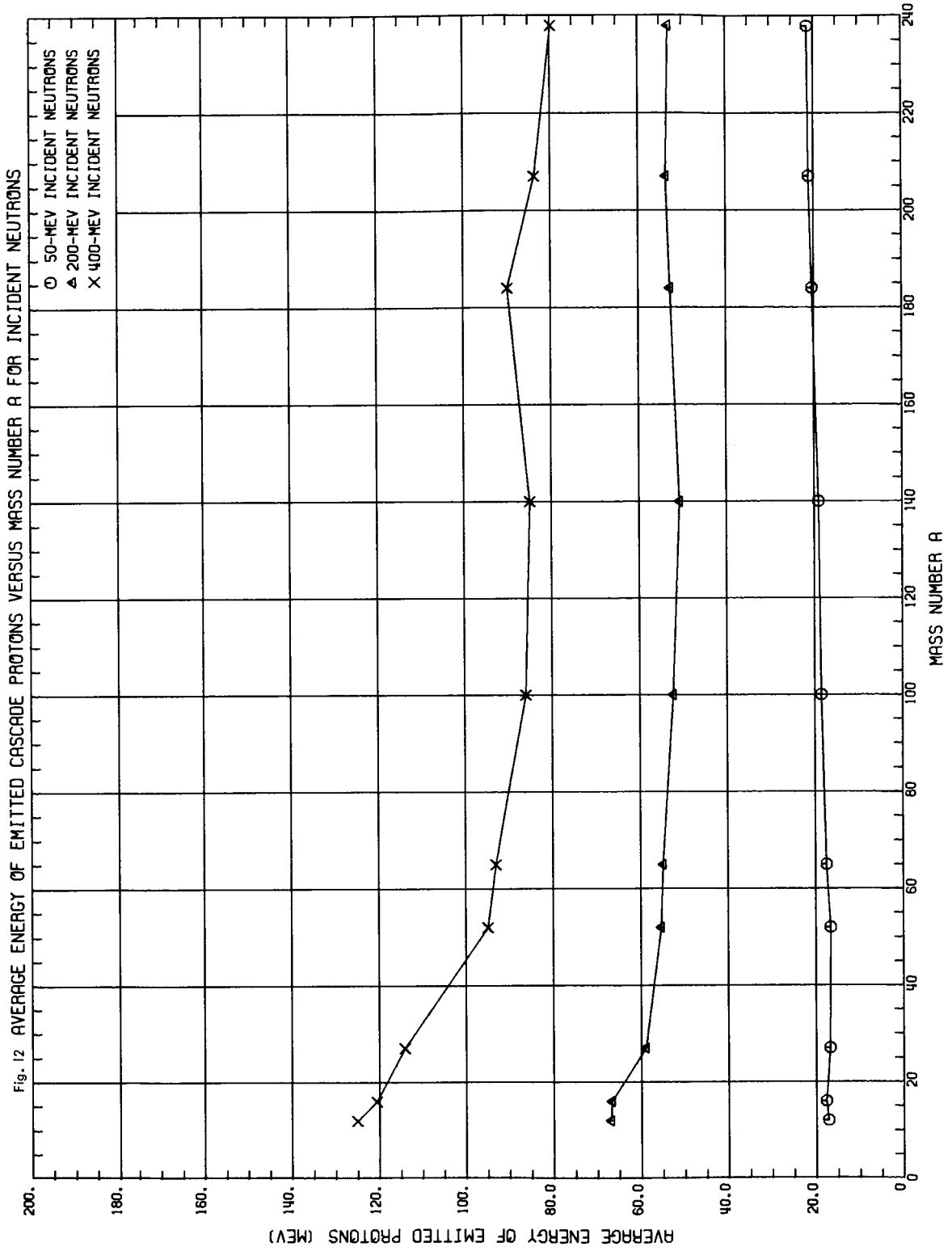
ORNIL DWG 67-5540



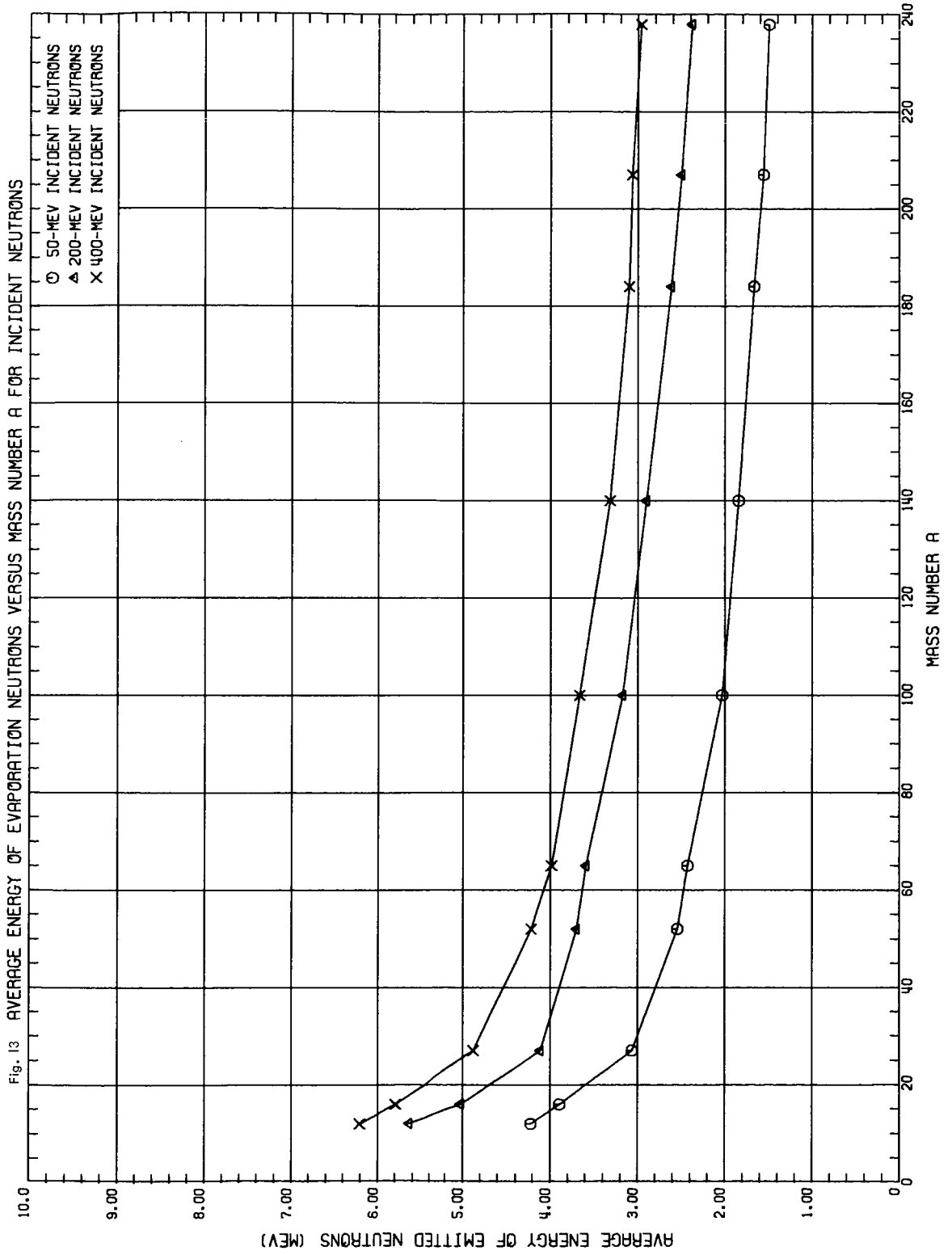
ORNL DWG 67-5541



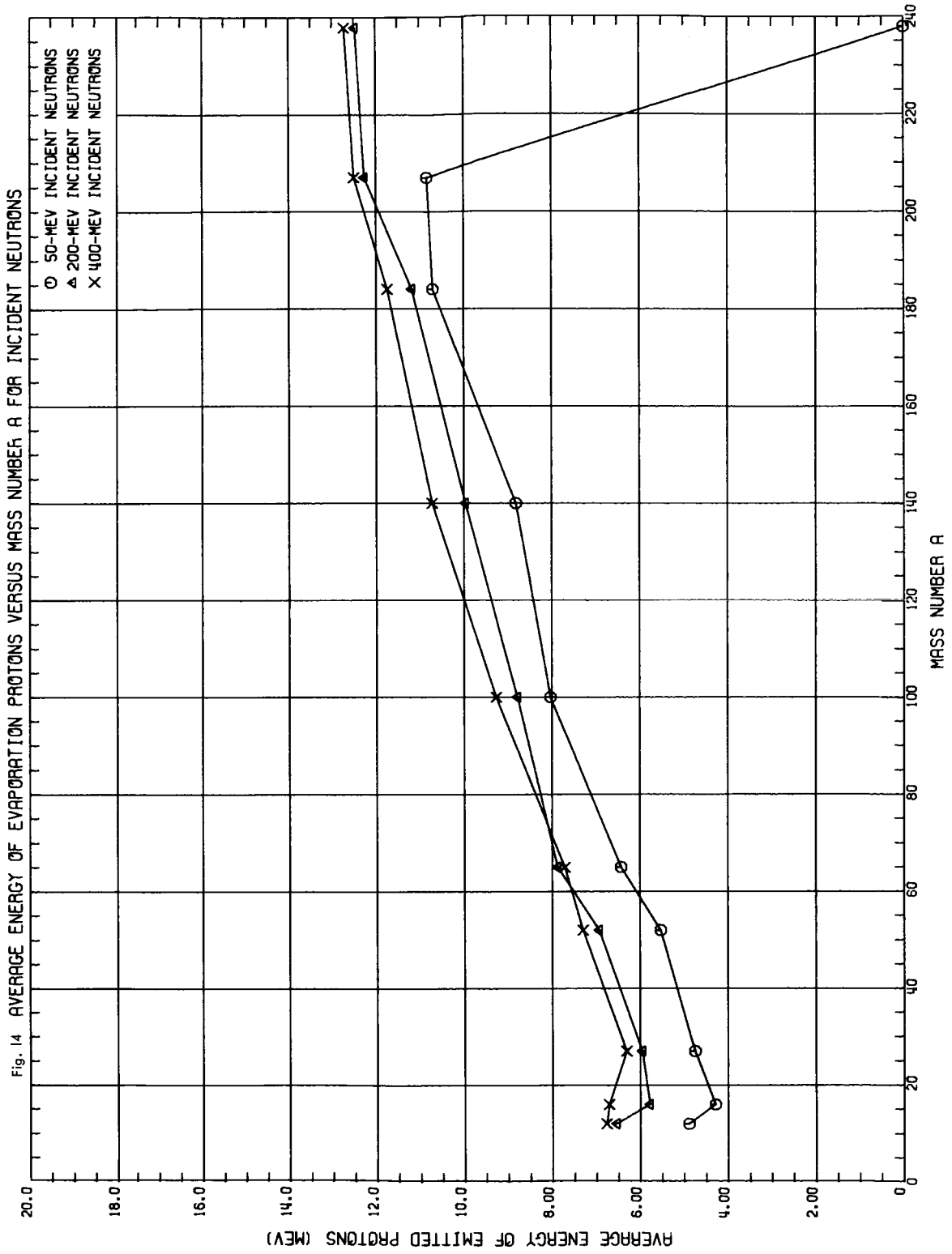
ORNL DWG 67-5542



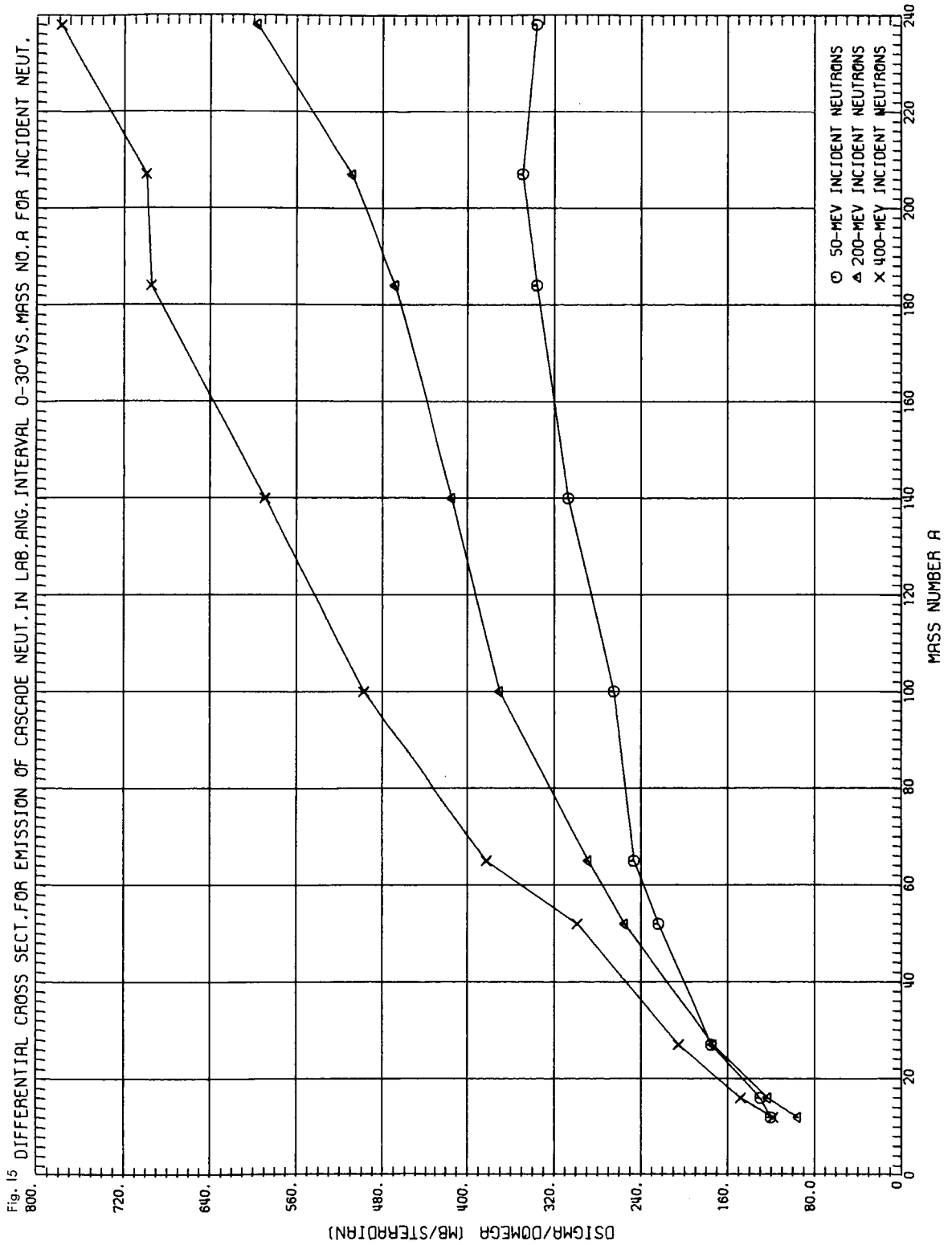
ORNL DWG 67-5543



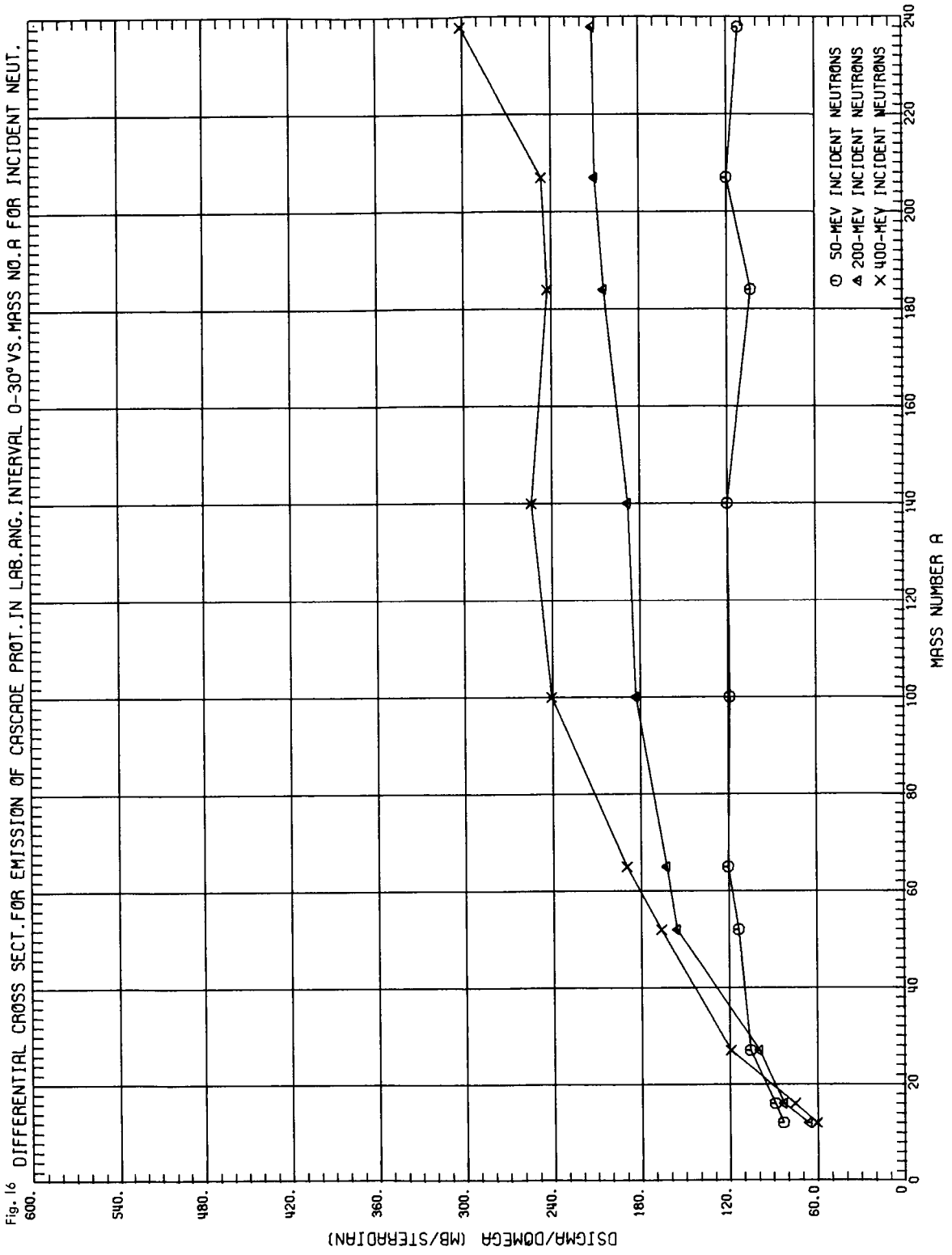
ORNL DWG 67-5544



ORNL DWG 67-5545

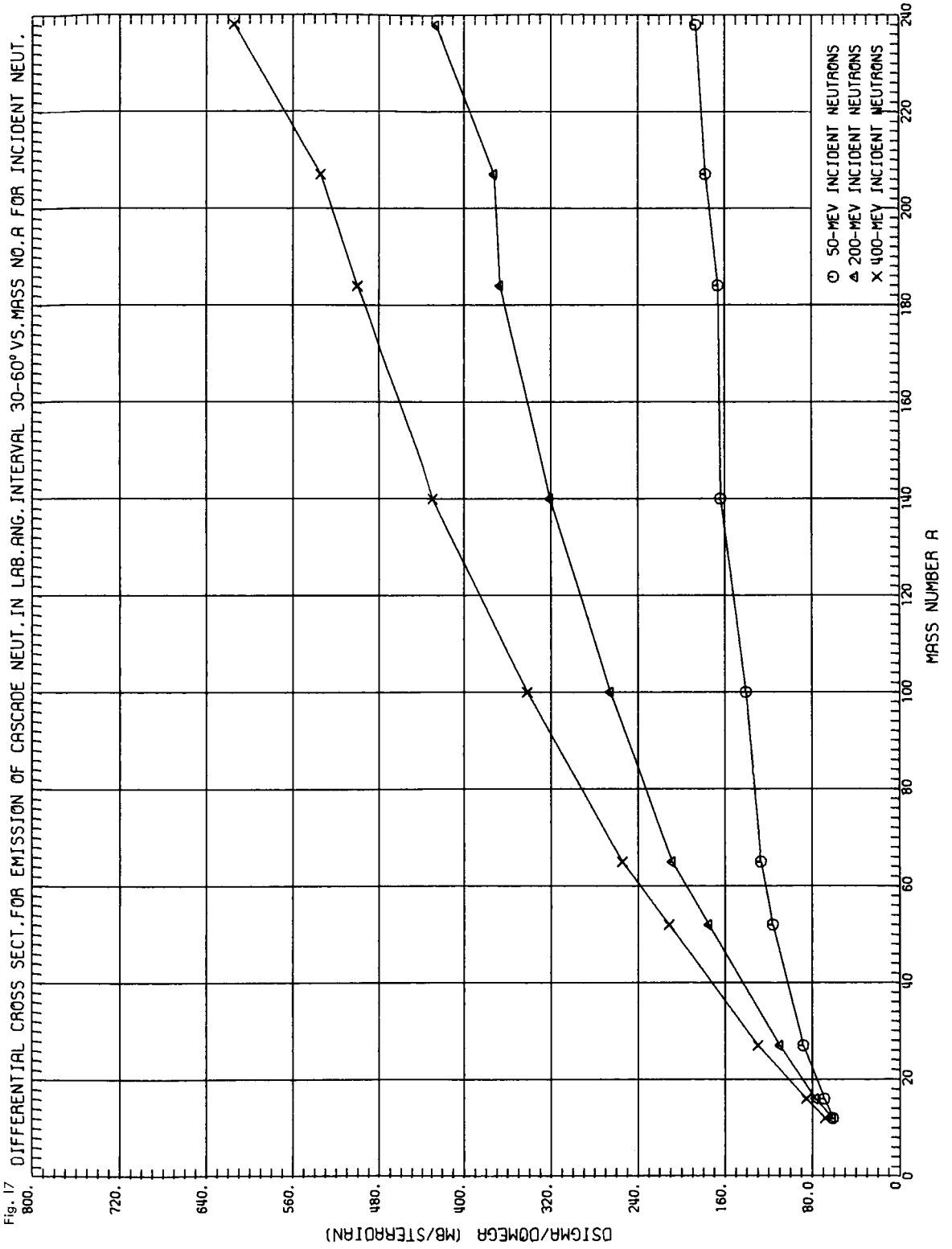


ORNL DWG 67-5546

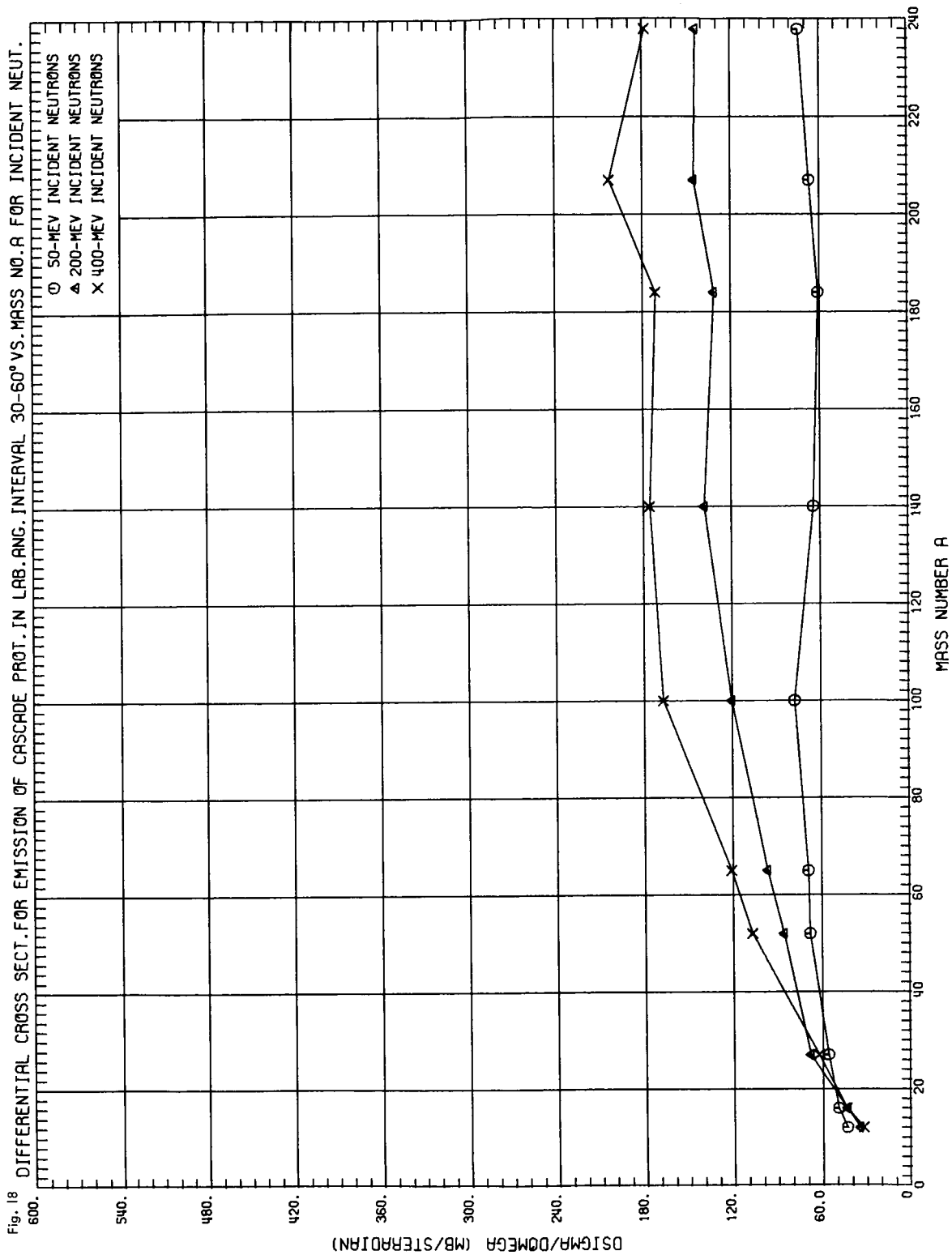




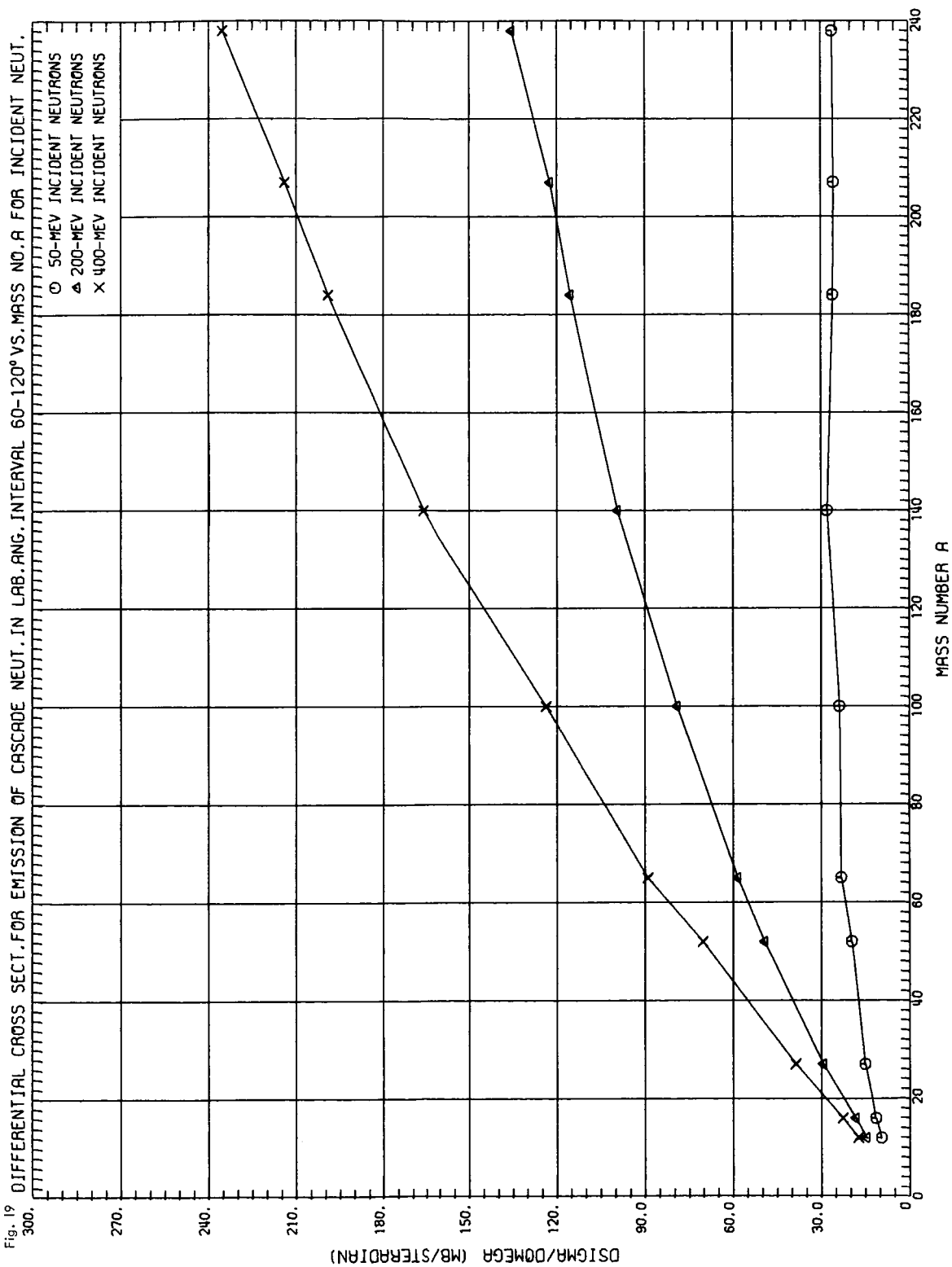
ORNL DWG 67-5547



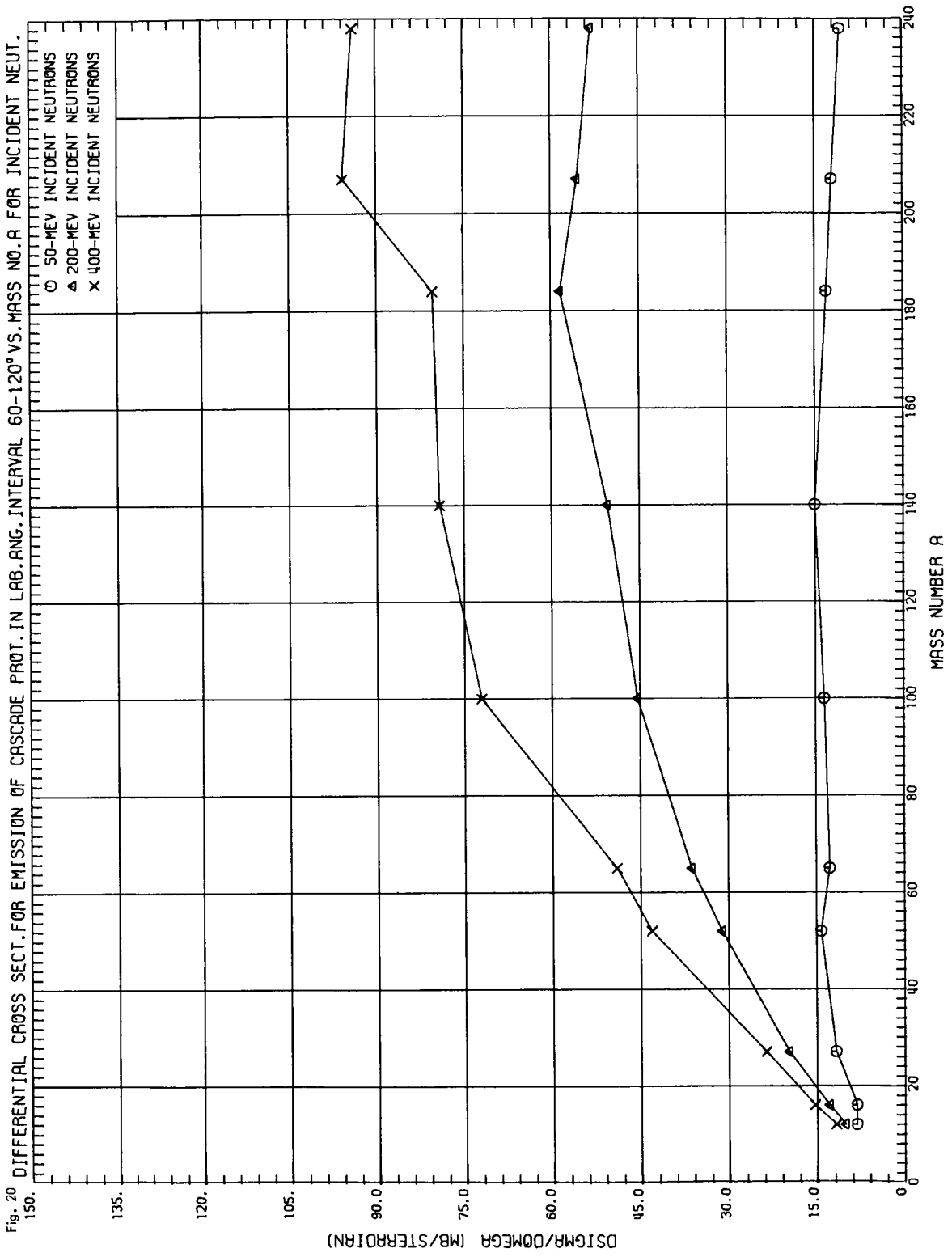
ORNL DWG 67-5548



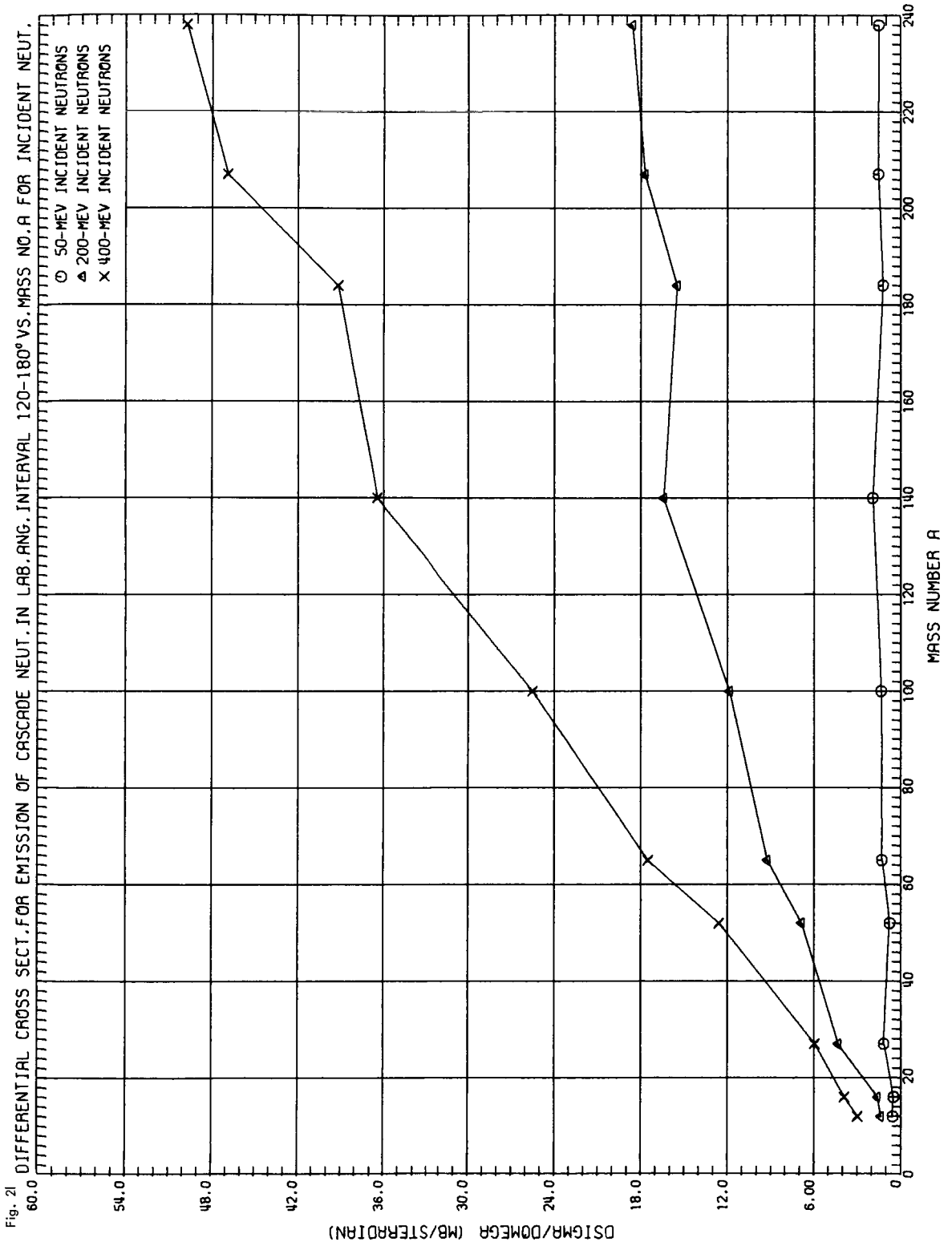
ORNL DWG 67-5549



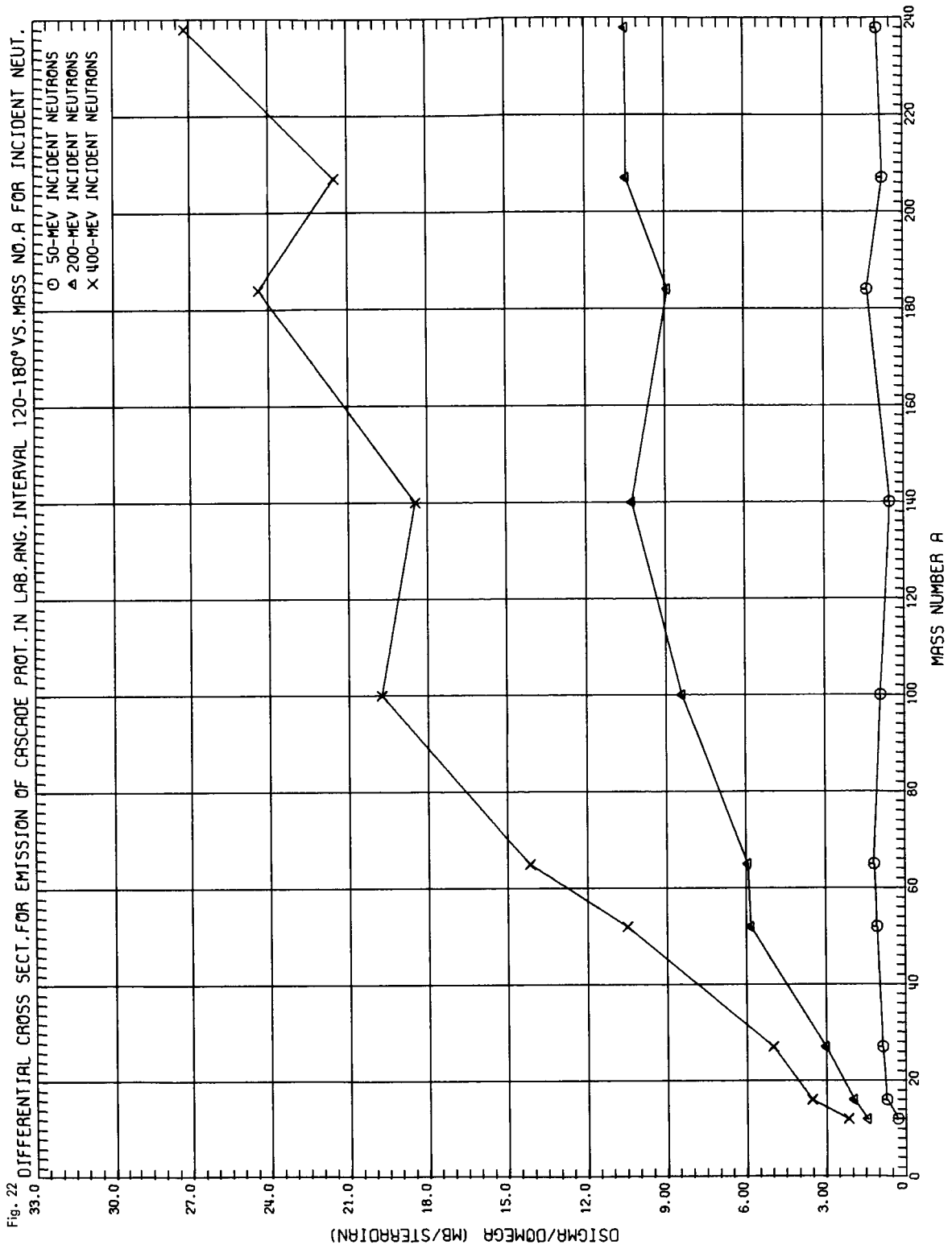
ORNL DWG 67-5550



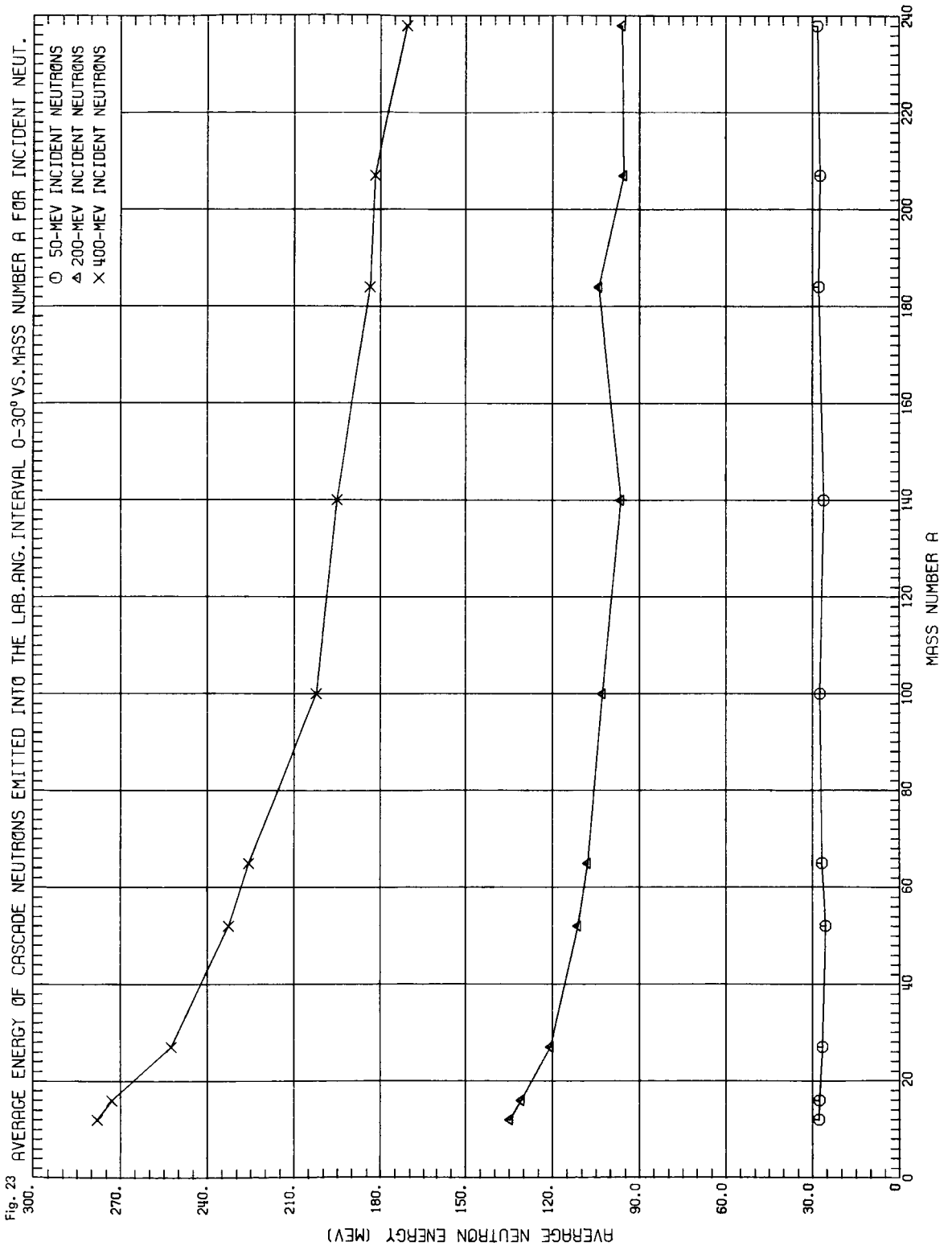
ORNL DWG 67-5551



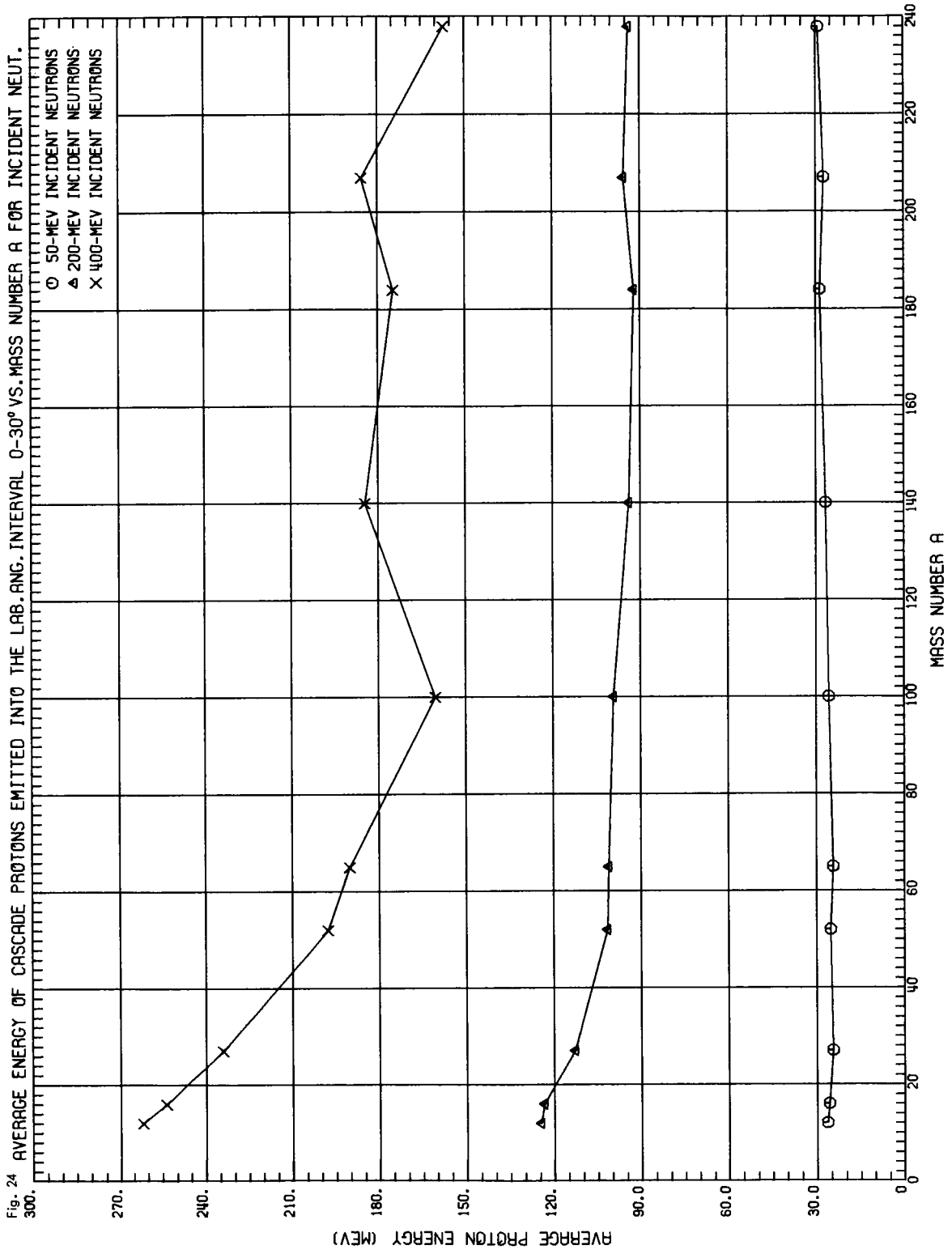
ORNL DWG 67-5552



ORNL DWG 67-5553

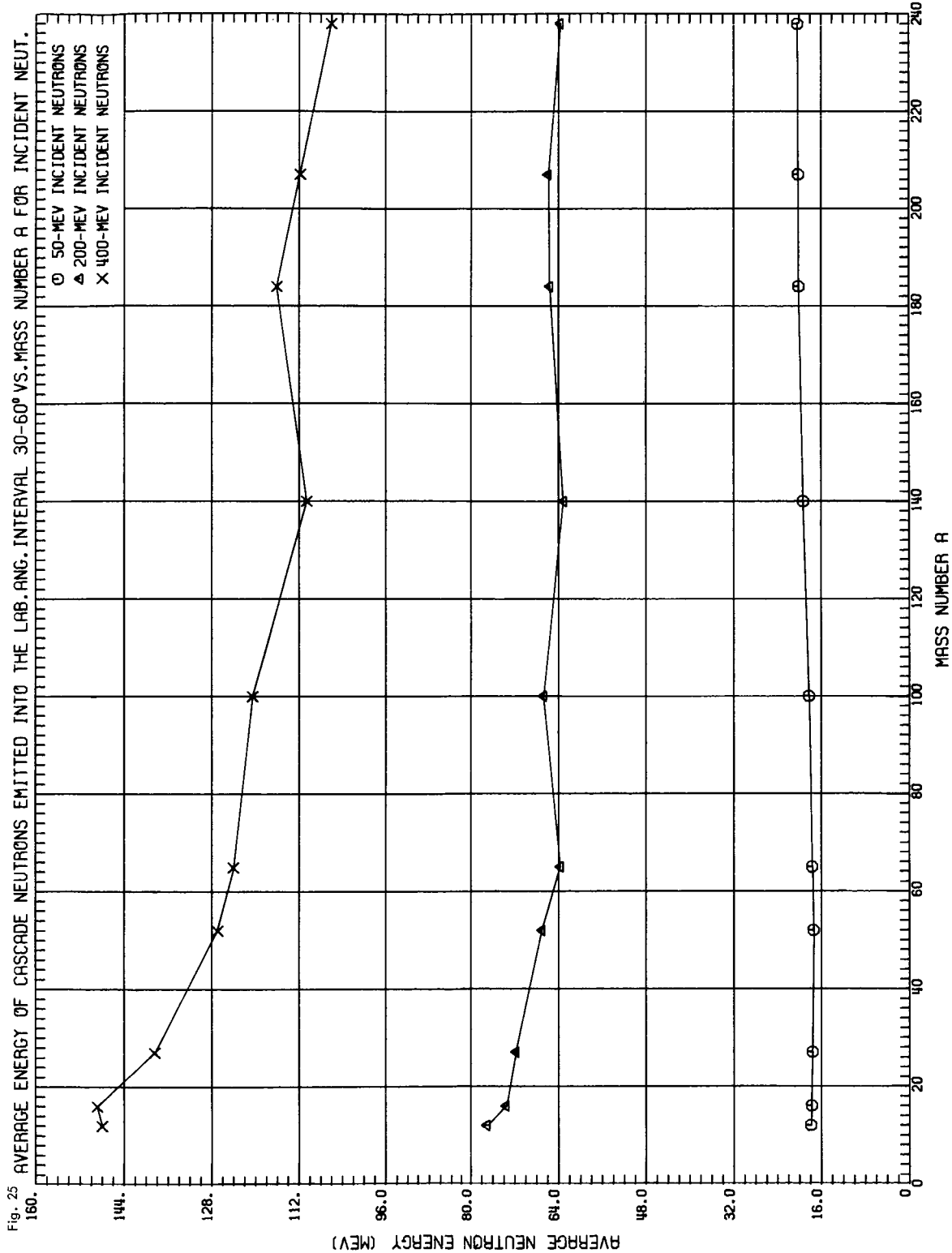


ORNL DWG 67-5554

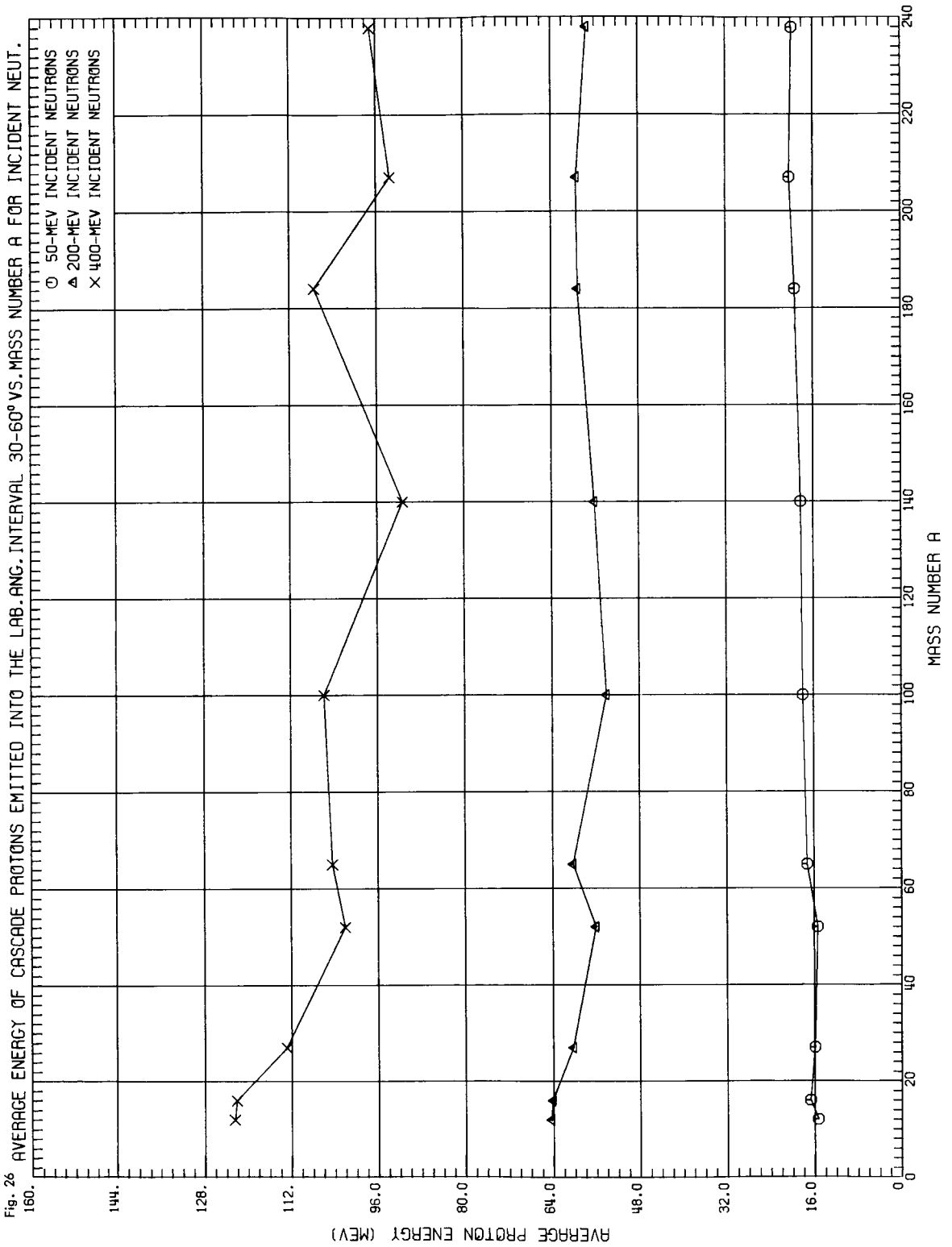




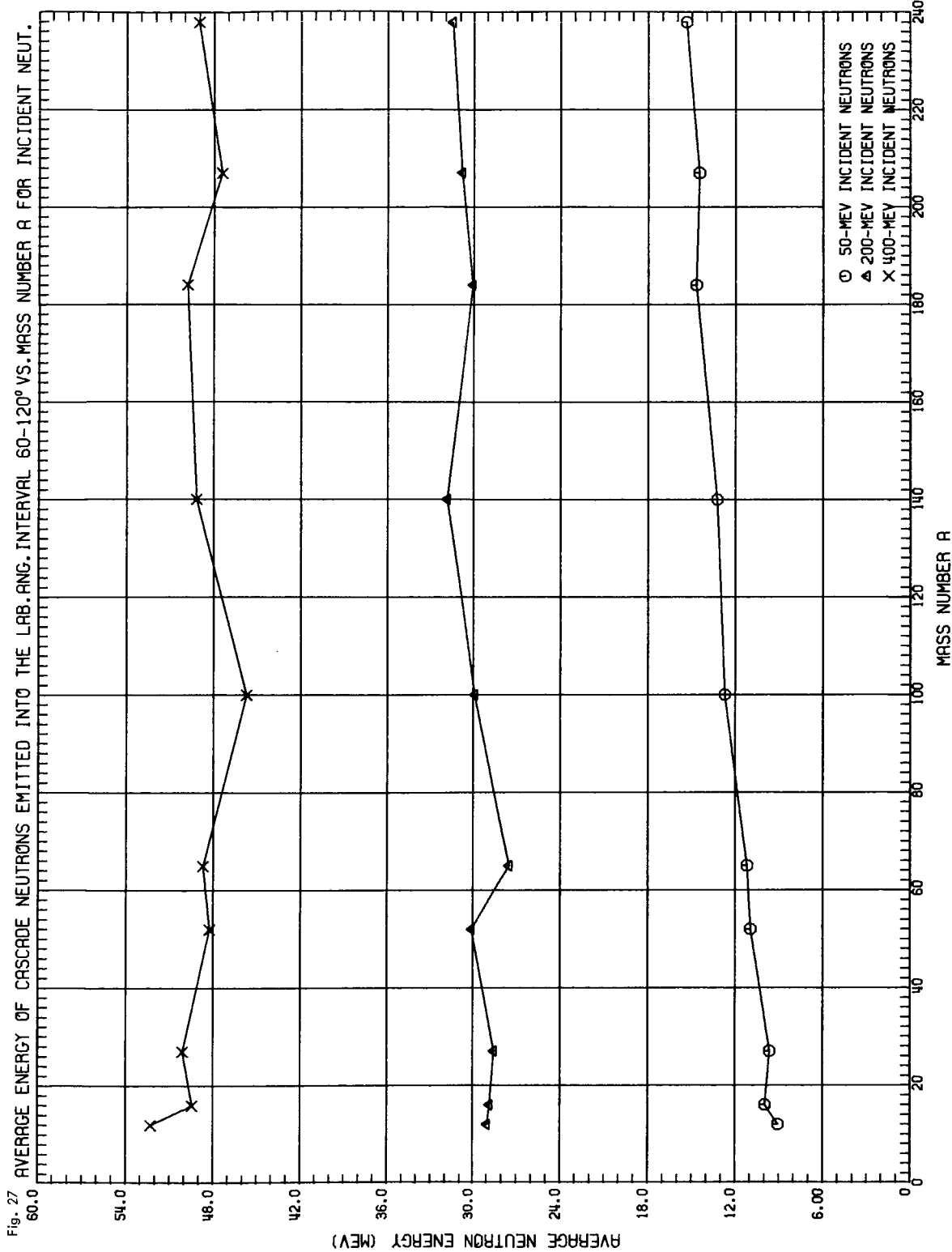
ORNL DWG 67-5555



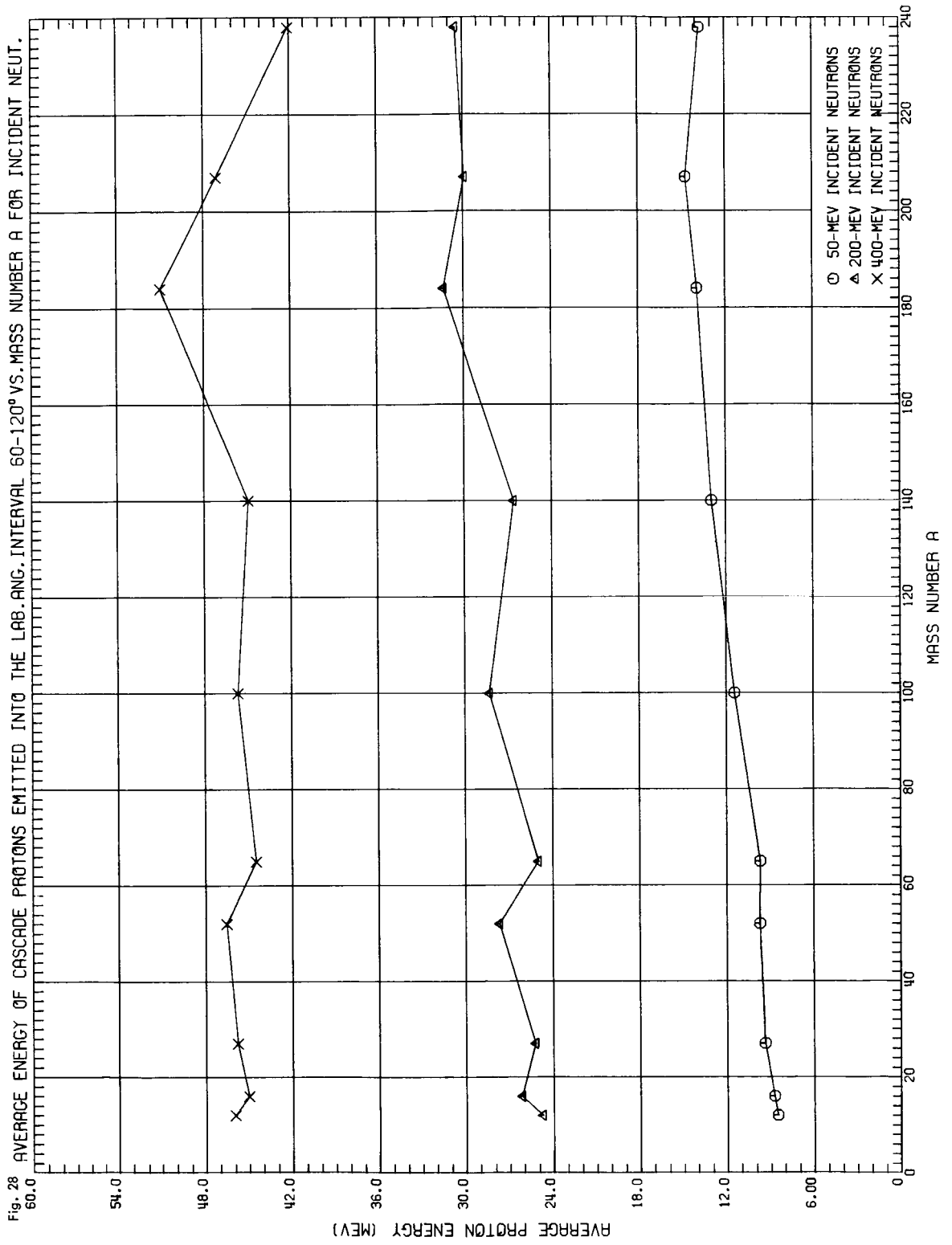
ORNL DWG 67-5556



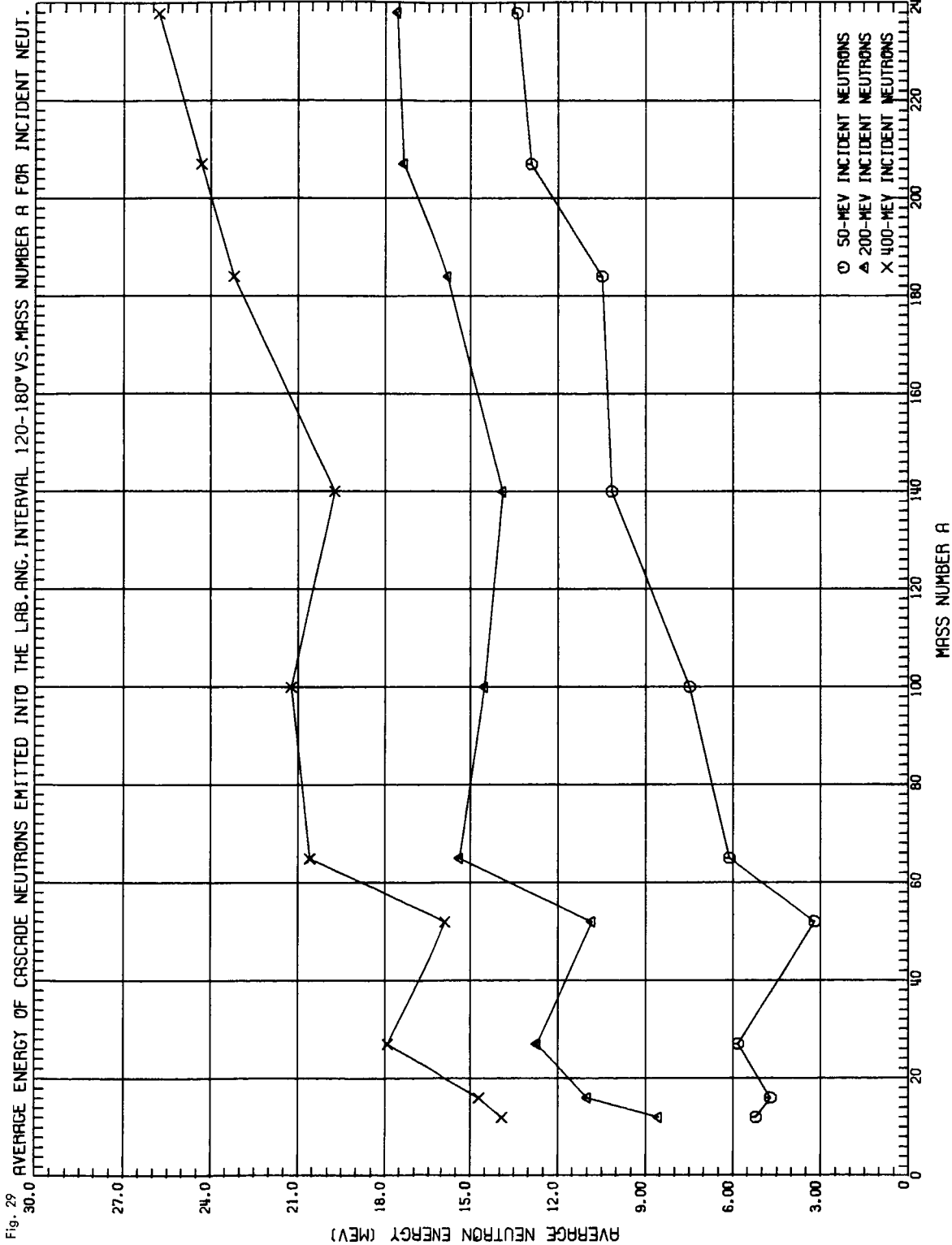
ORNL DWG 67-5557



ORNL DWG 67-5538

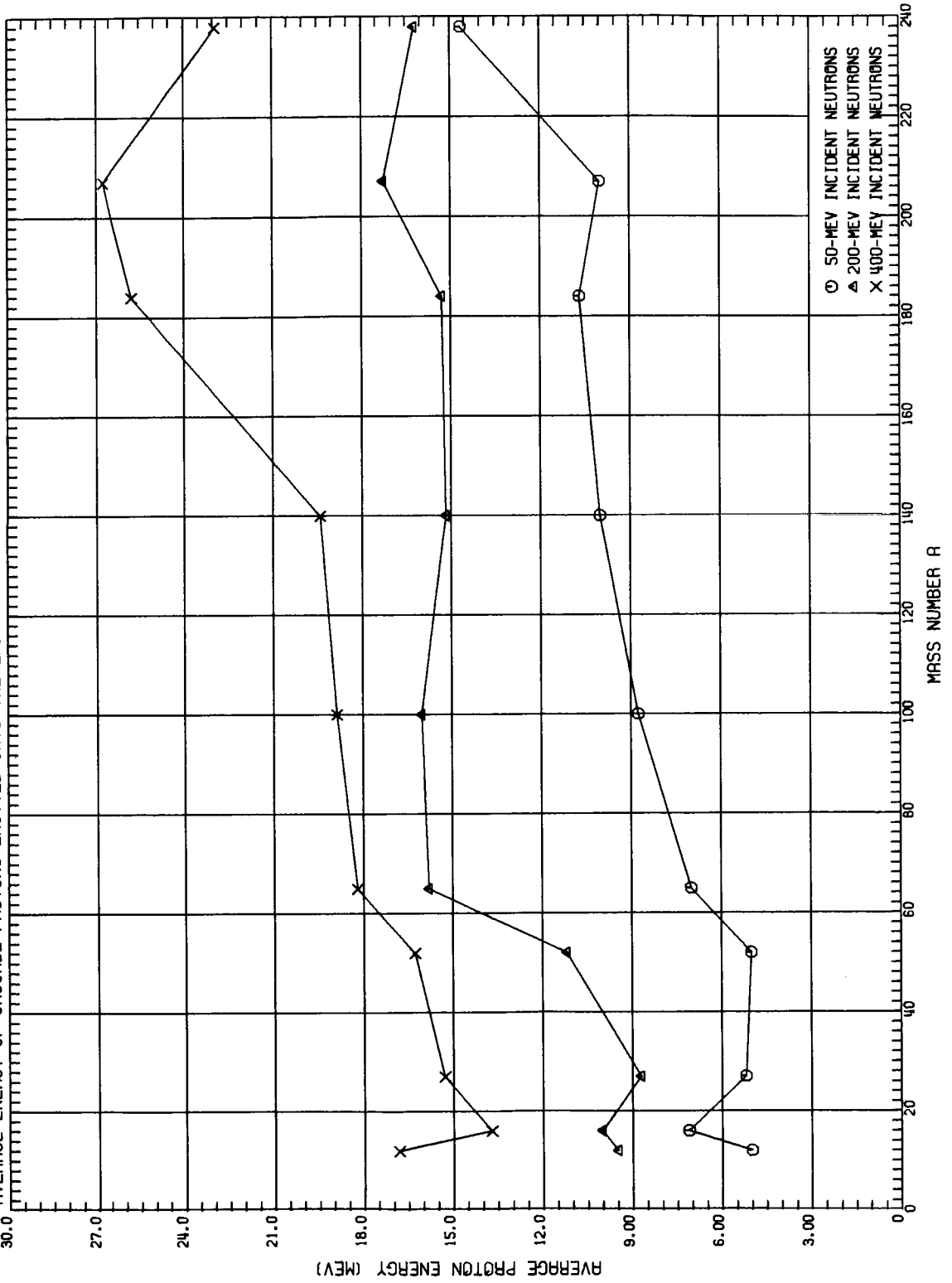


ORNL DWG 67-5559

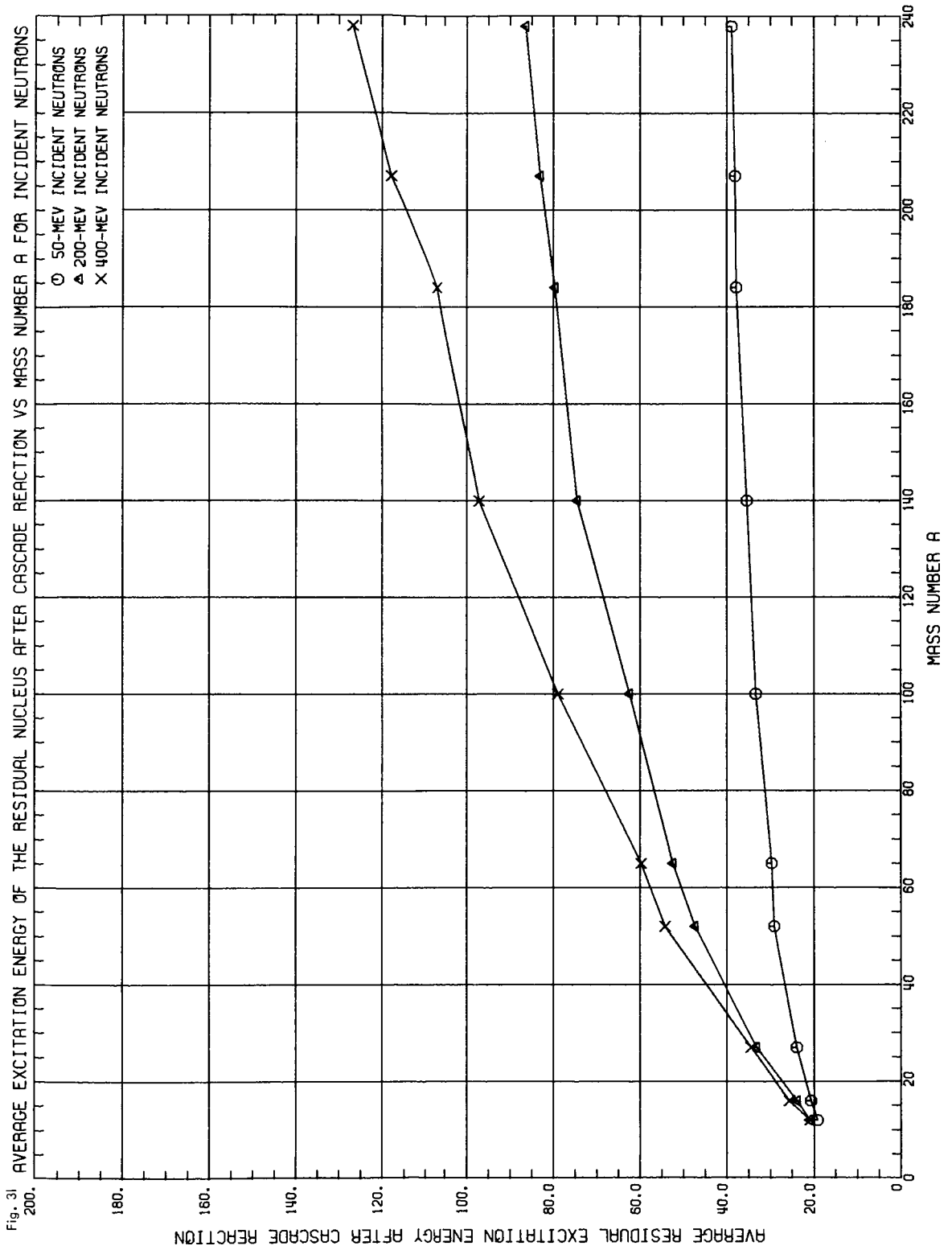


ORNL DWG 67-5560

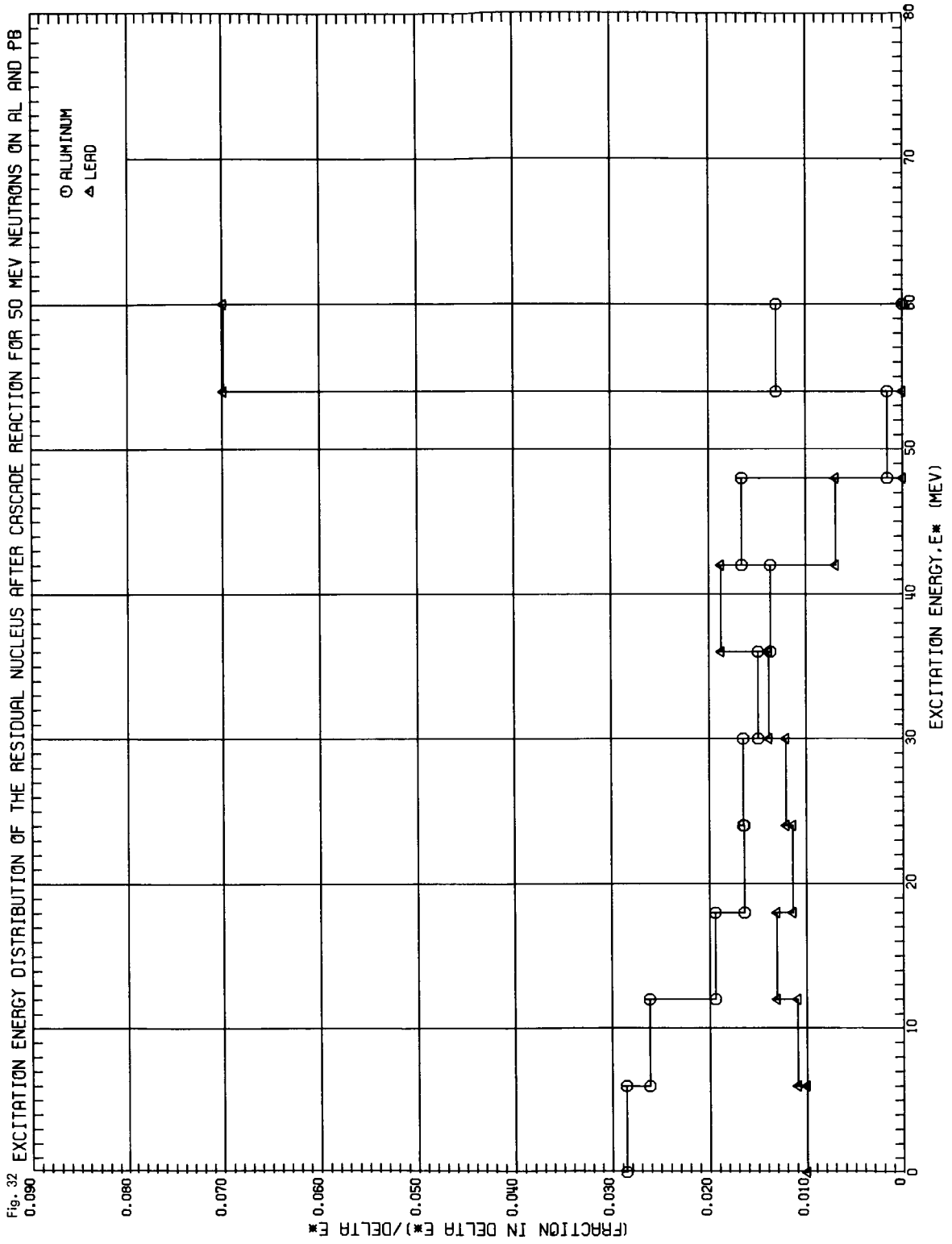
Fig. 30 AVERAGE ENERGY OF CASCADE PROTONS EMITTED INTO THE LAB. ANG. INTERVAL 120-180° VS. MASS NUMBER A FOR INCIDENT NEUT.



ORNL DWG 67-5561

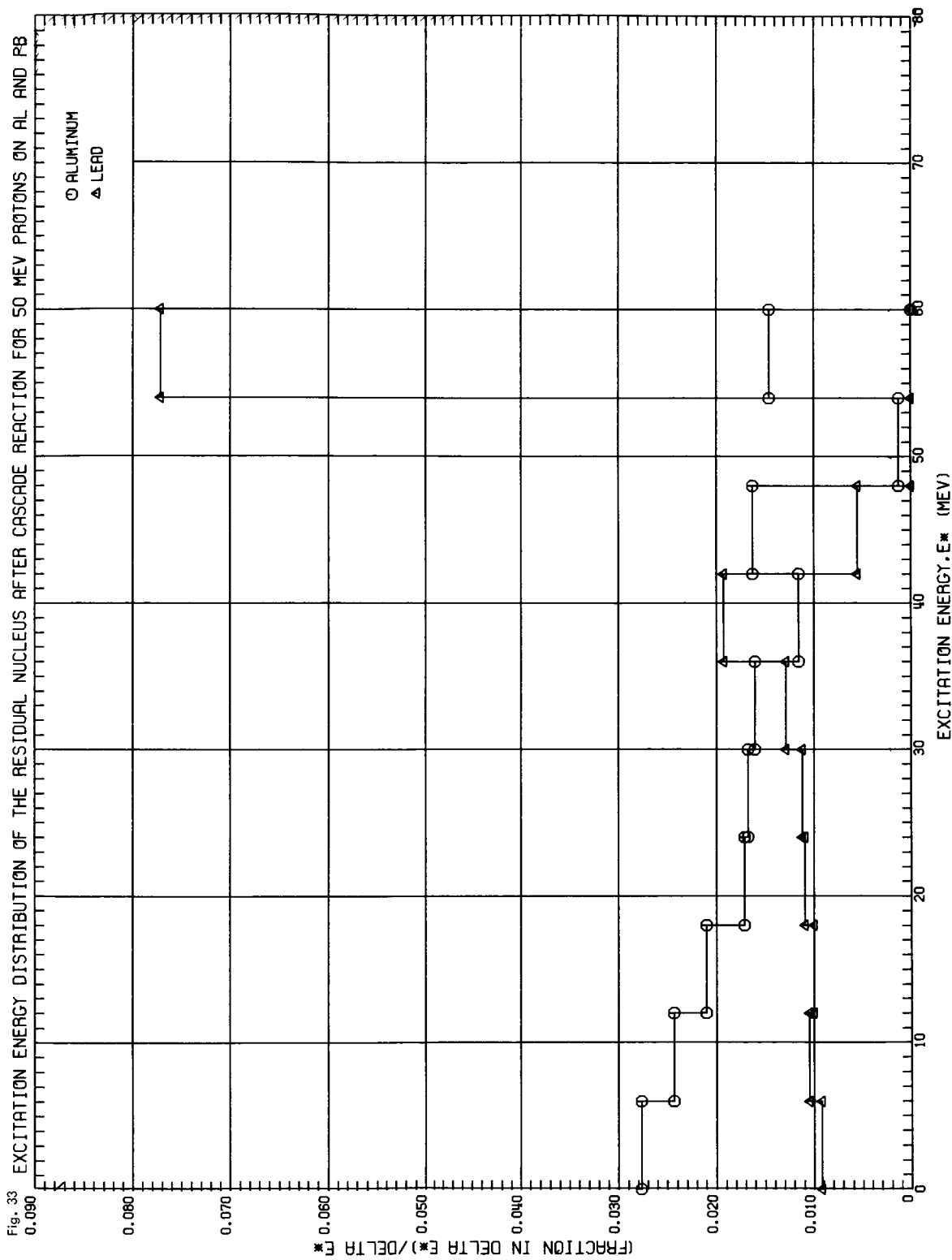


ORNL DWG 67-5562

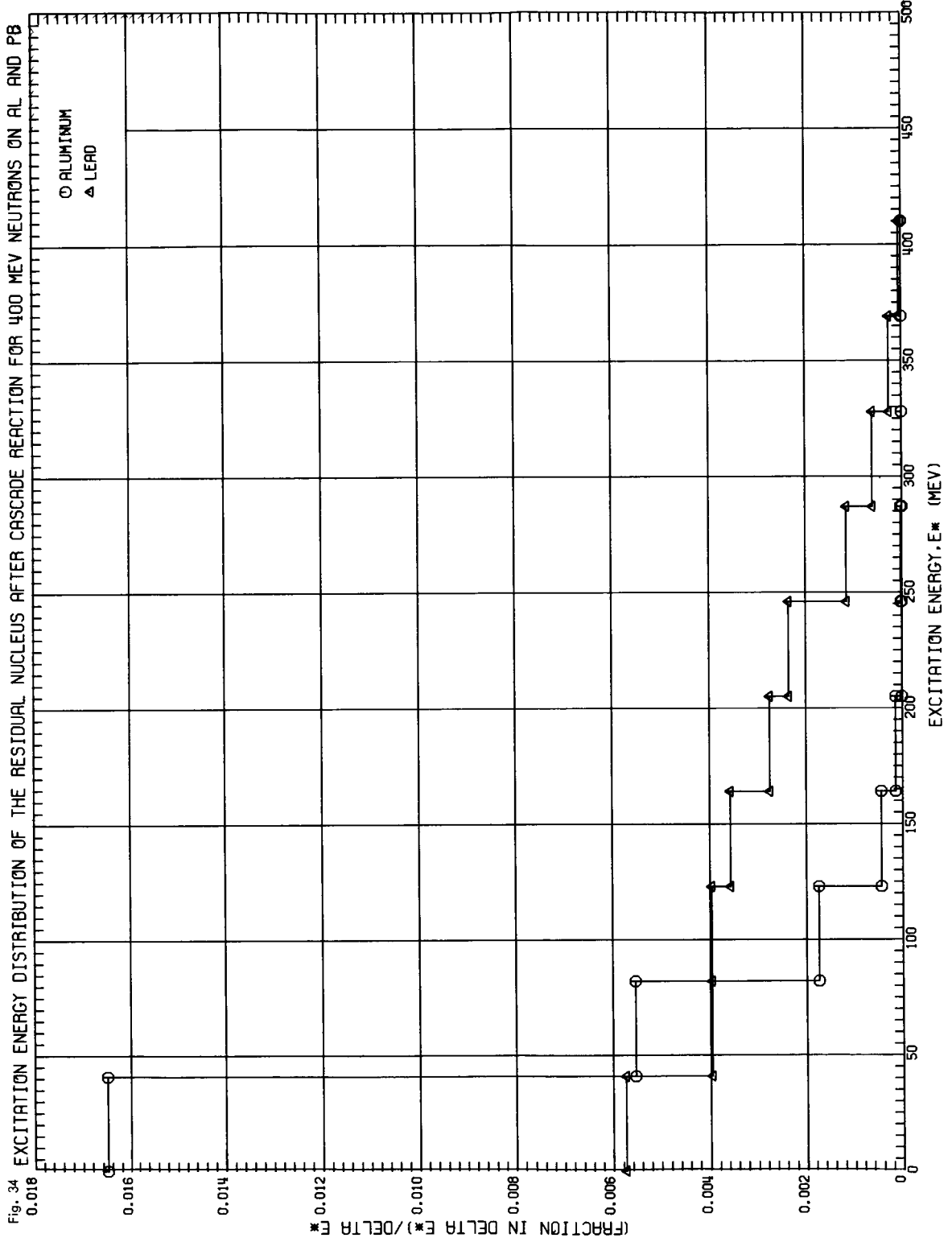




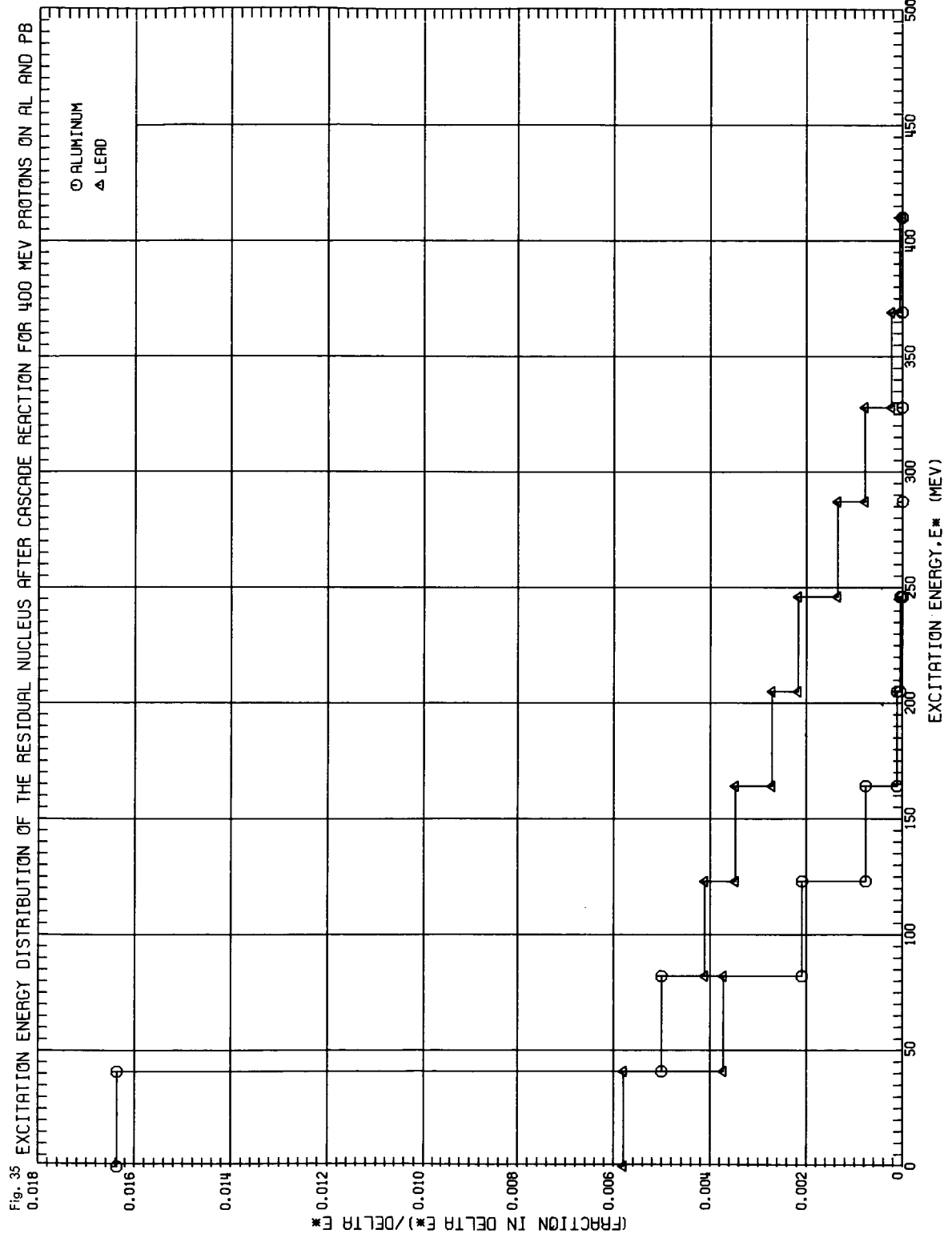
ORNL DWG 67-5563



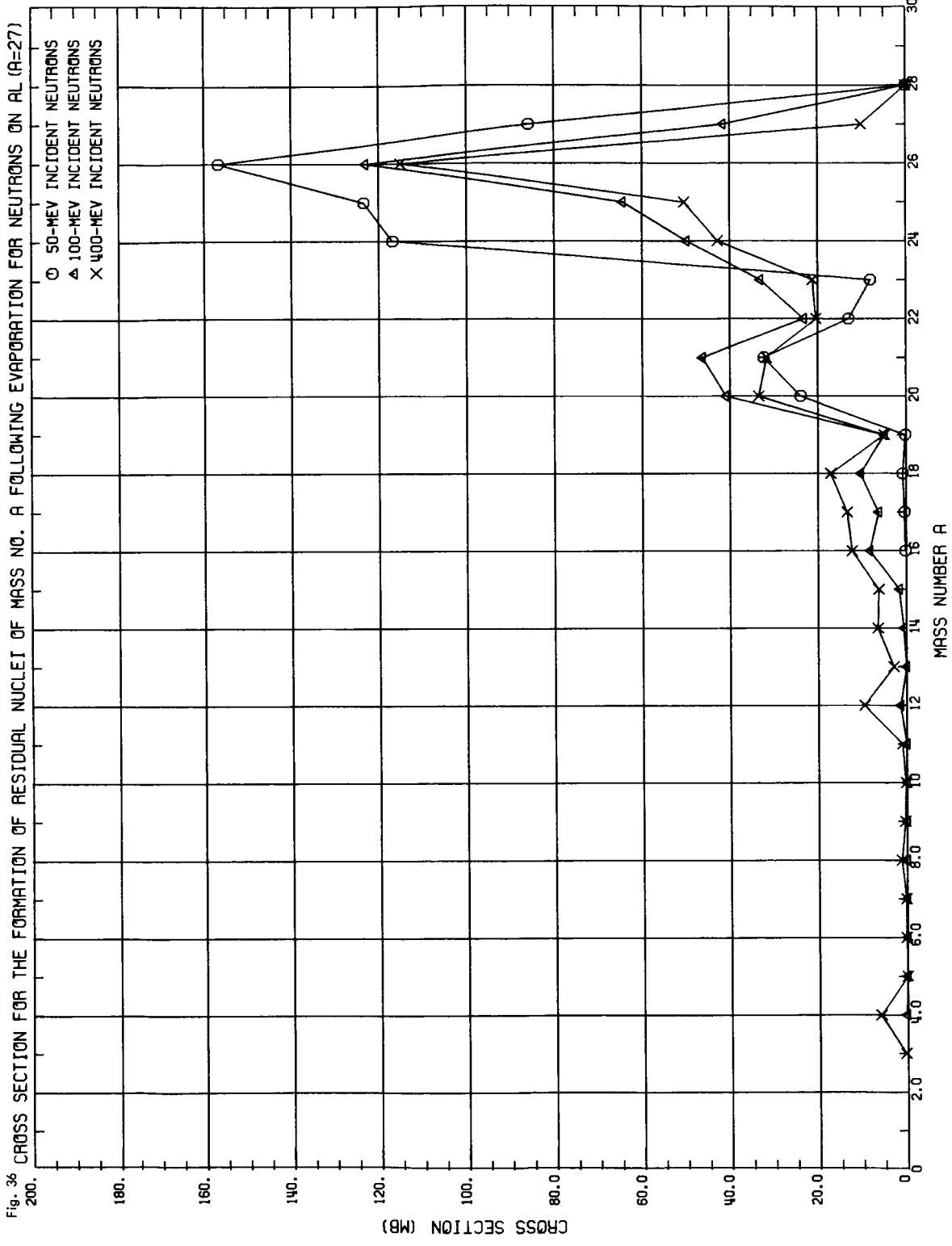
ORNL DWG 67-5564



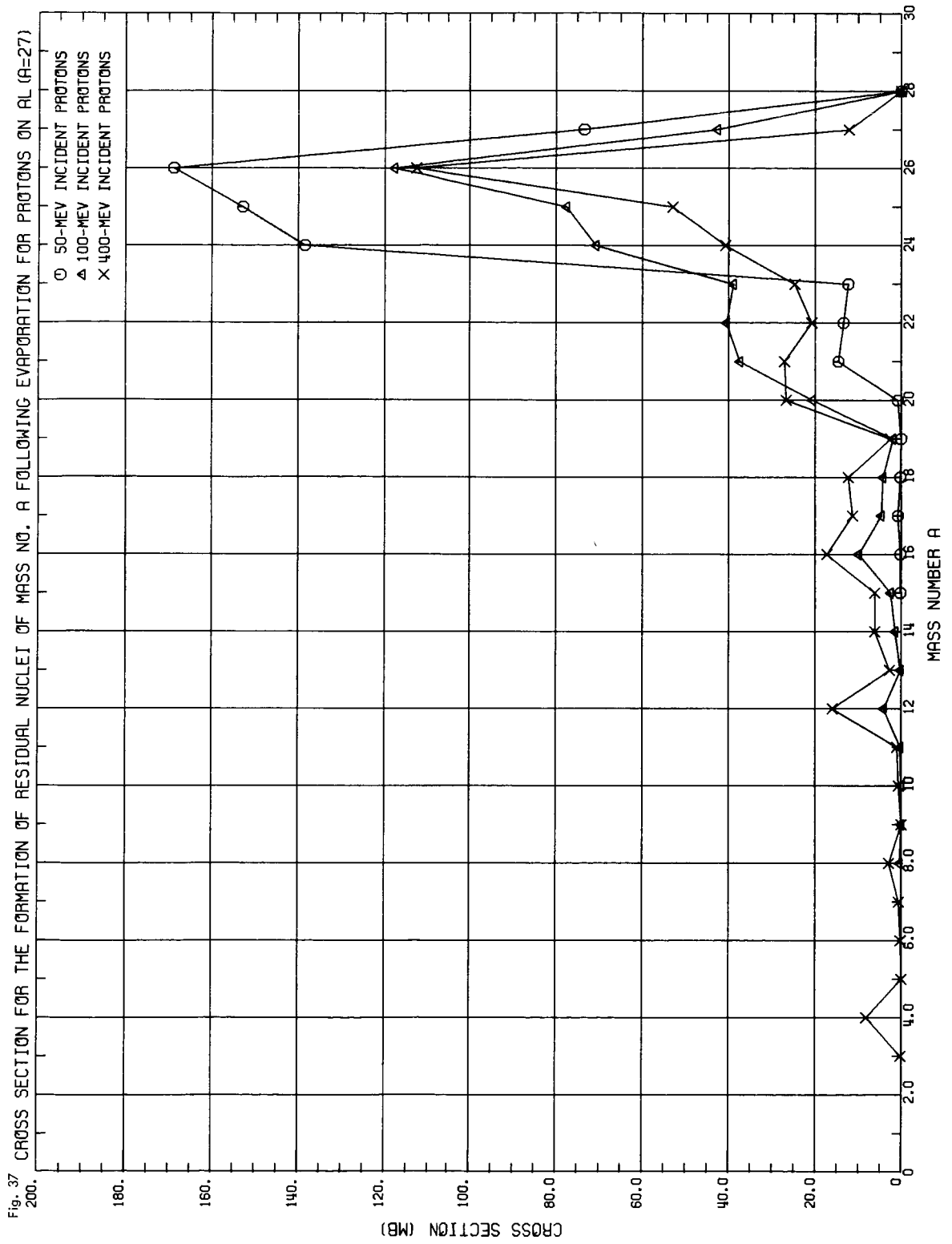
ORNL DWG 67-5565



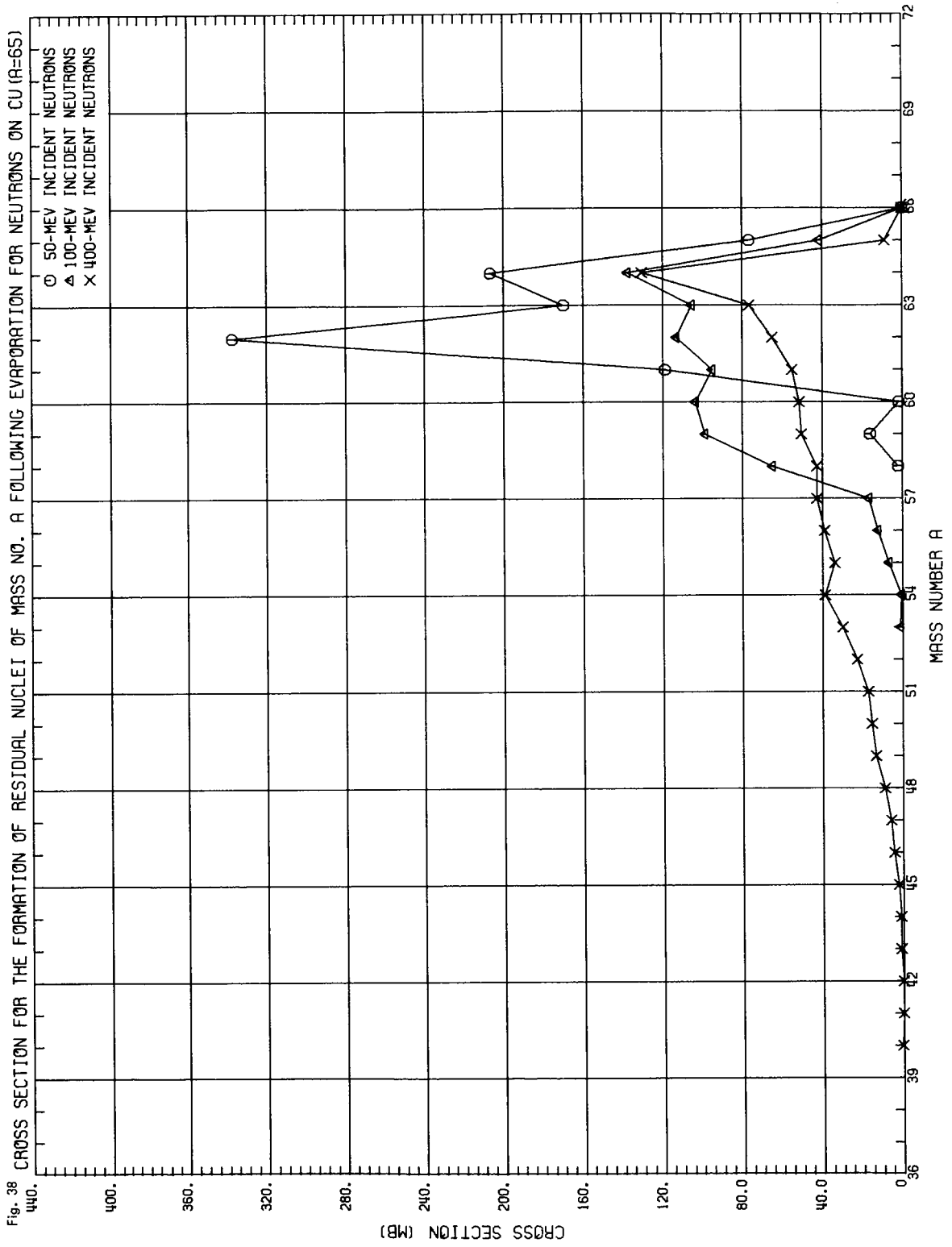
ORNL DWG 67-5566



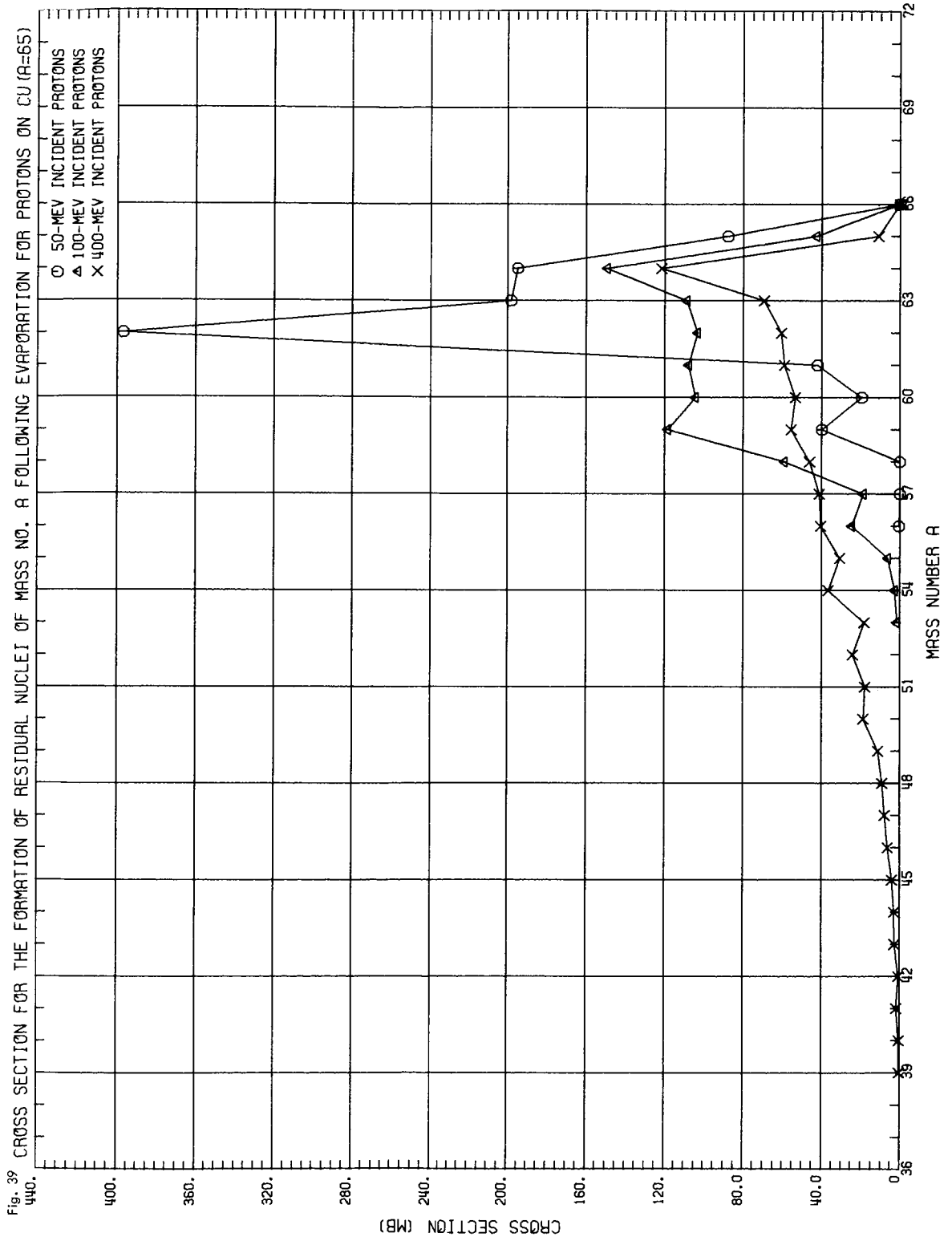
ORNL DWG 67-5567



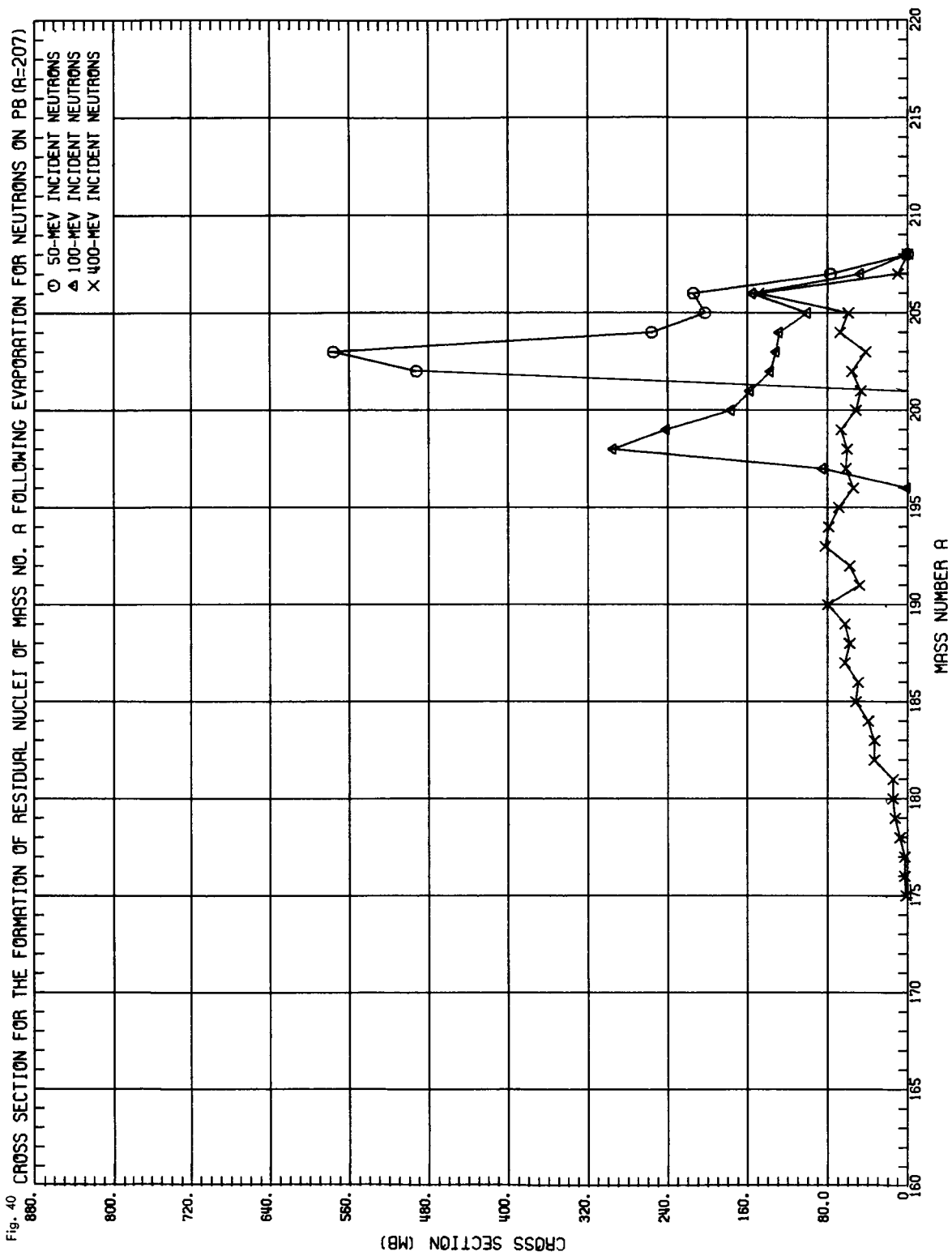
ORNL DWG 67-5568



ORNL DWG 67-5569

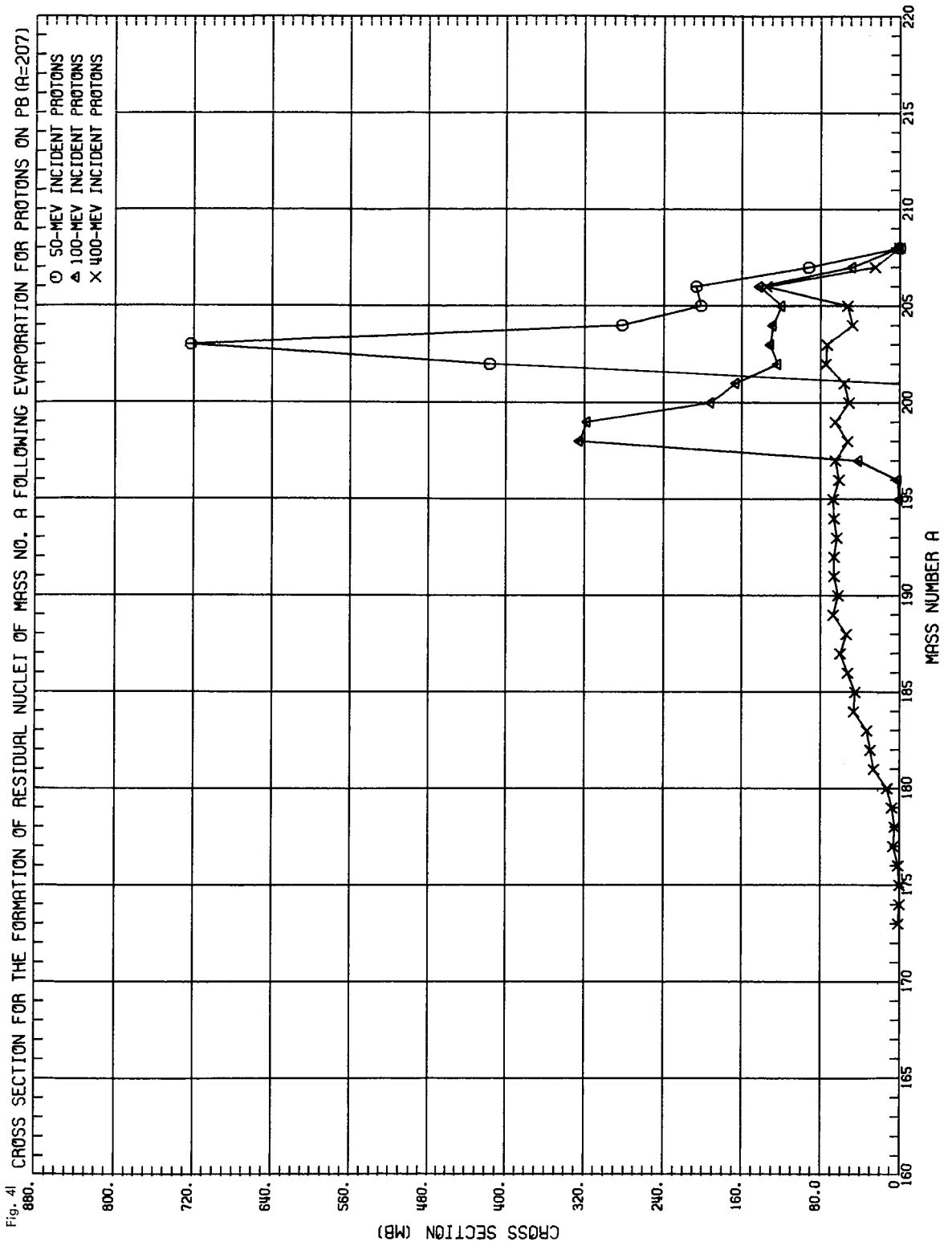


ORNL DWG 67-5570

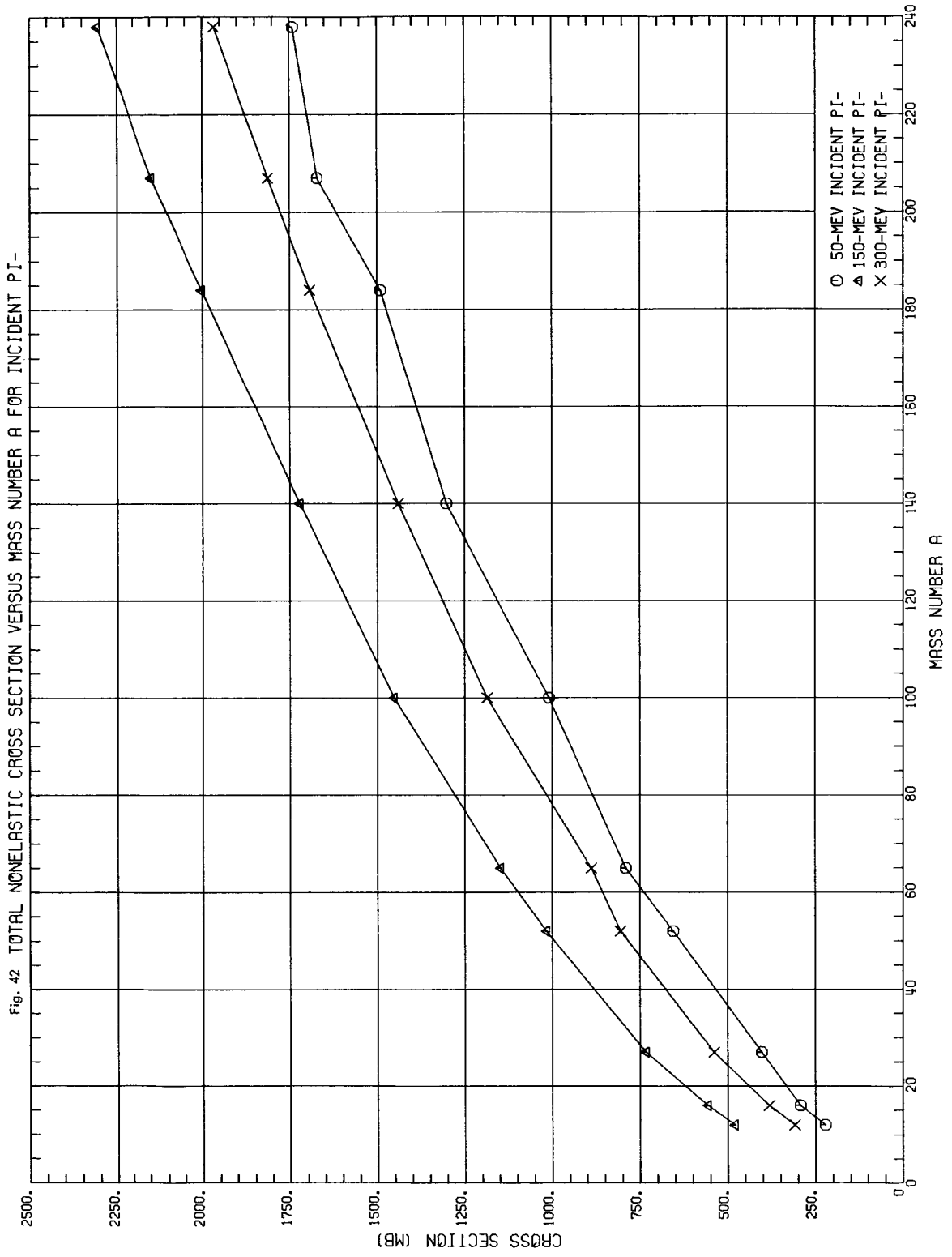




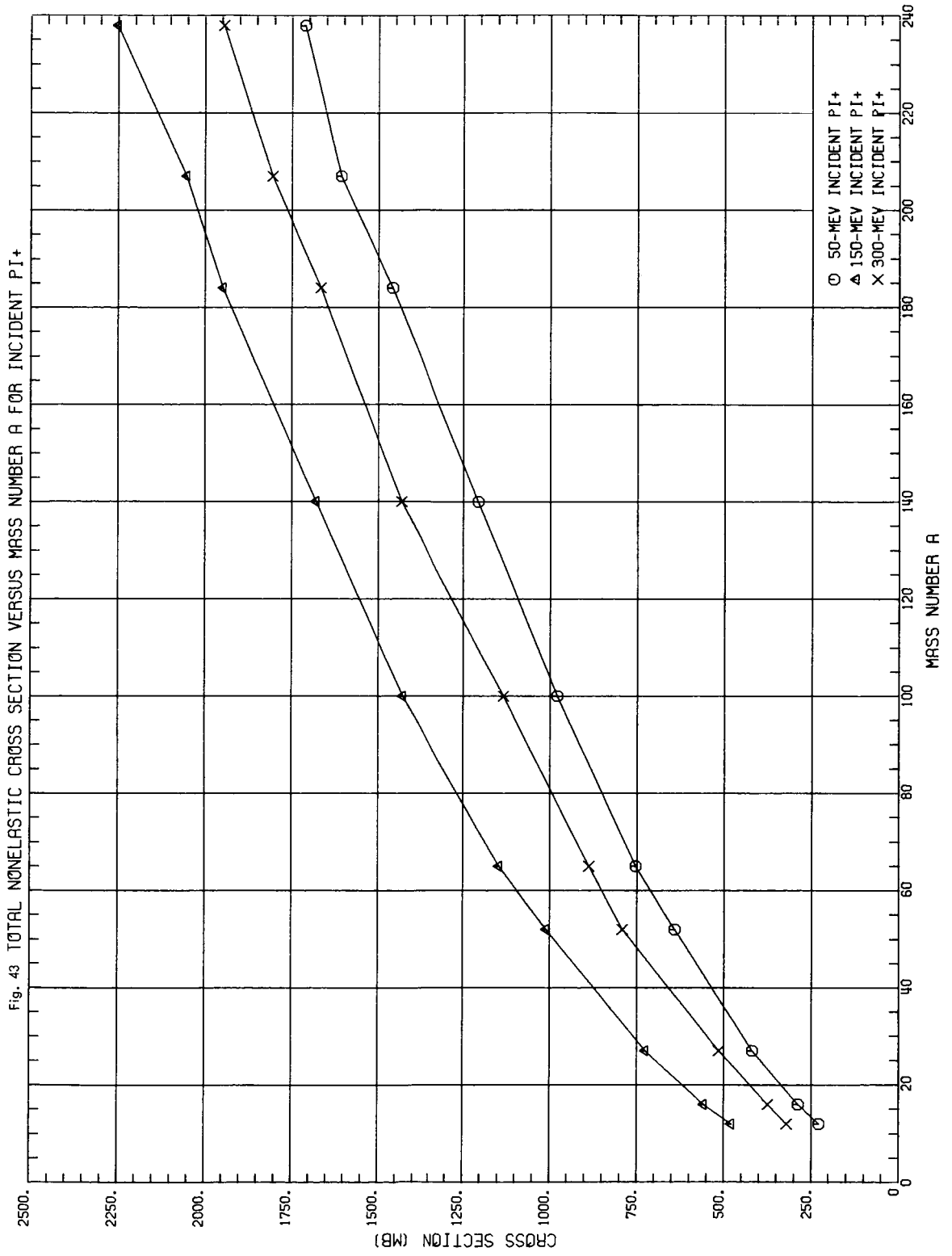
ORNL DWG 67-5571



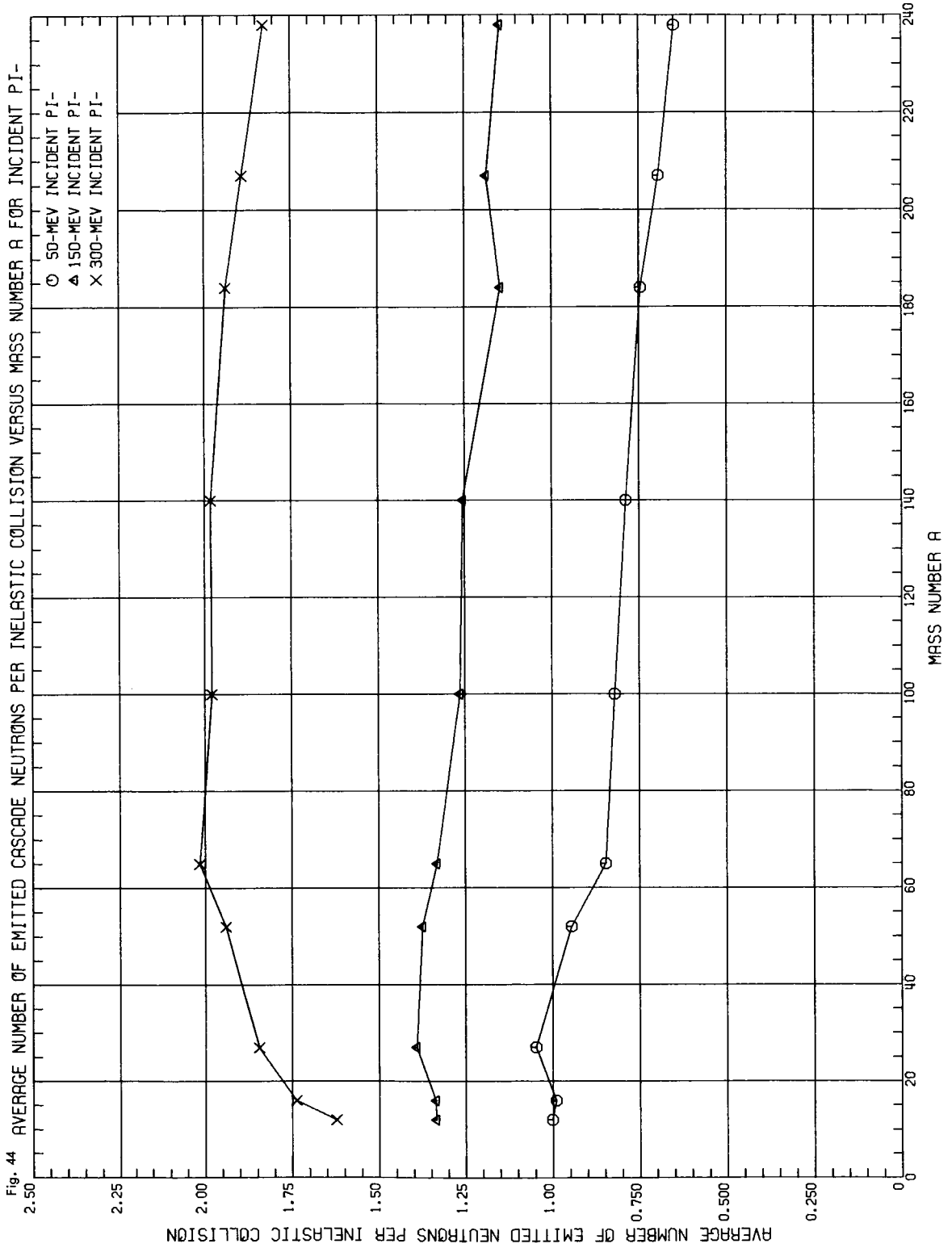
ORNL DWG 67-5572



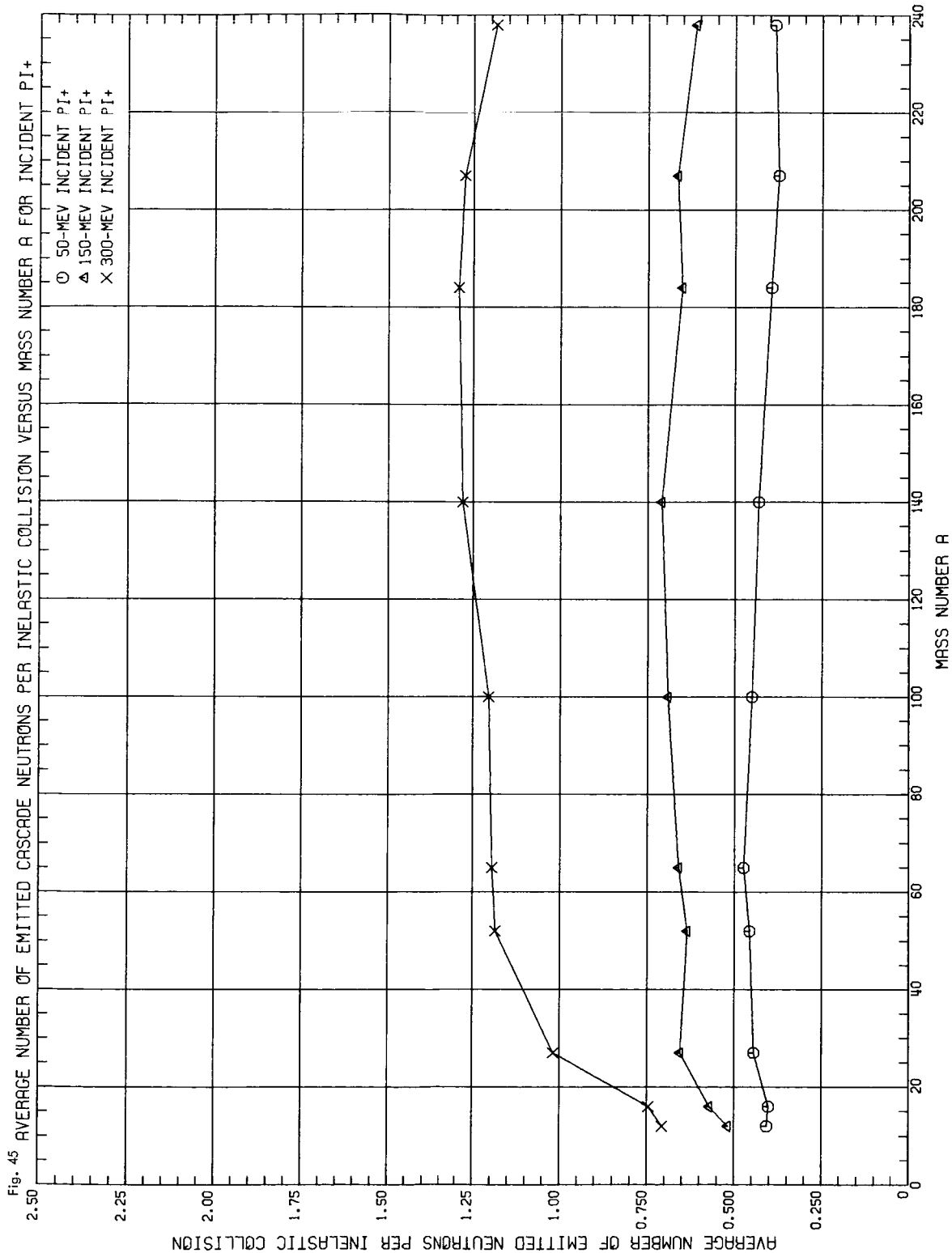
ORNL DWG 67-5573



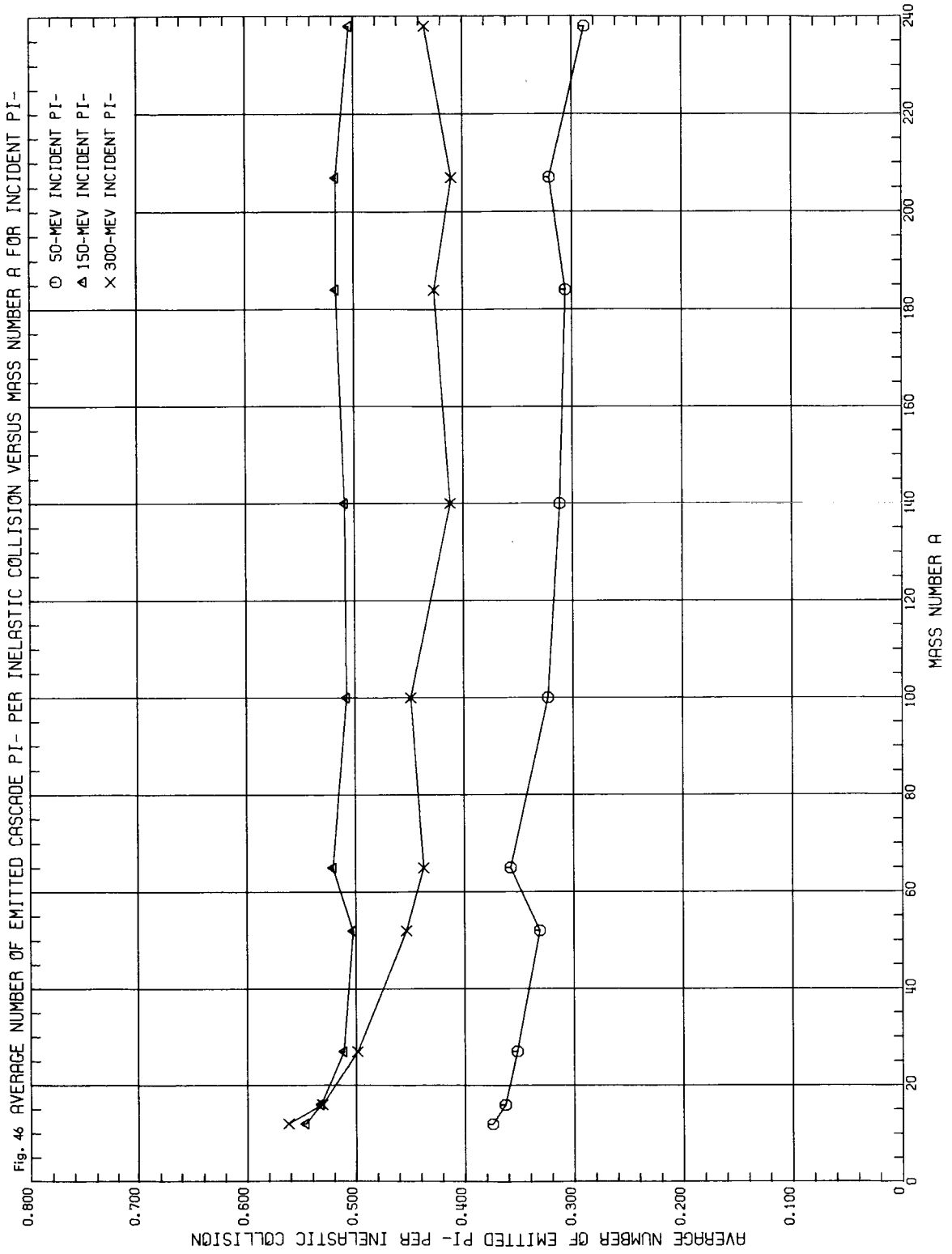
ORNL DWG 67-5574



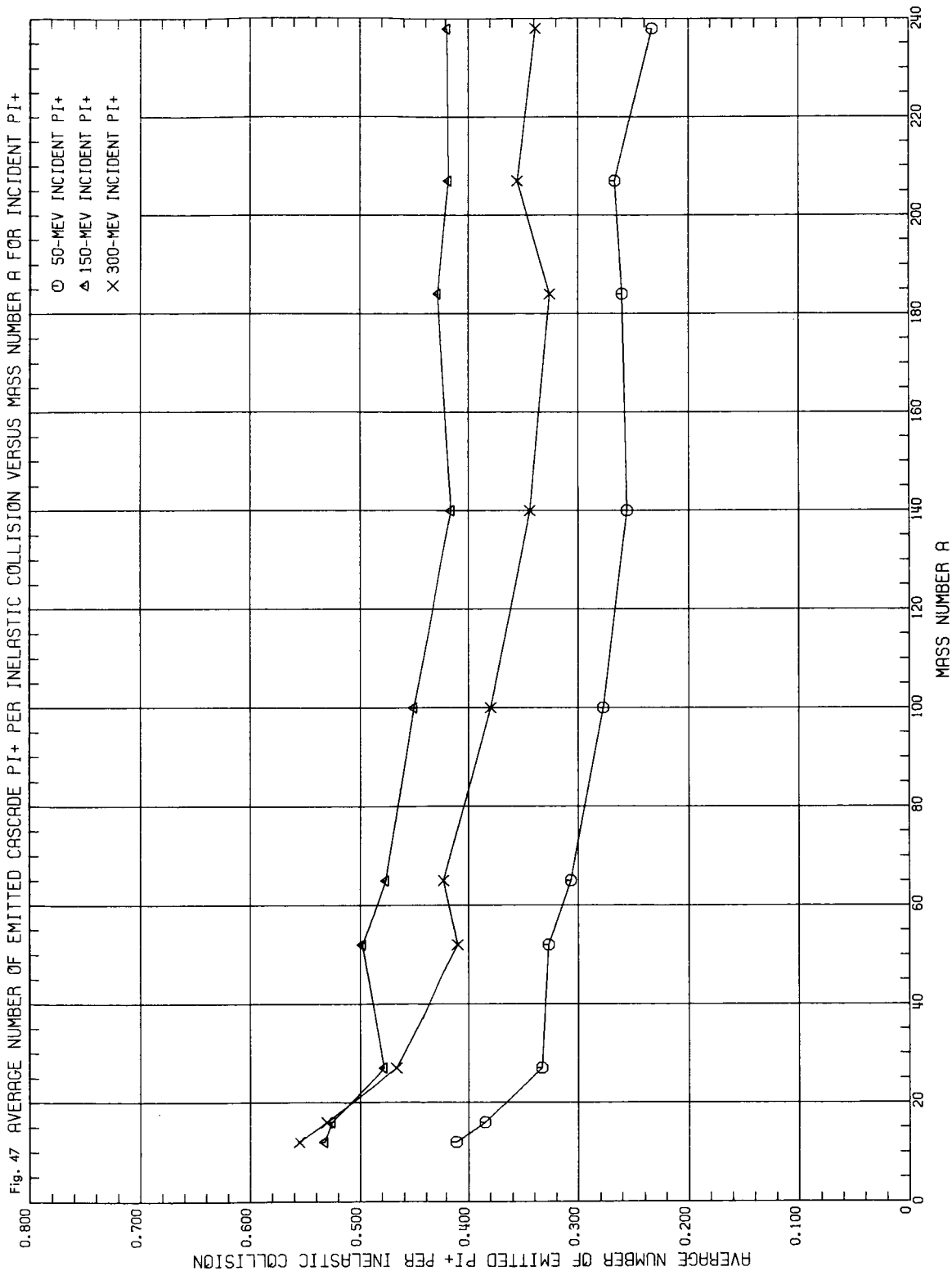
ORNL DWG 67-5575



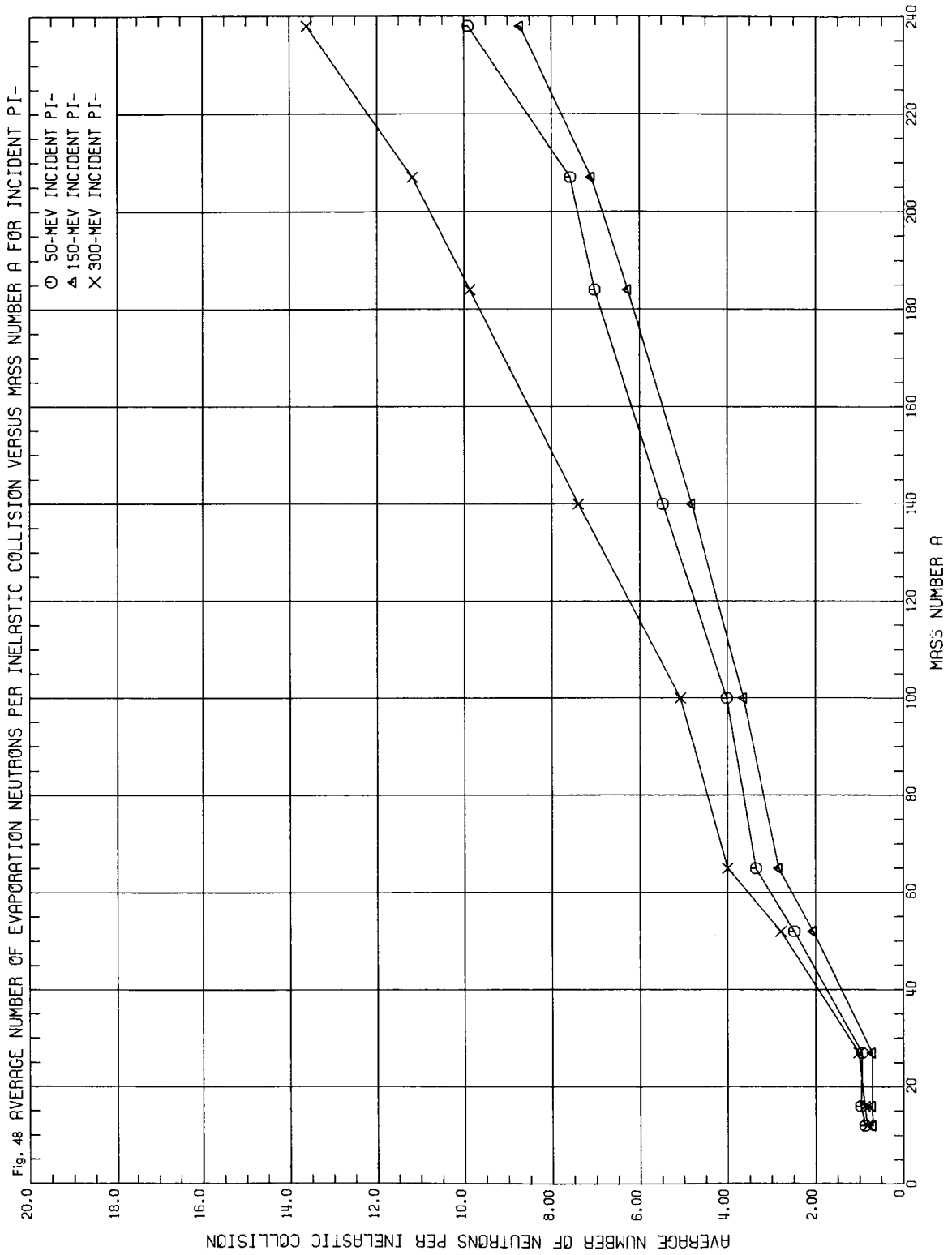
ORNL DWG 67-5576



ORNL DWG 67-5577

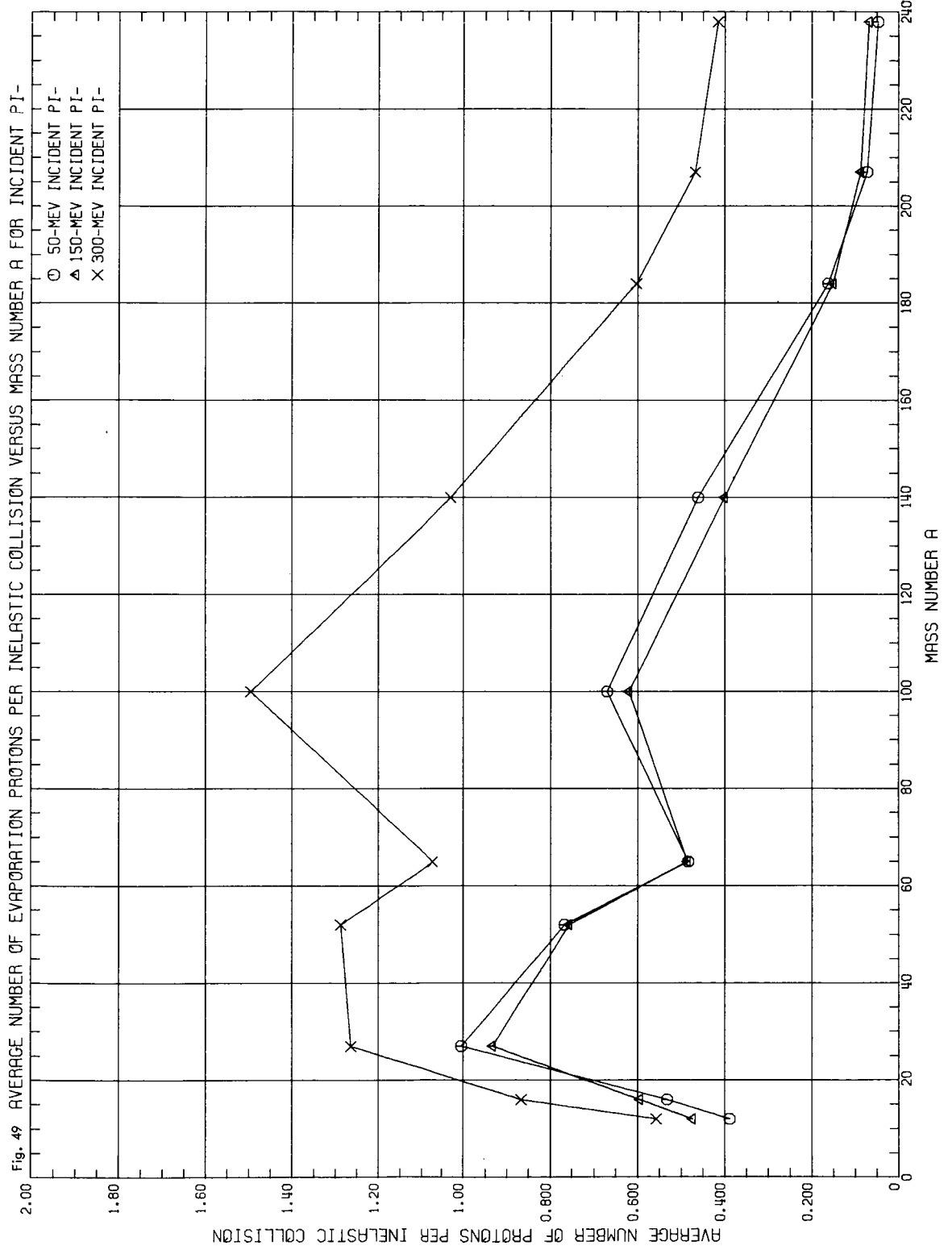


ORNL DWG 67-5578

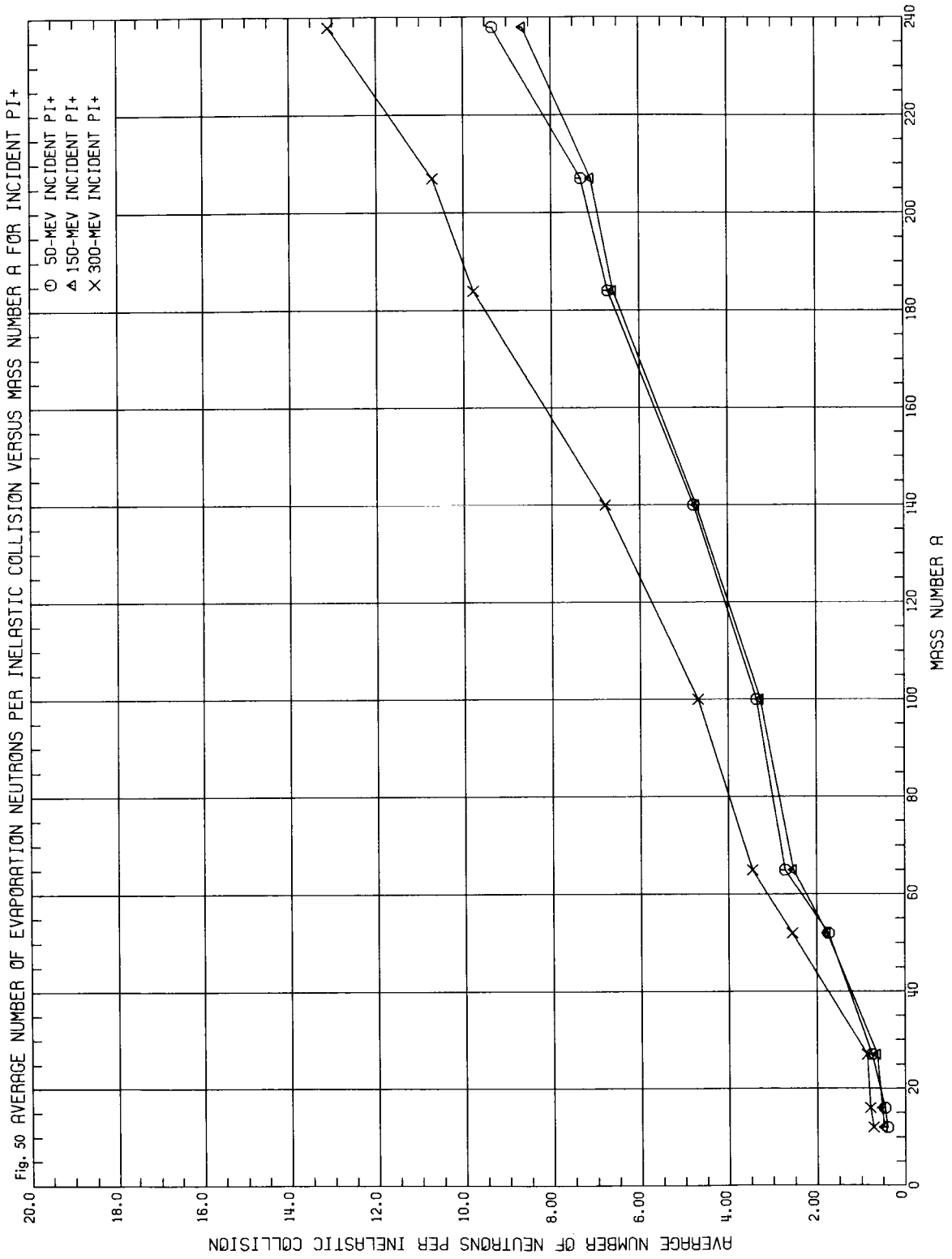




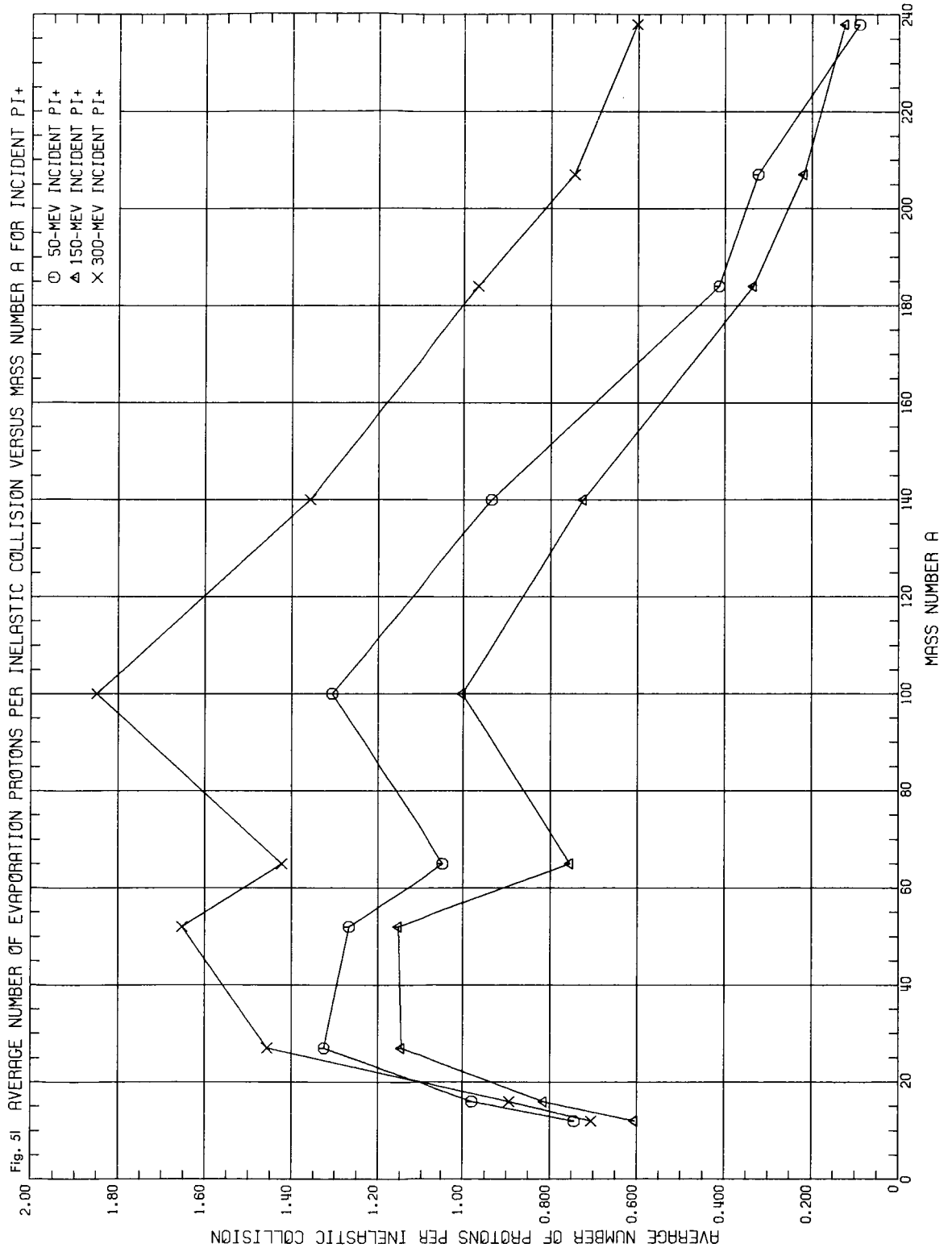
ORNL DWG 67-5579



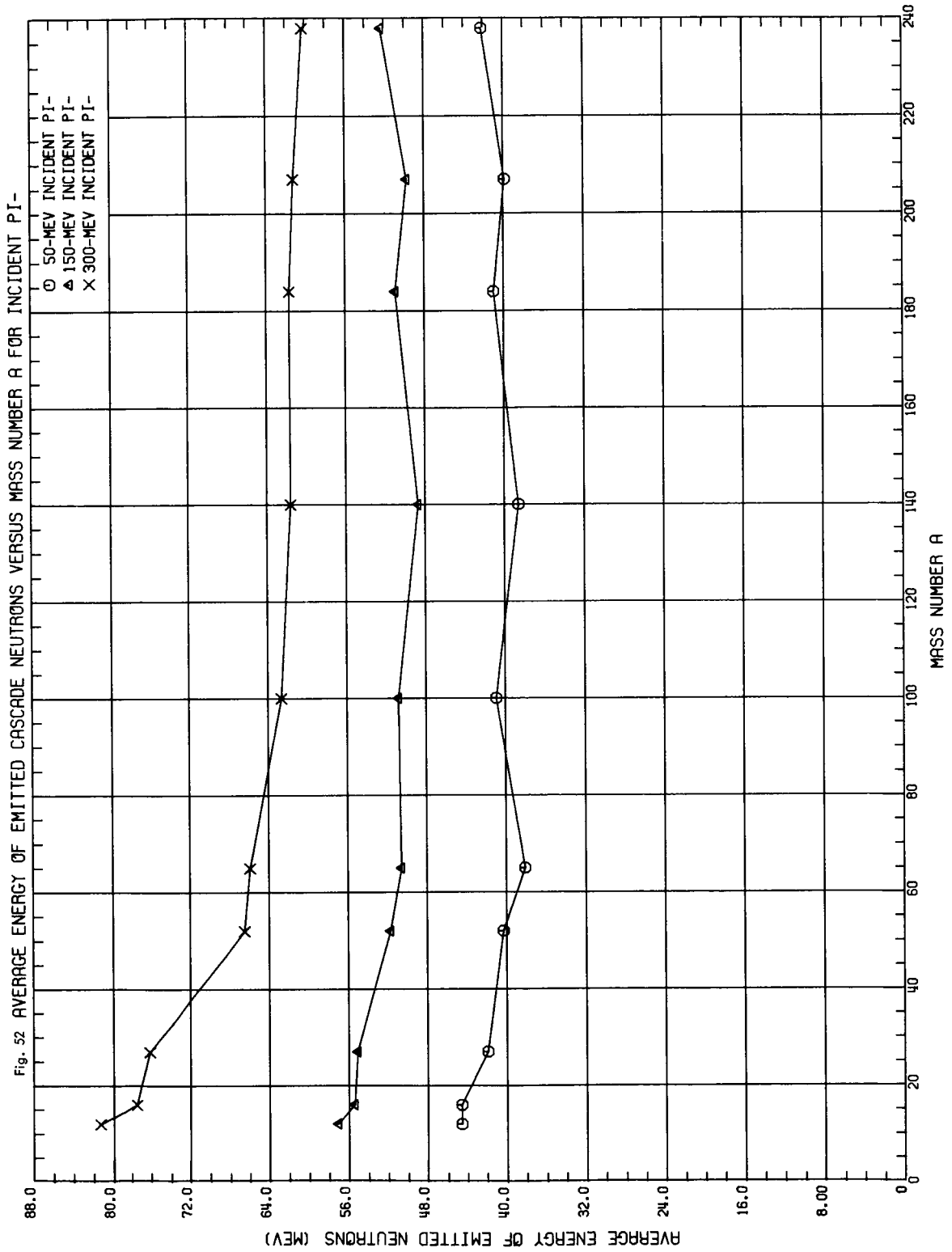
ORNL DWG 67-5580



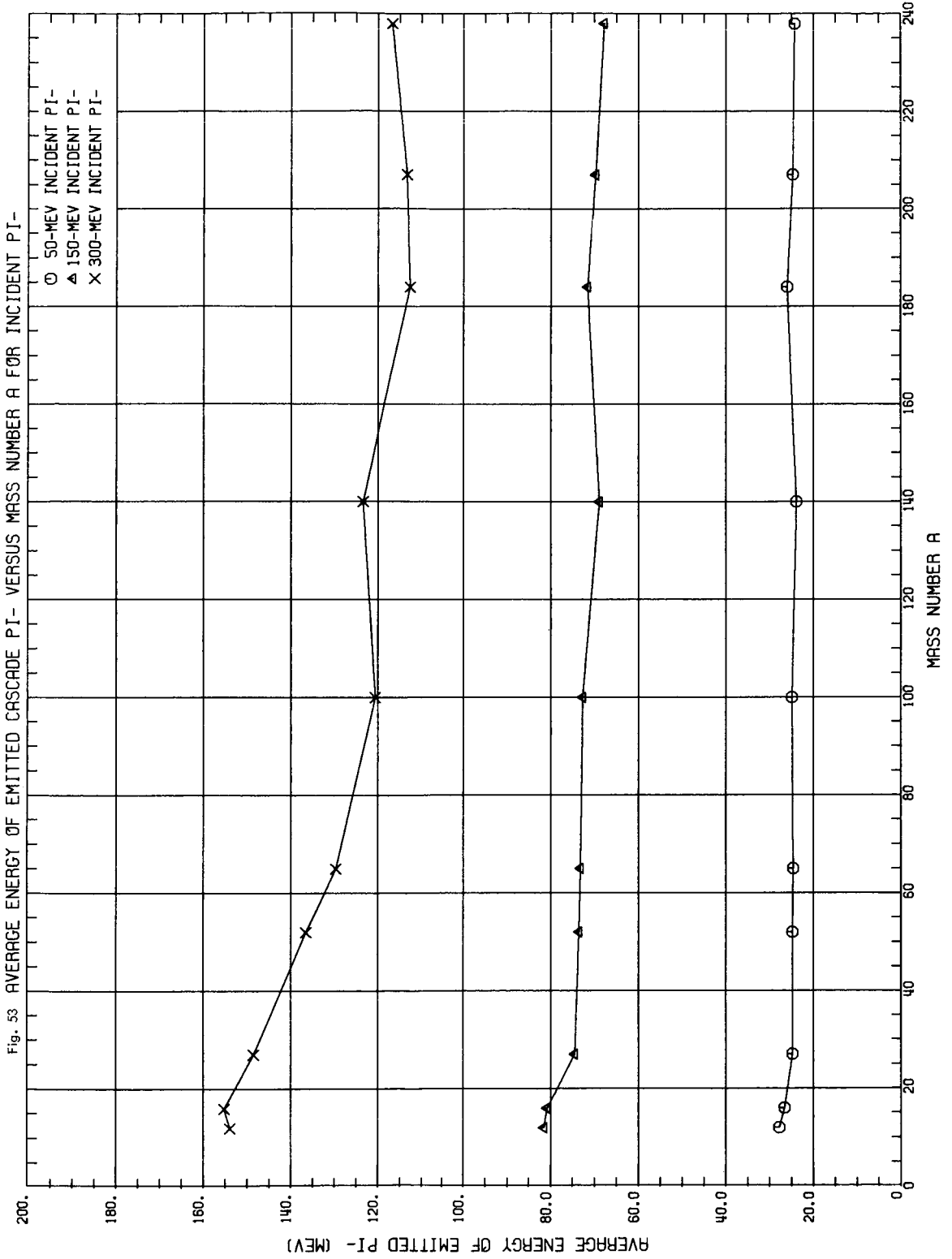
ORNL DWG 67-5581



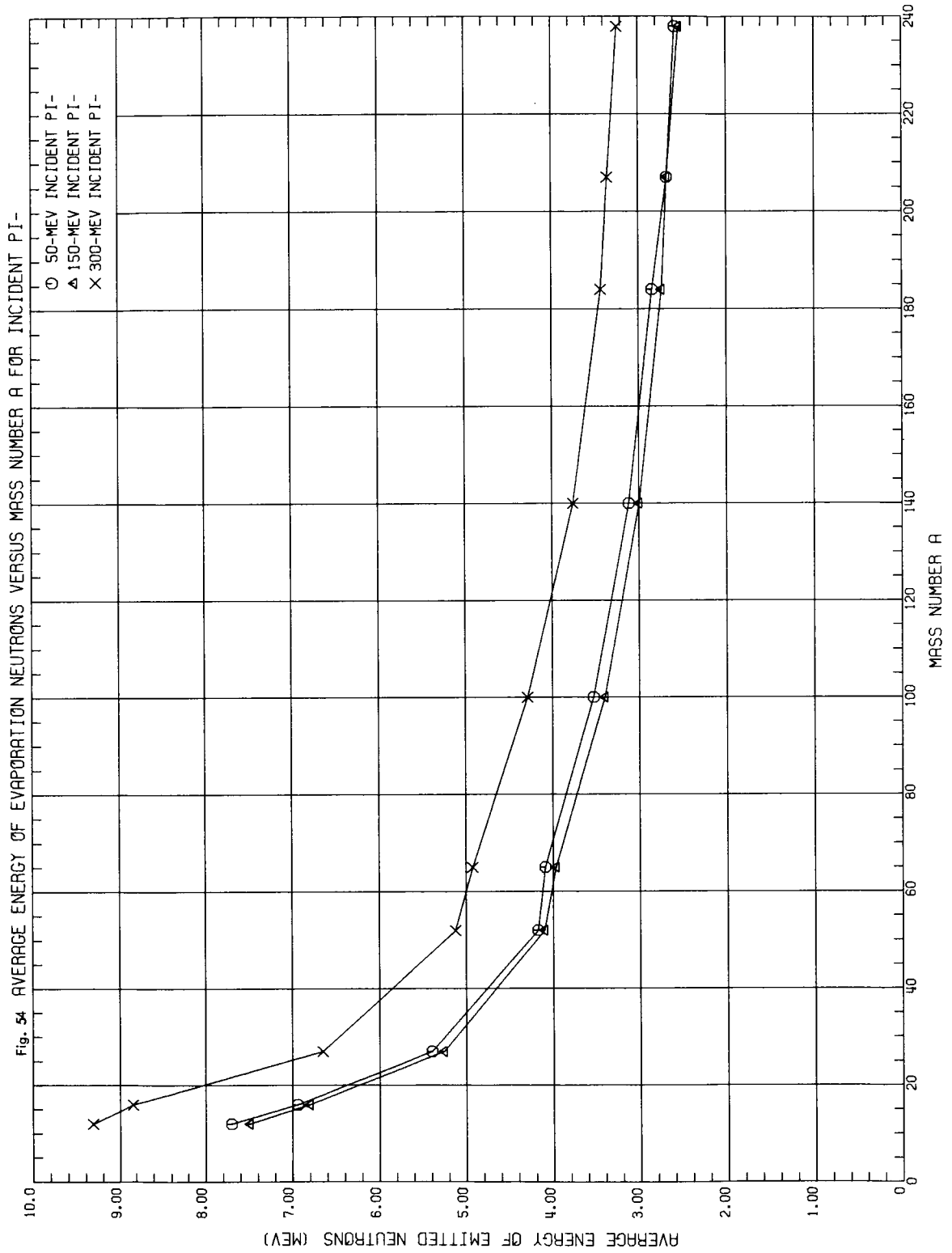
ORNL DWG 67-5582



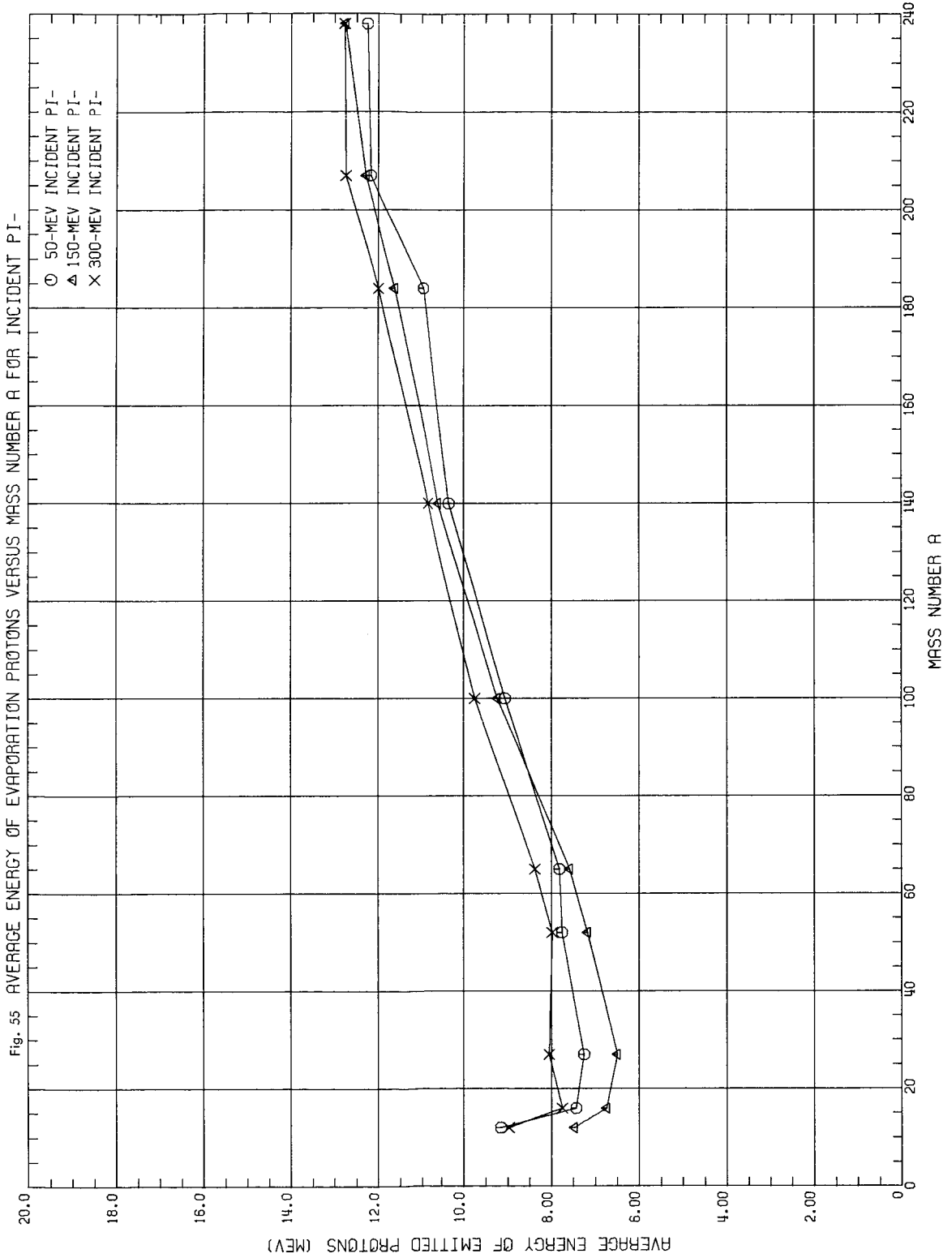
ORNL DWG 67-5583



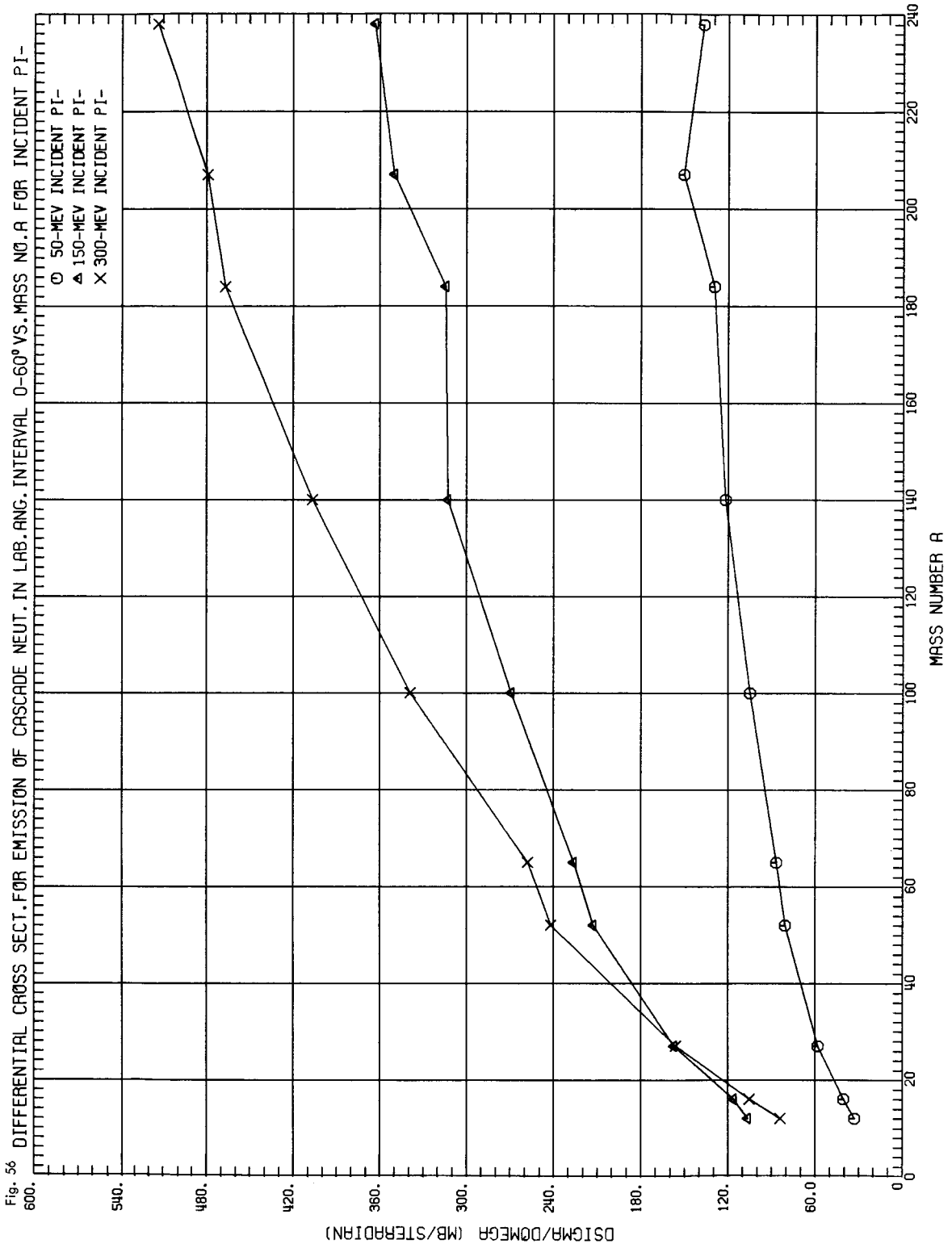
ORNL DWG 67-5584



ORNL DWG 67-5585

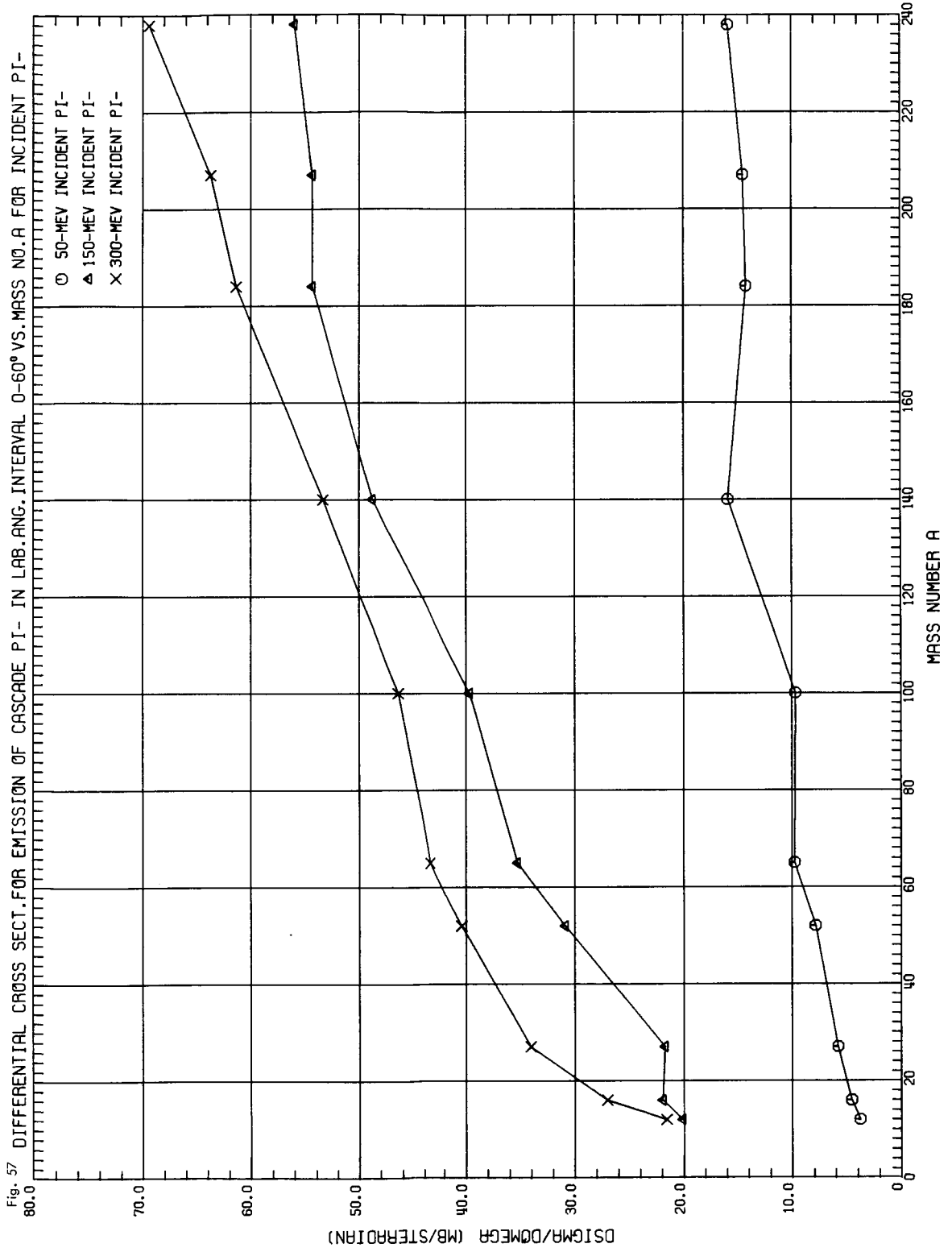


ORNL DWG 67-5586

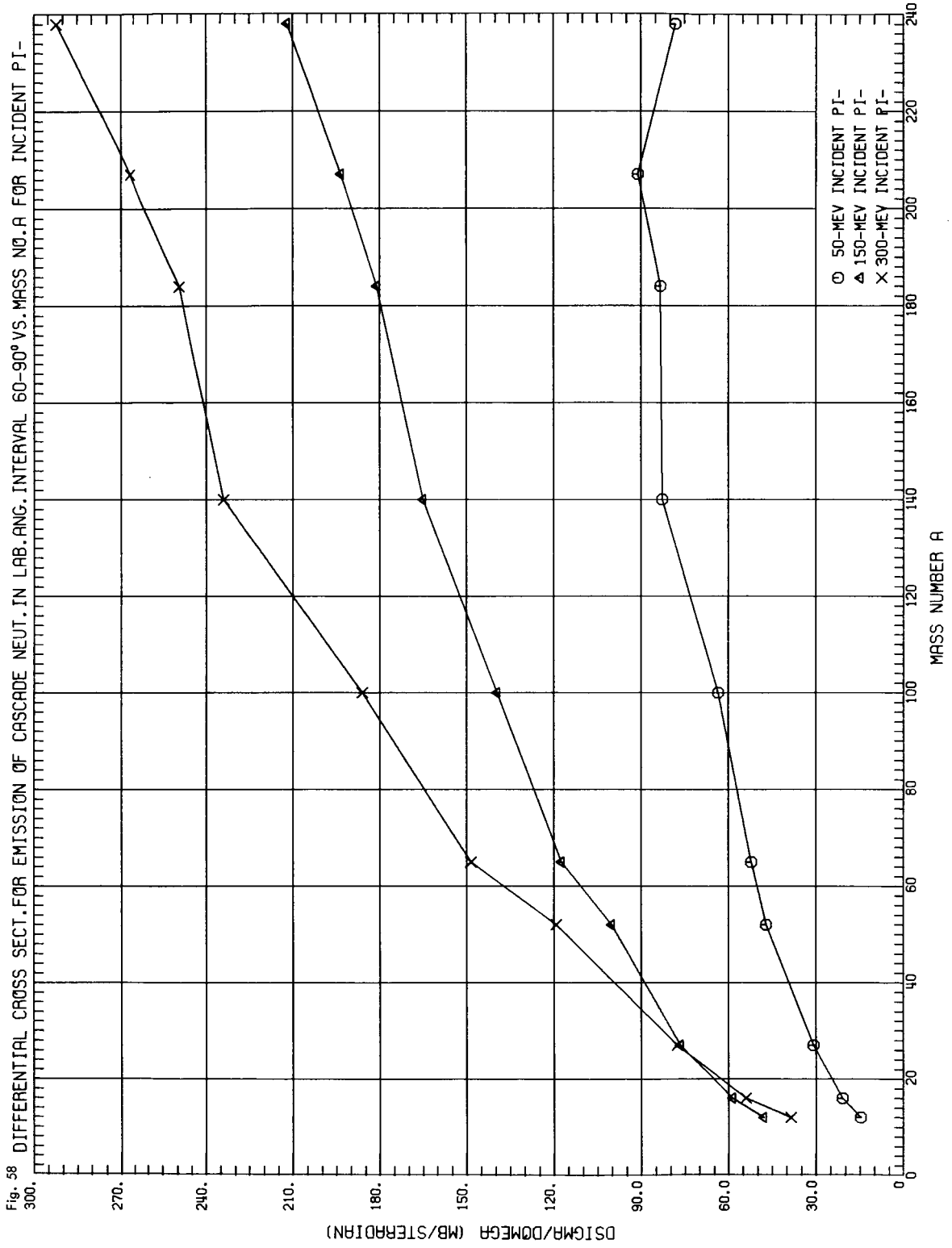




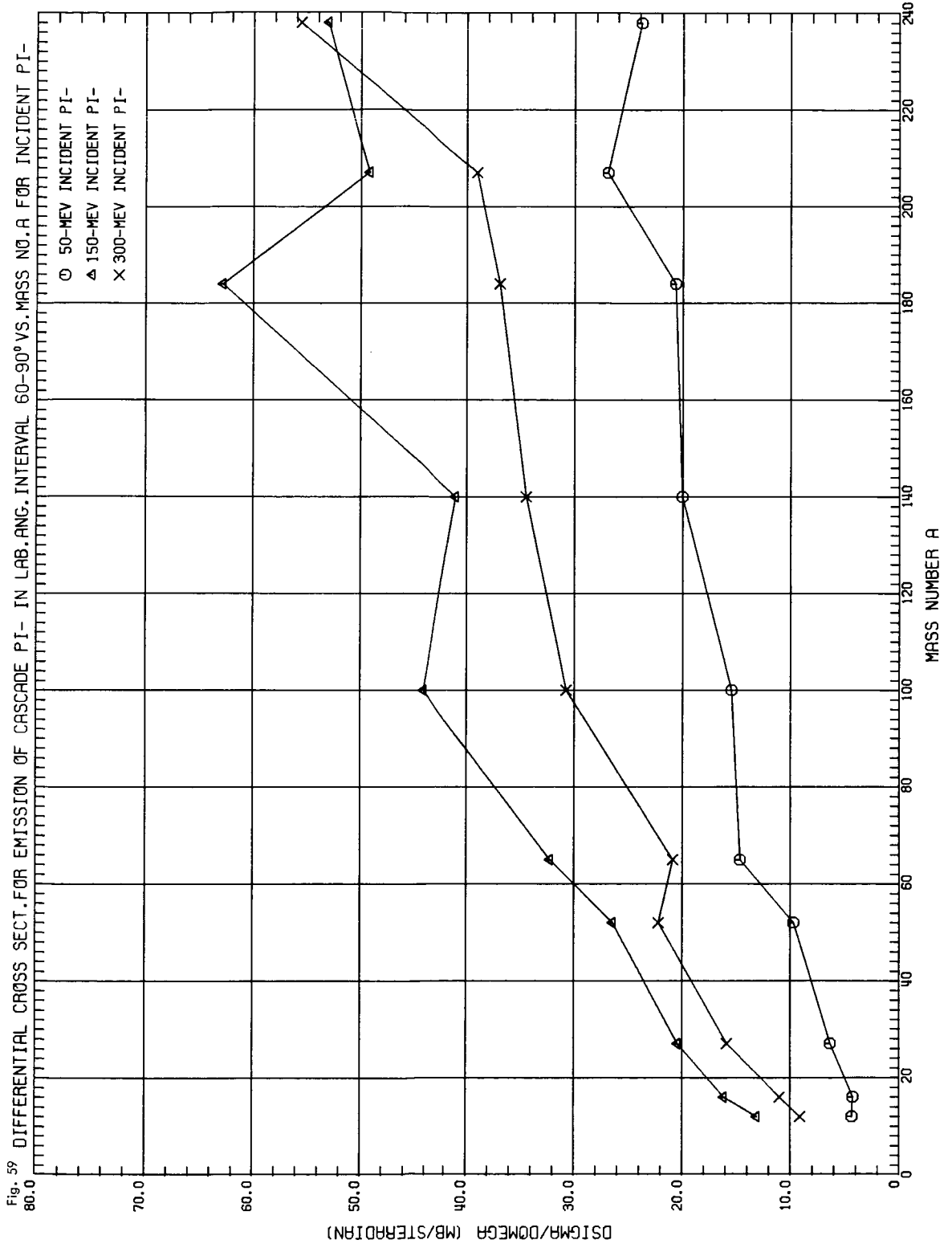
ORNL DWG 67-5587



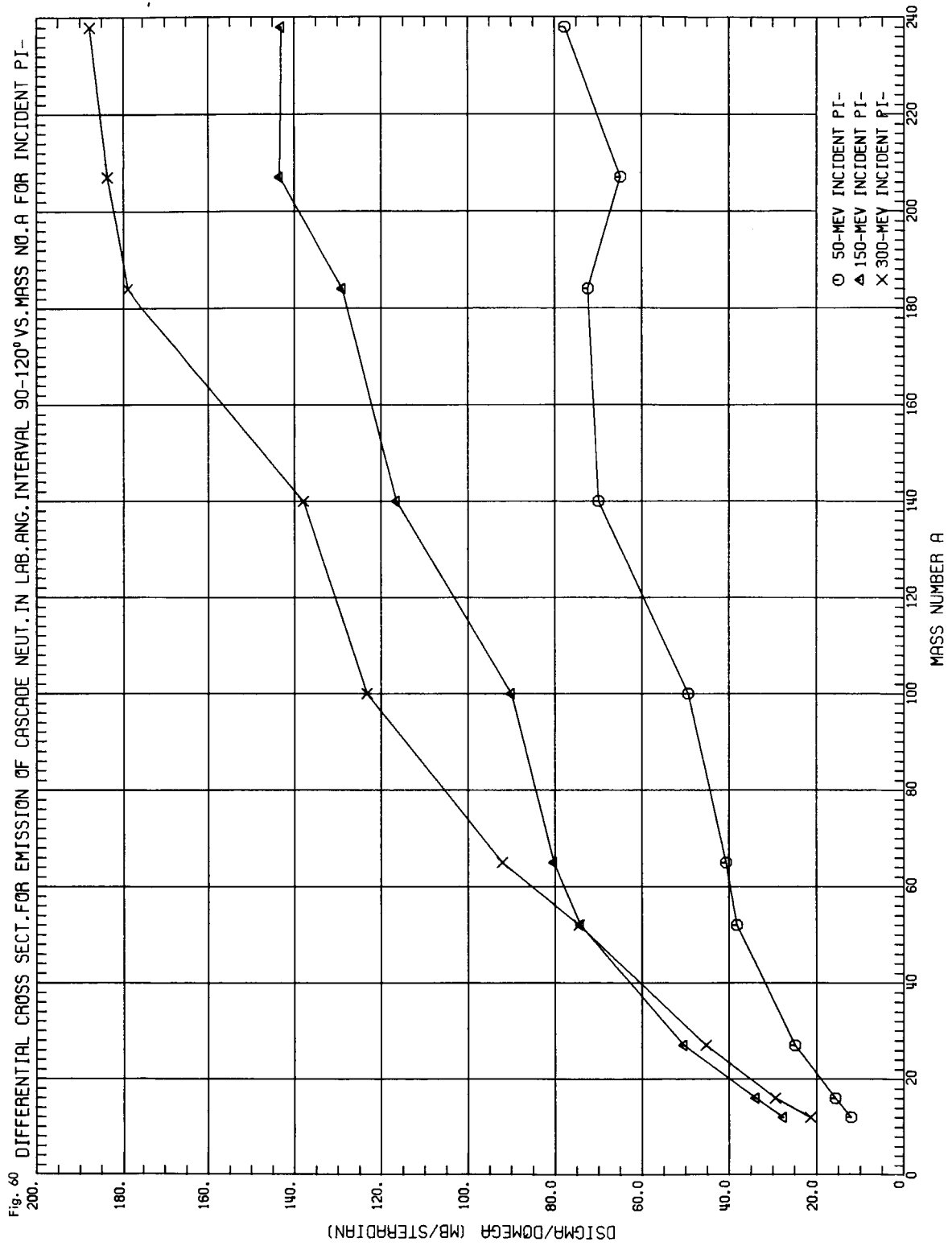
ORNL DWG 67-5588



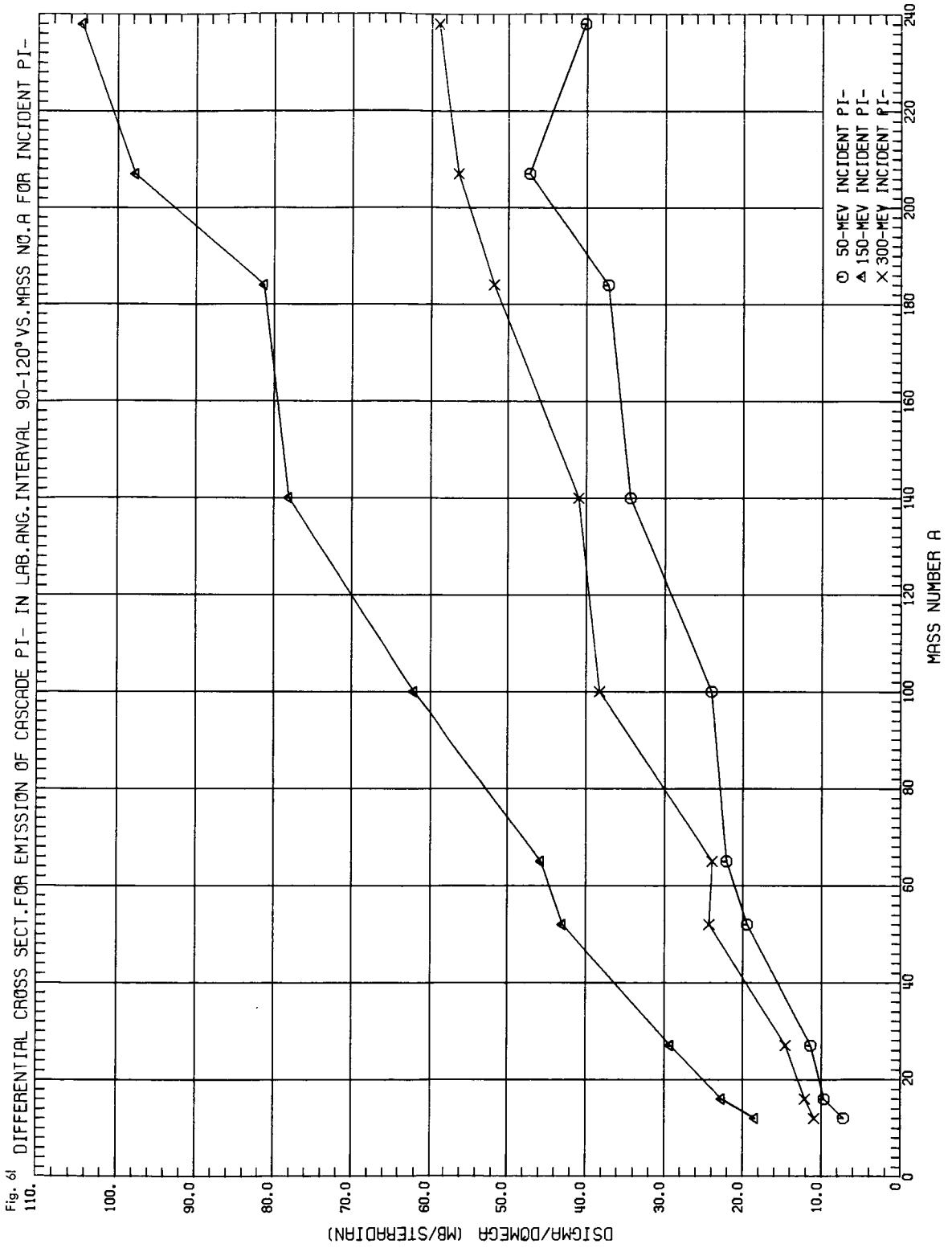
ORNL DWG 67-5589



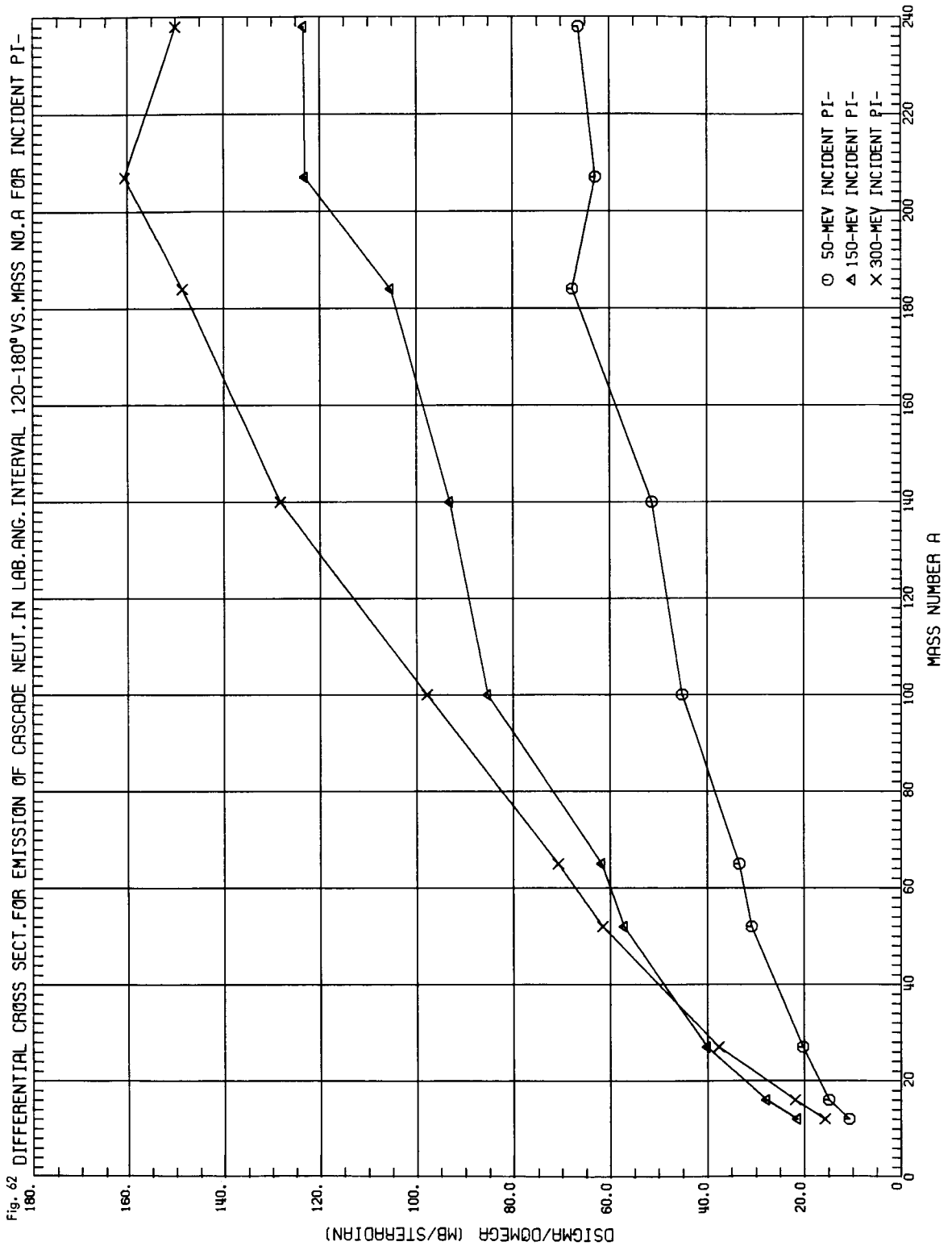
ORNL DWG 67-5590



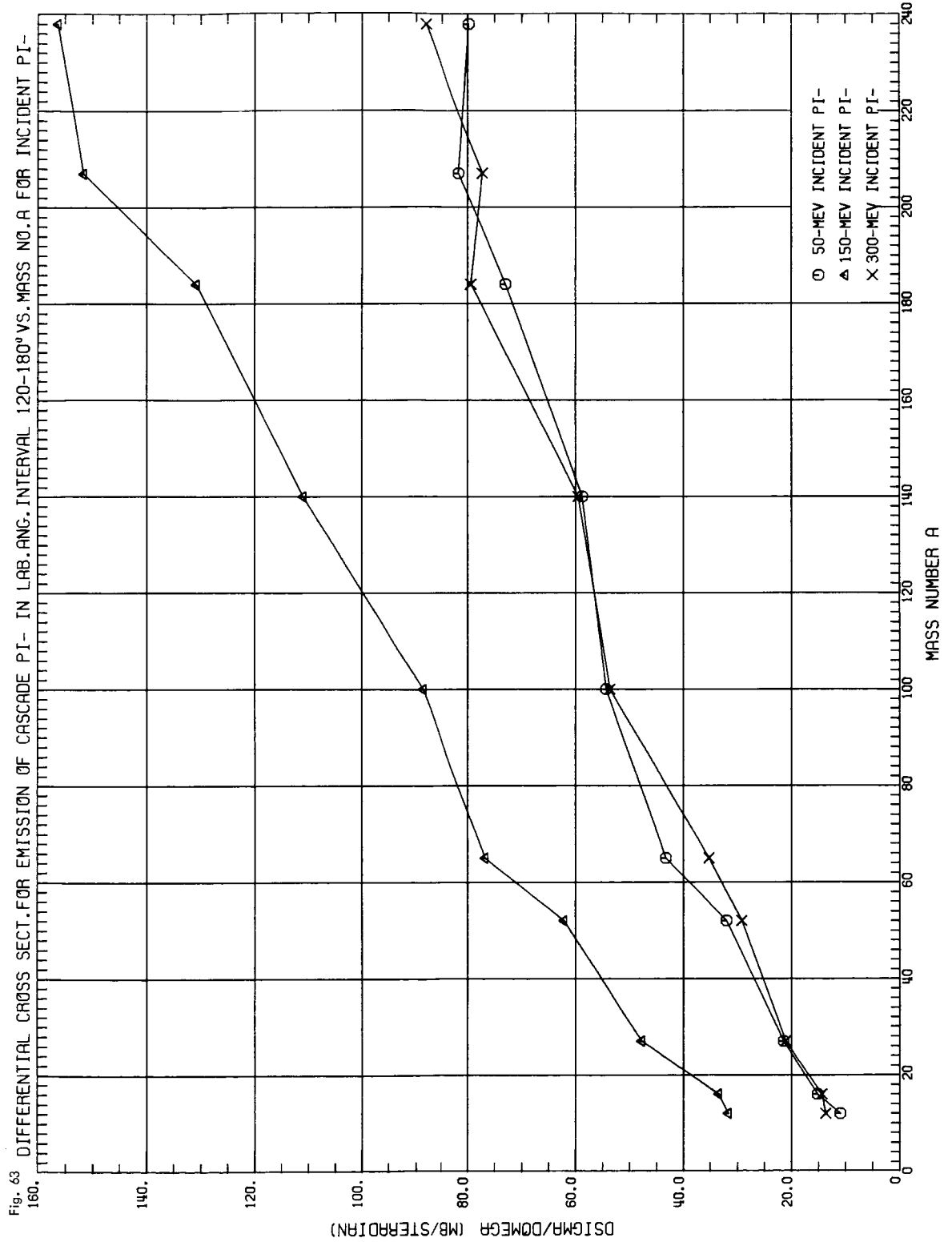
ORNL DWG 67-5591



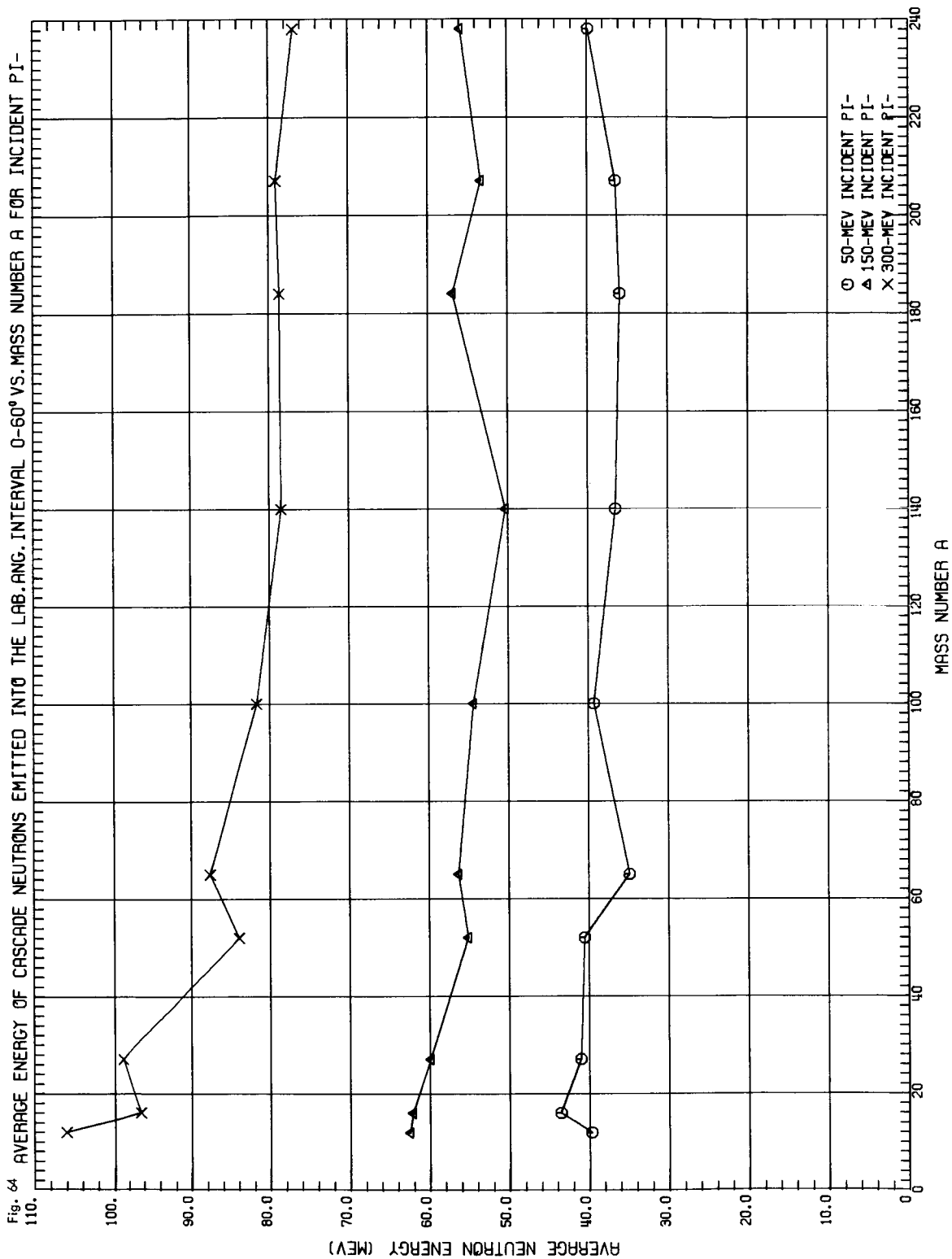
ORNL DWG 67-5592



ORNL DWG 67-5593

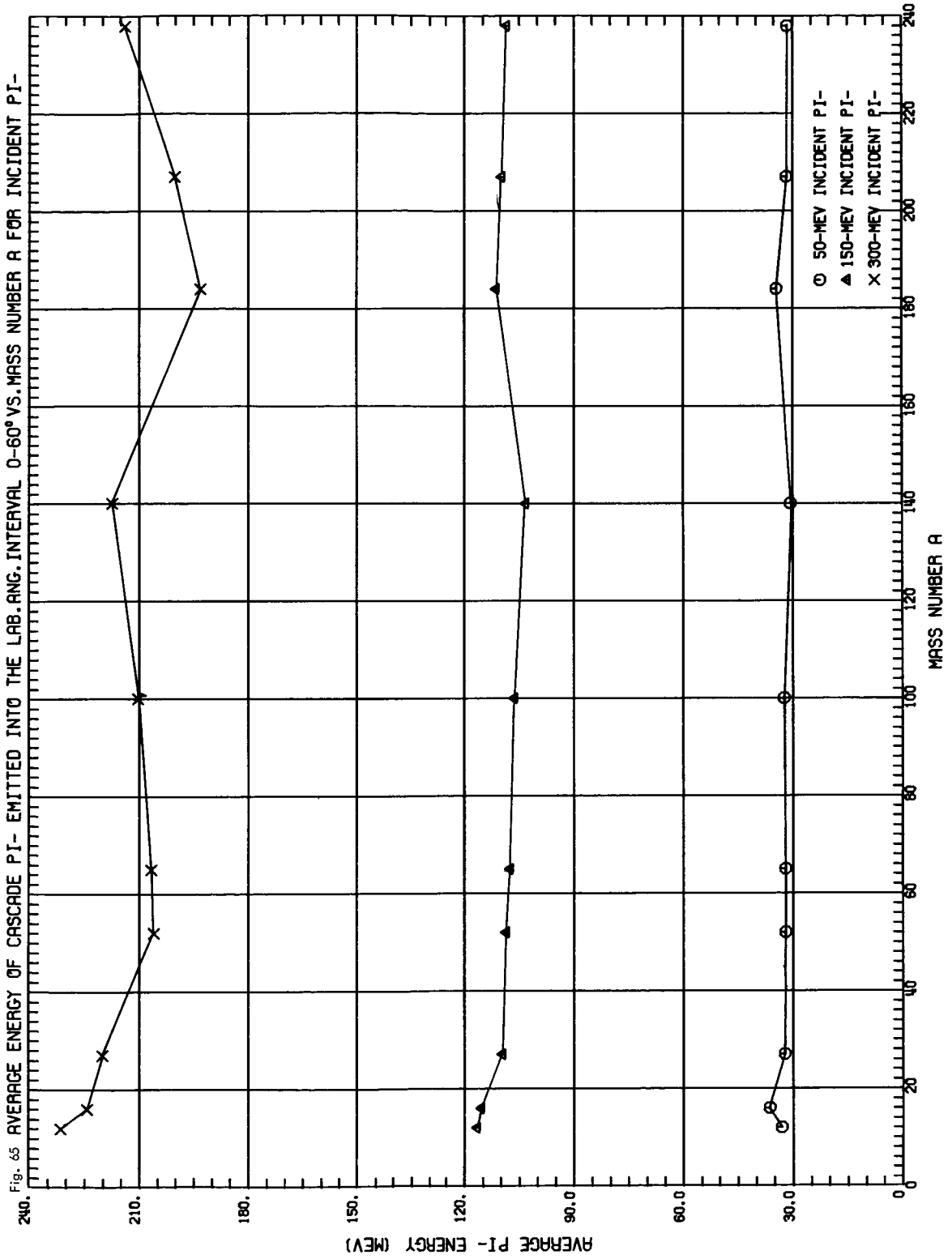


ORNL DWG 67-5594

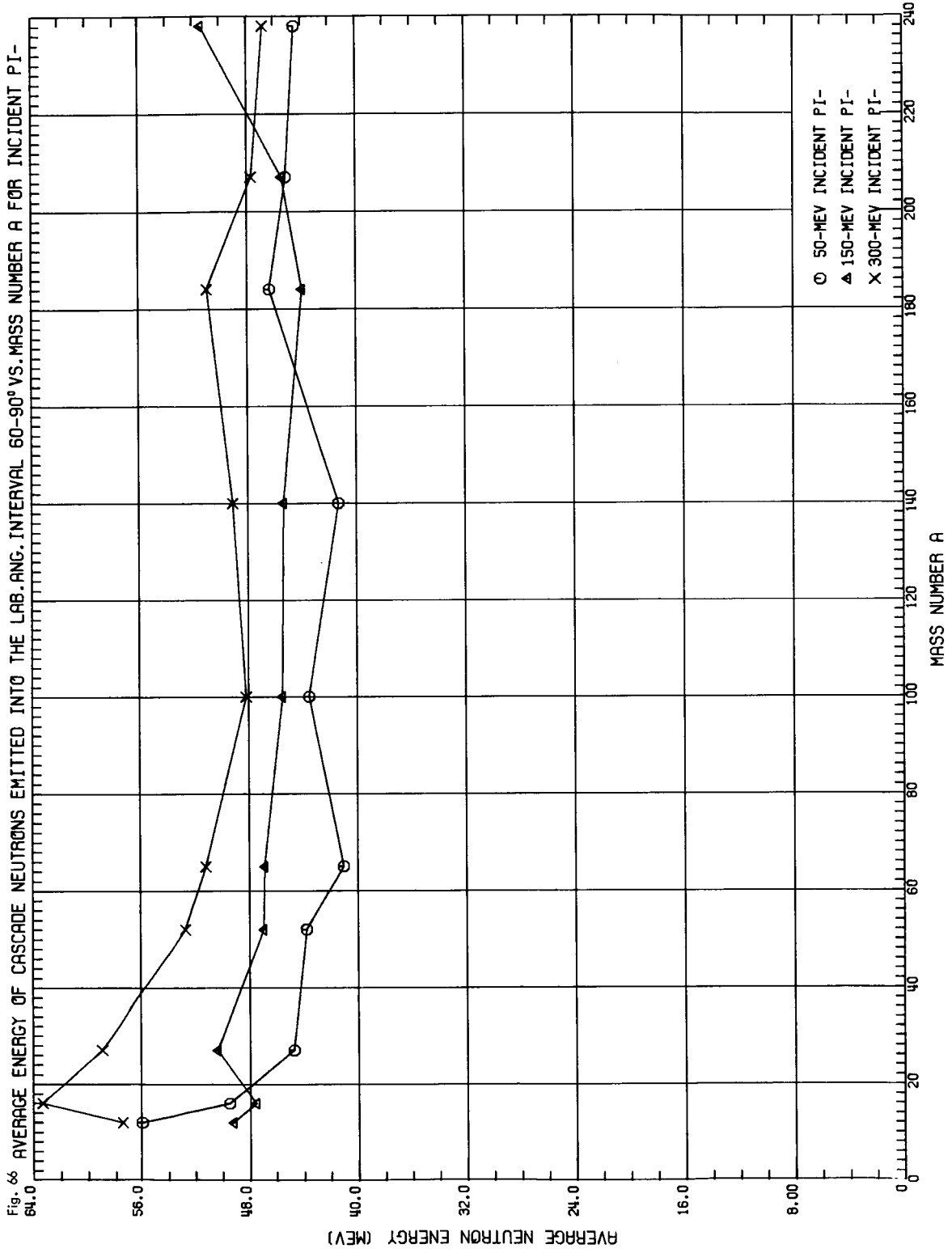




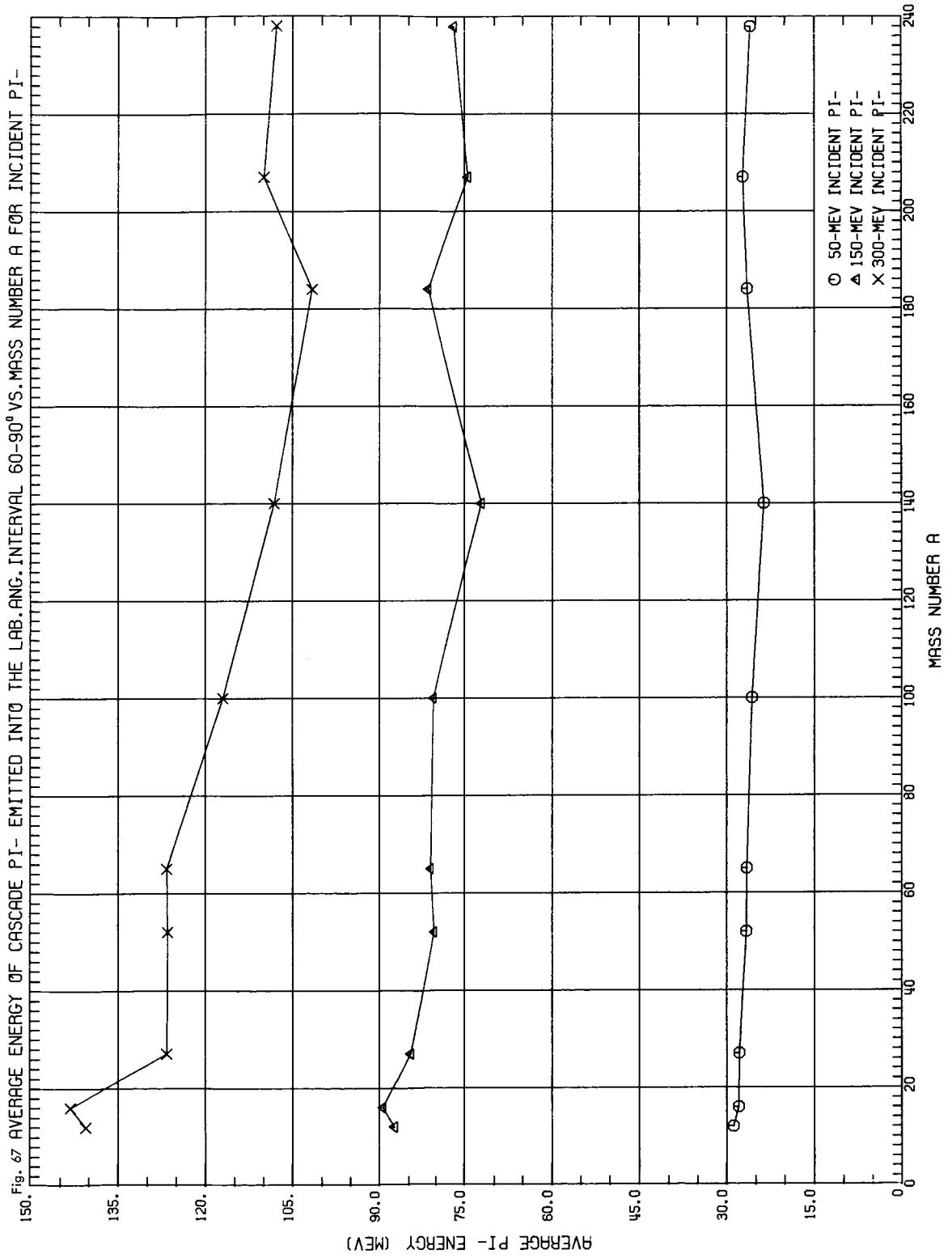
ORNL DWG 67-5595



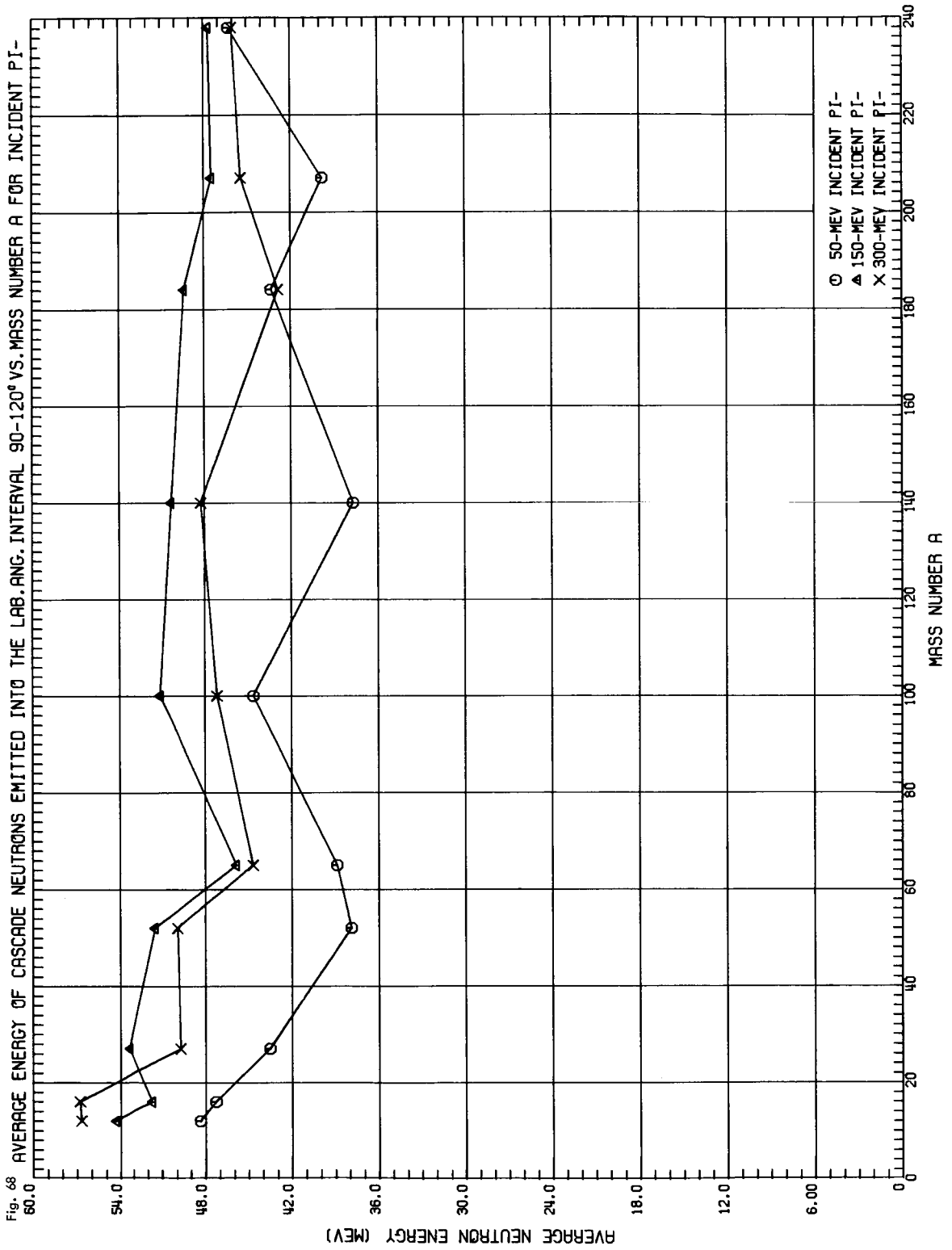
ORNL DWG 67-5596



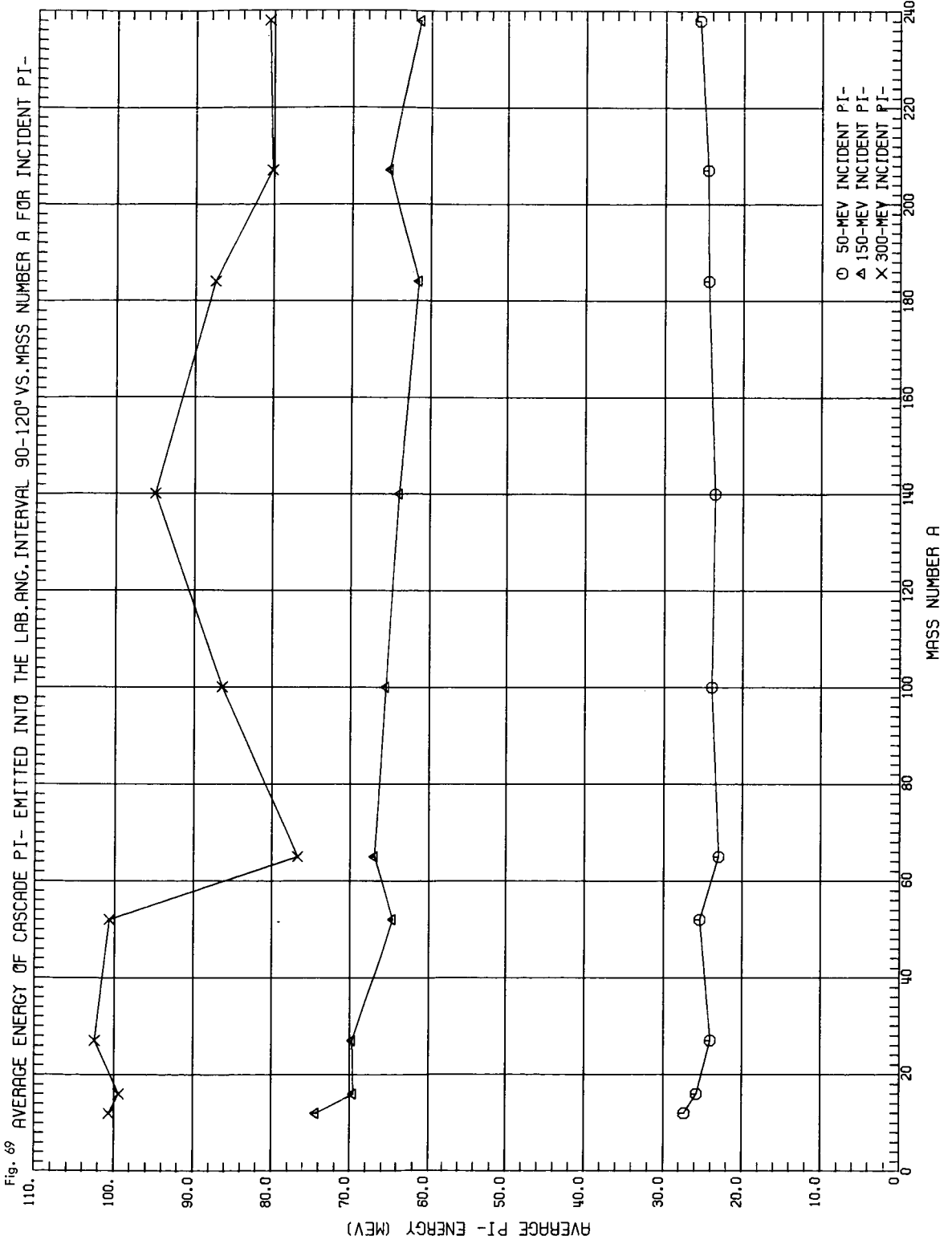
ORNL DWG 67-5597



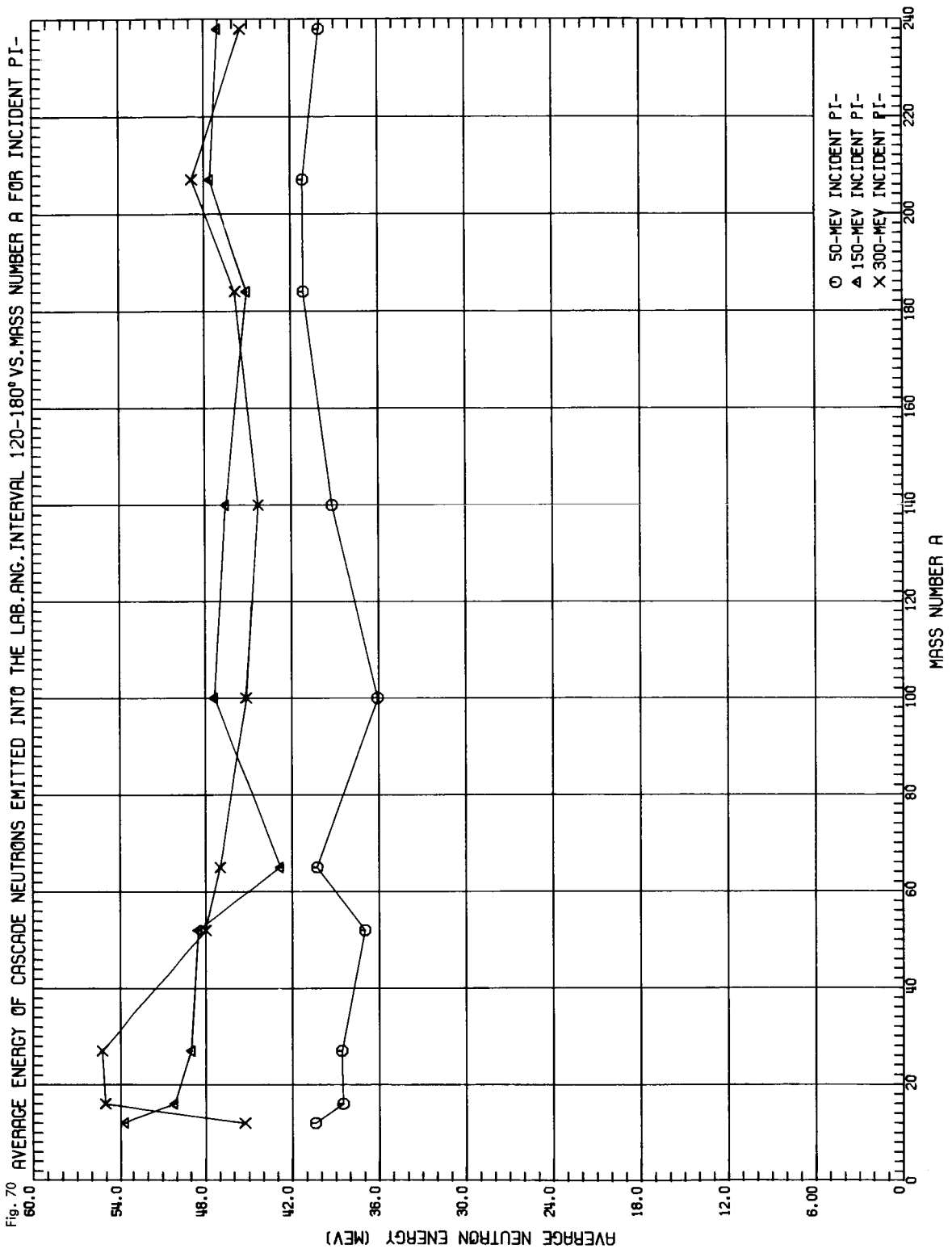
ORNL DWG 67-5598



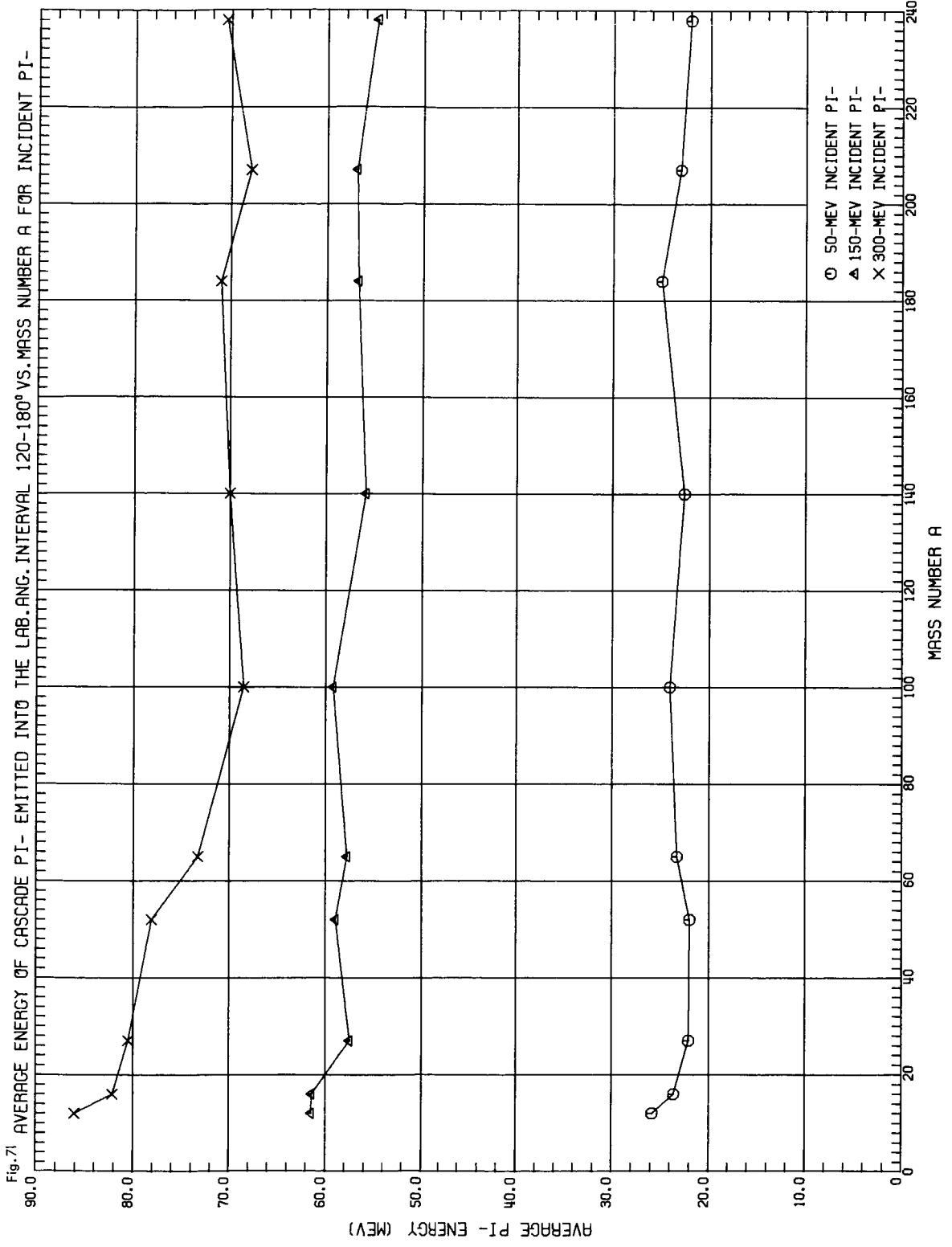
ORNL DWG 67-5599



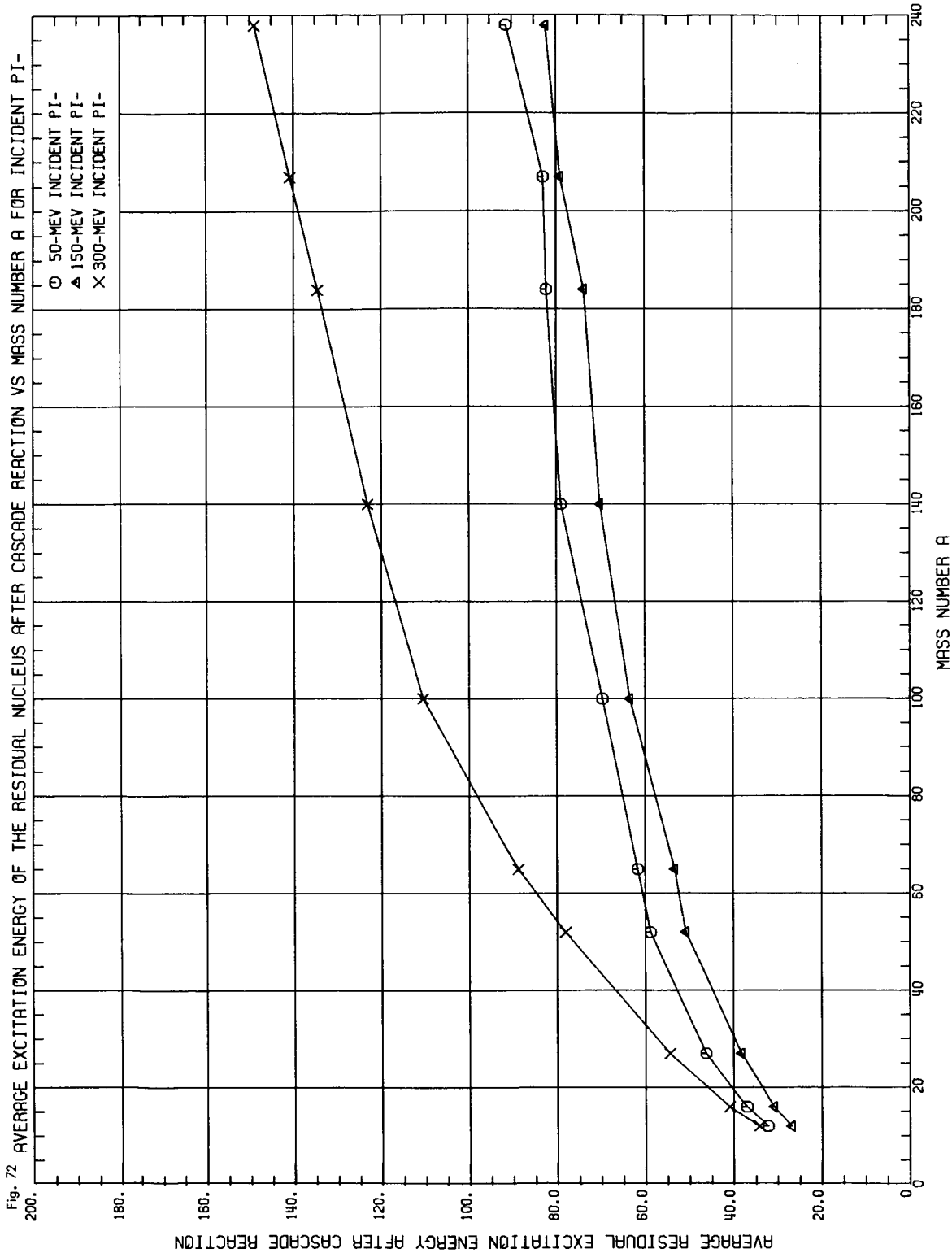
ORNL DWG 67-5600



ORNL DWG 67-5601

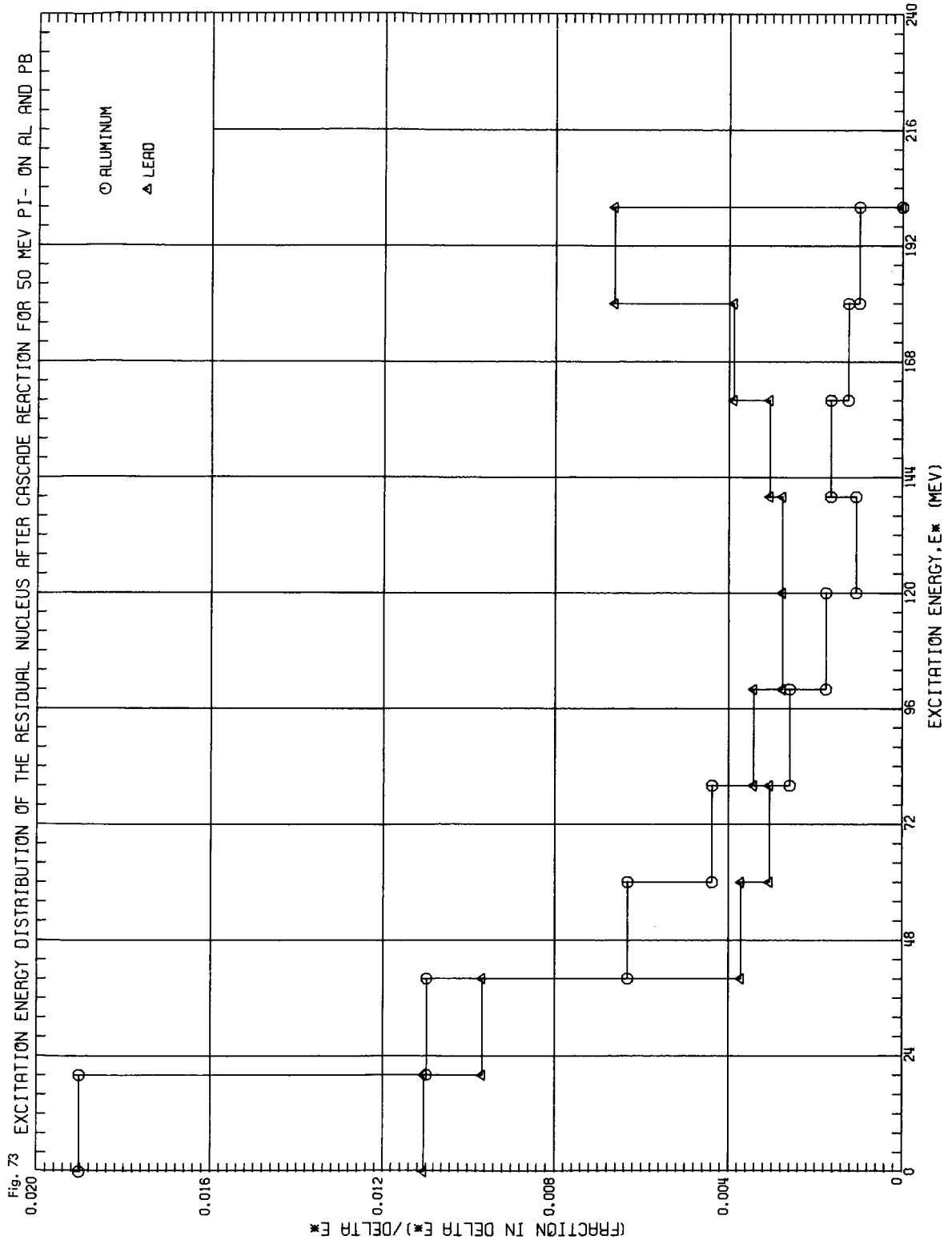


ORNL DWG 67-5602

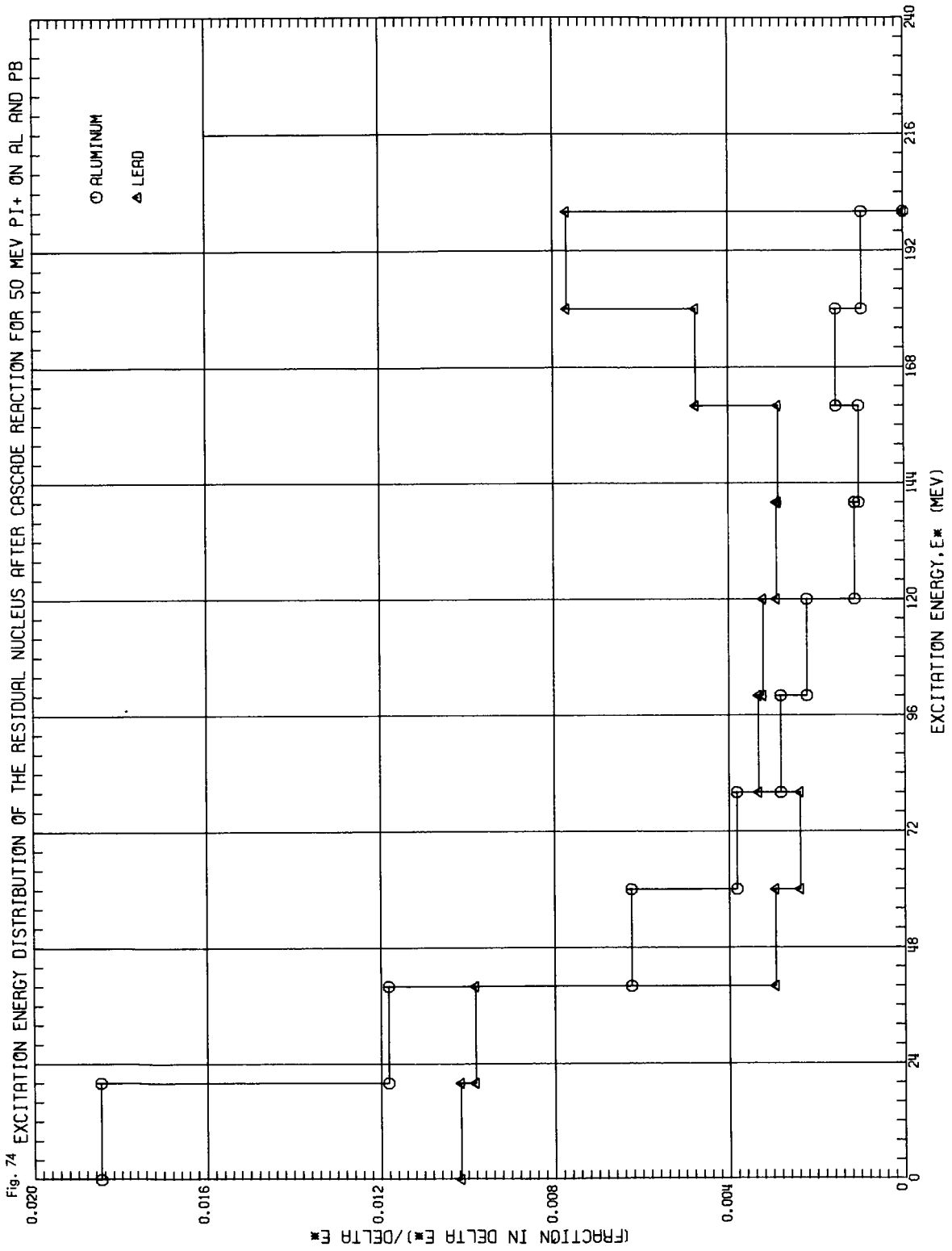




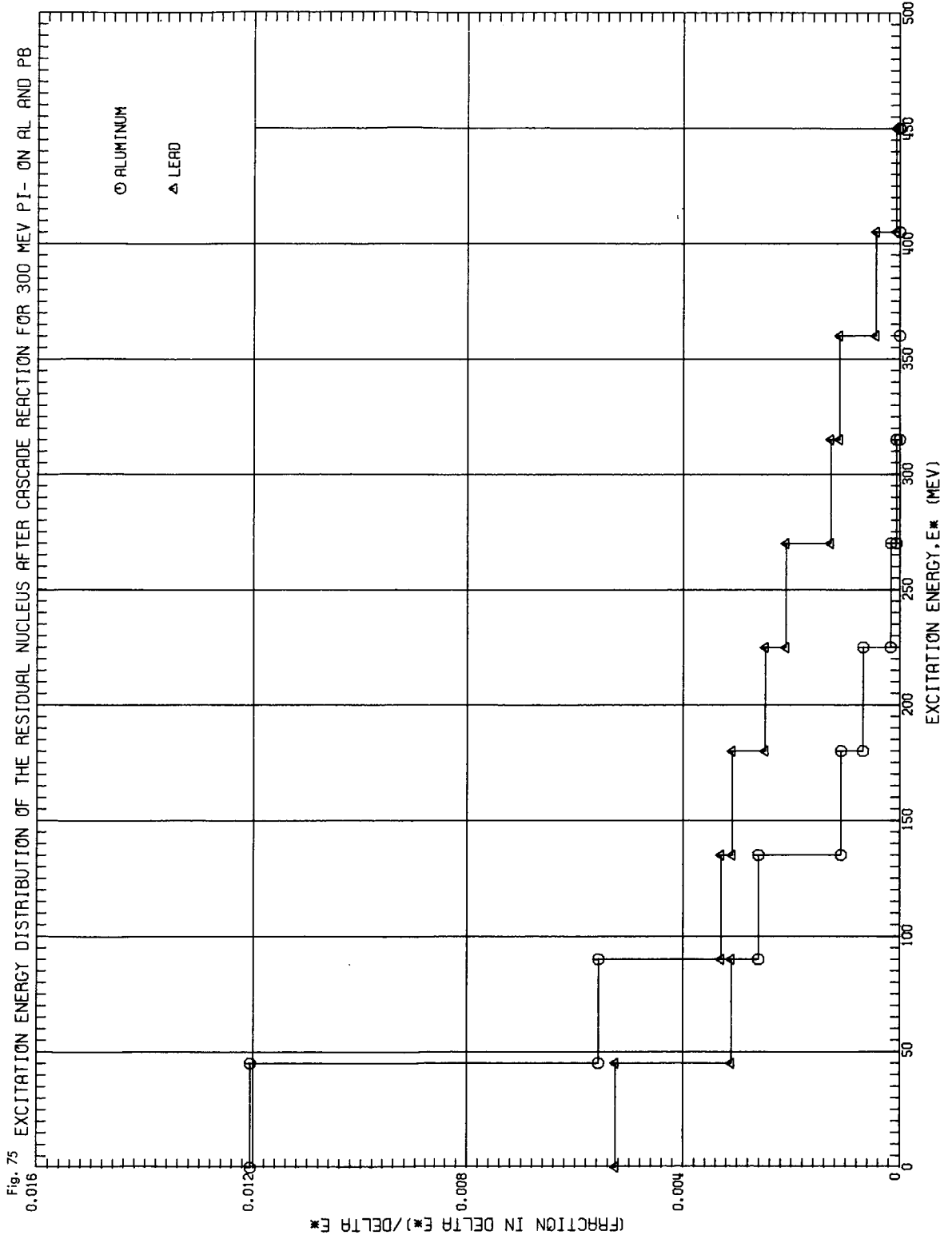
ORNL DWG 67-5603



ORNL DWG 67-5604

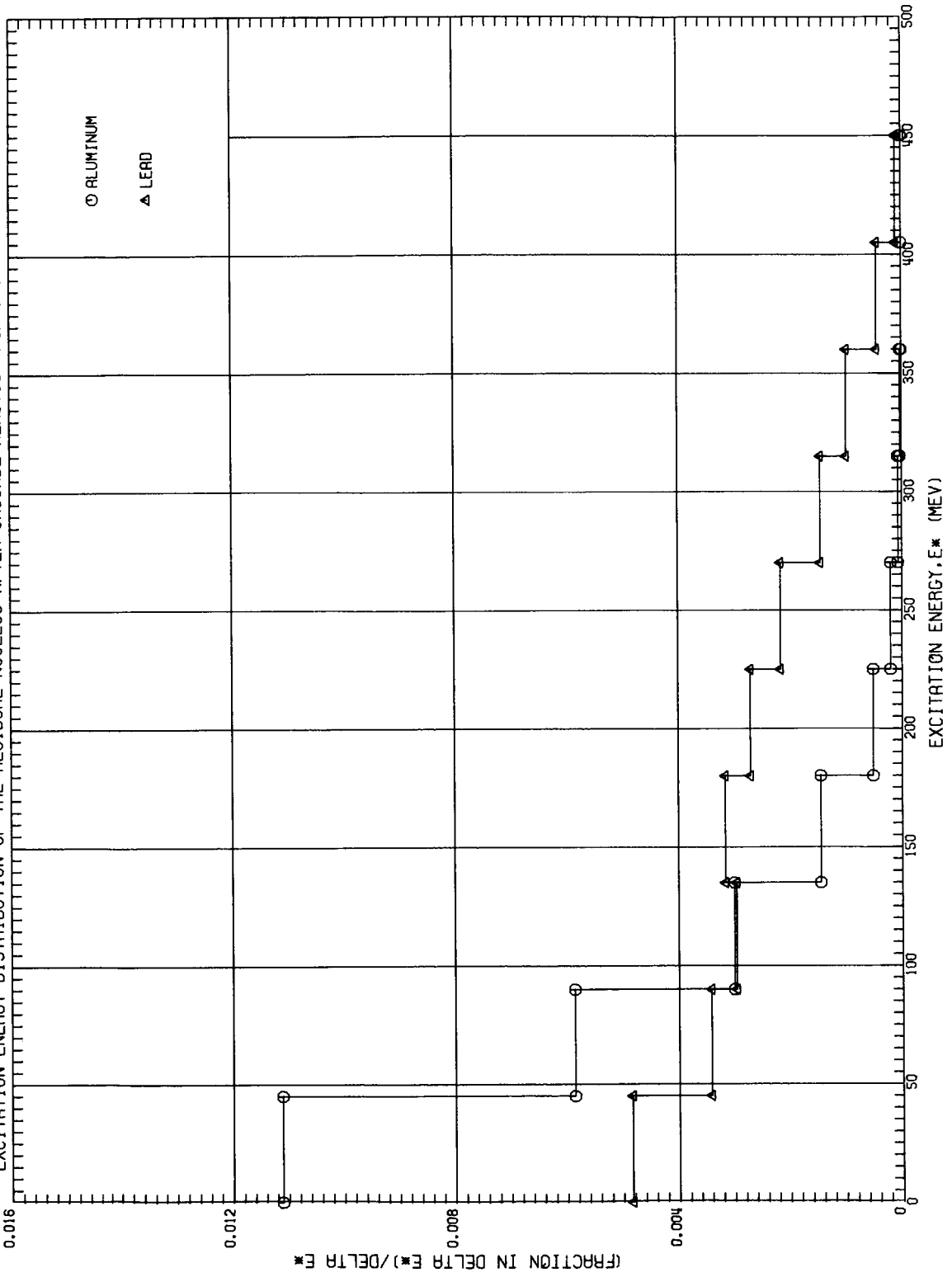


ORNL DWG 67-5605

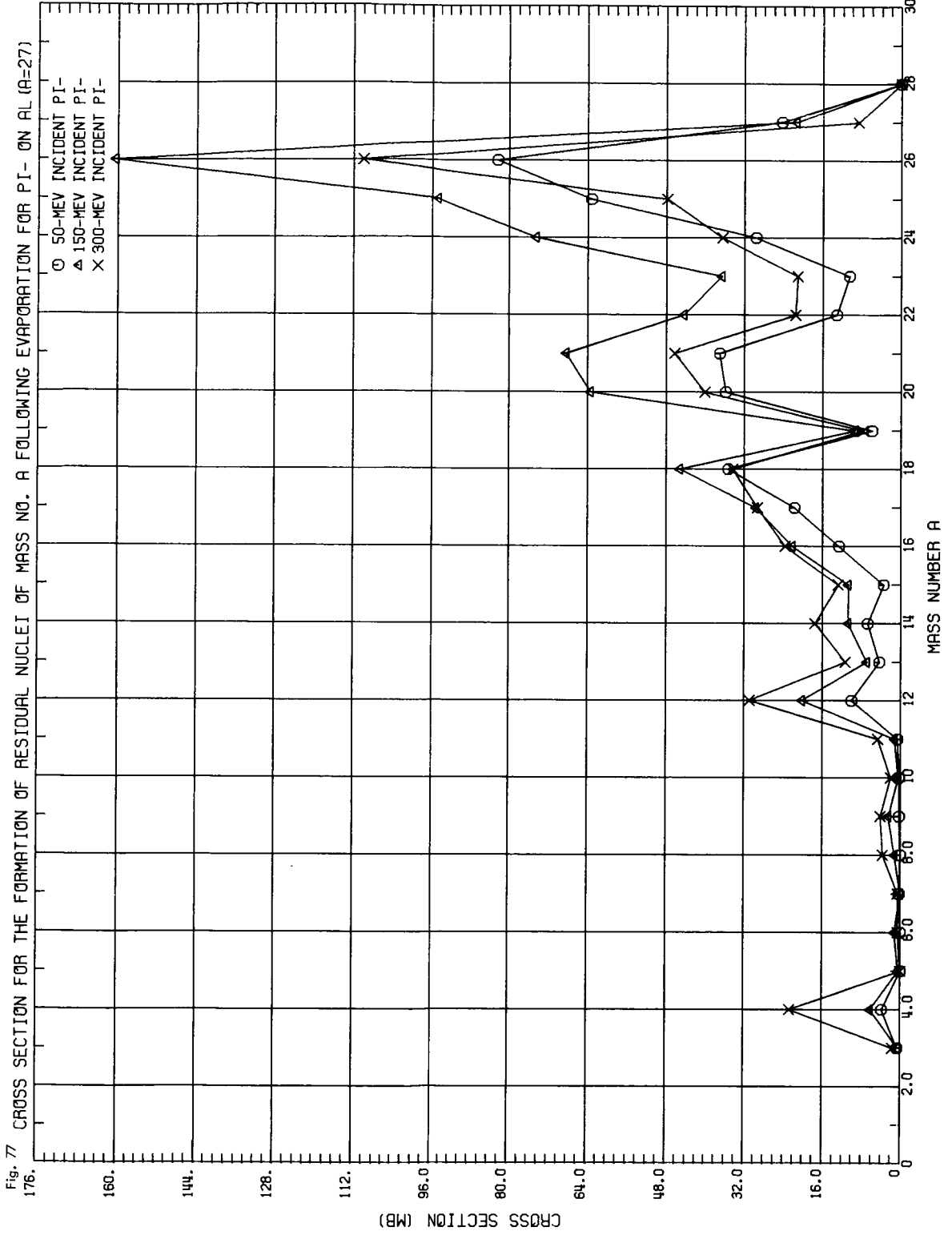


ORNL DWG 67-5606

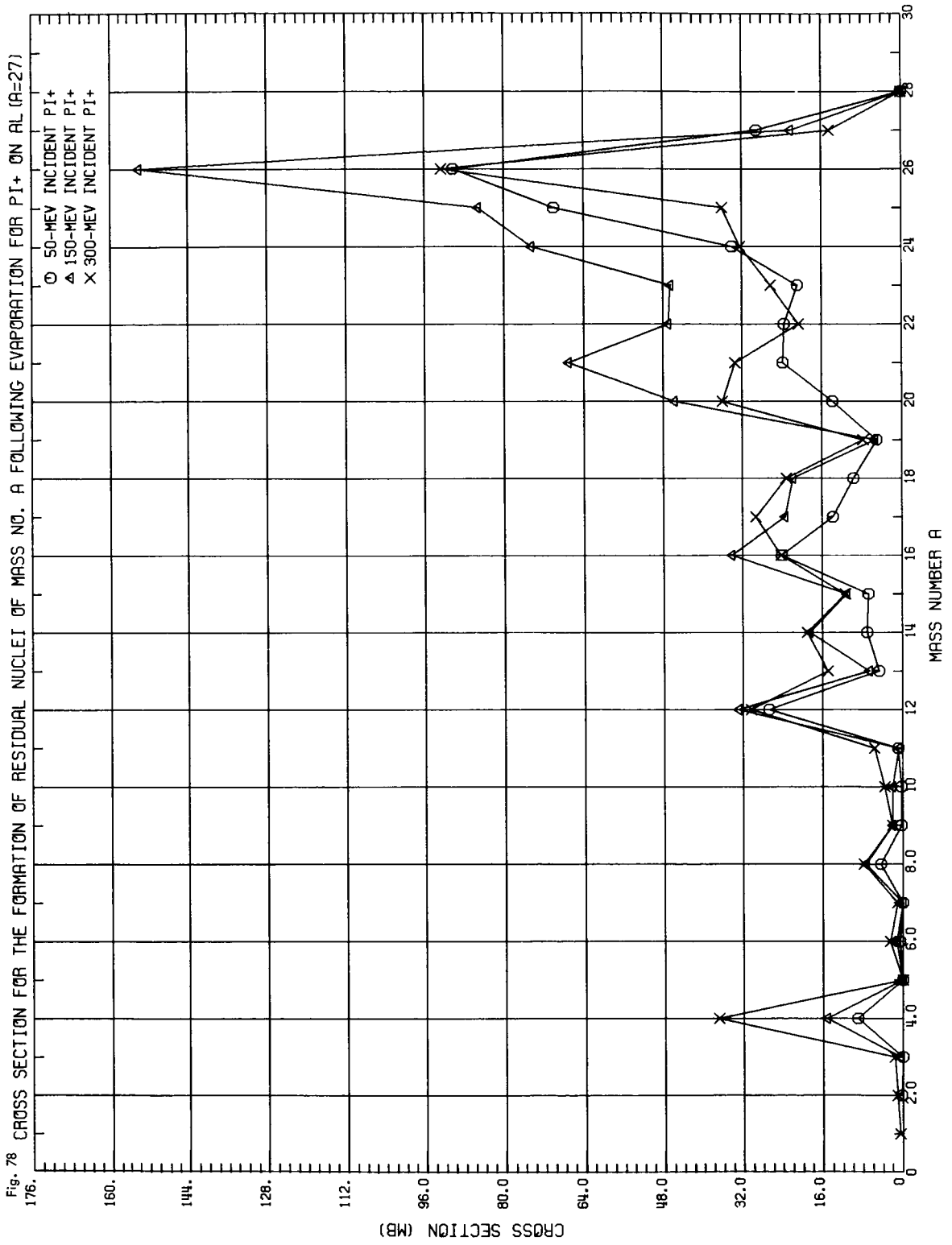
Fig. 76 EXCITATION ENERGY DISTRIBUTION OF THE RESIDUAL NUCLEUS AFTER CASCADE REACTION FOR 300 MEV PI+ ON AL AND PB



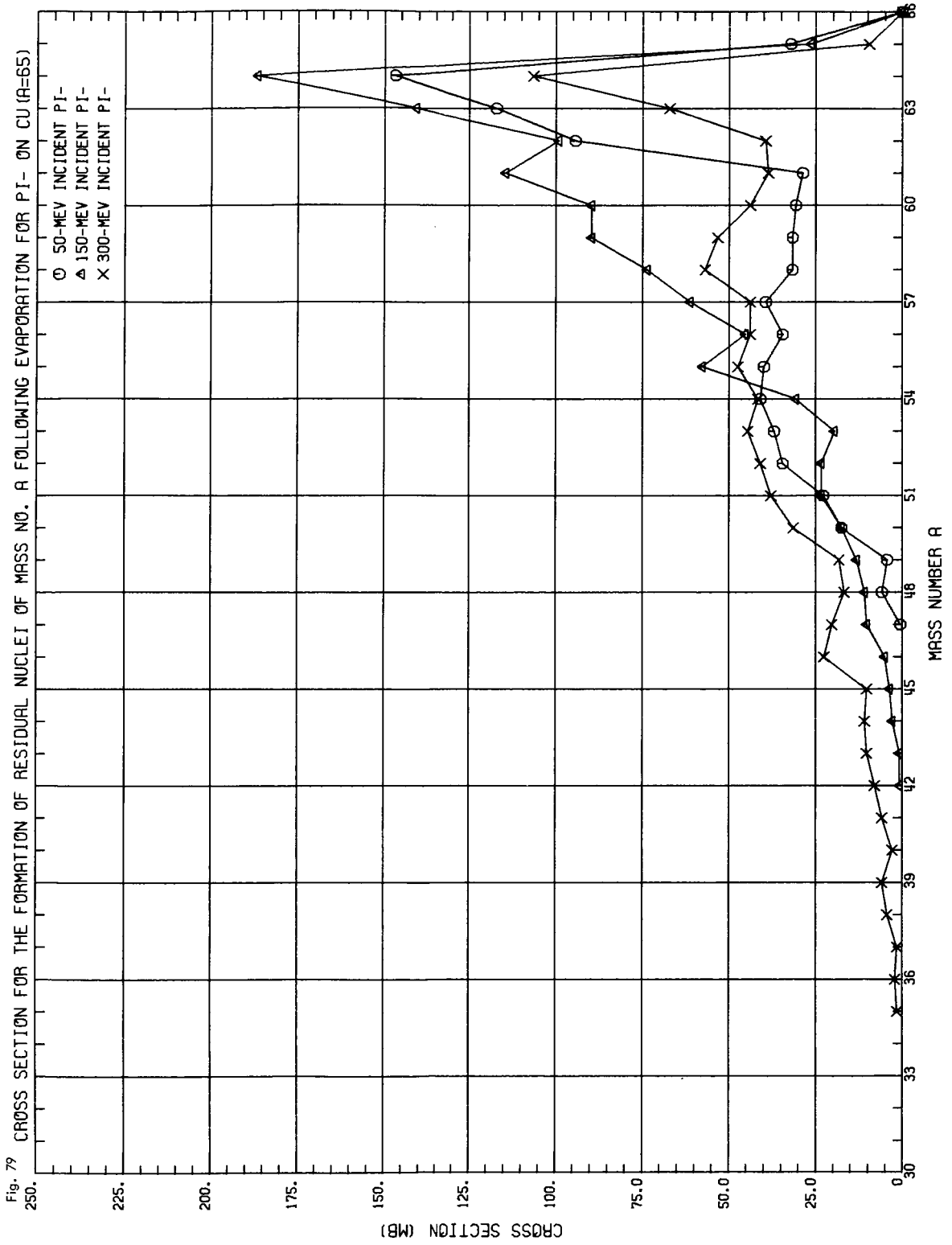
ORNL DWG 67-5607



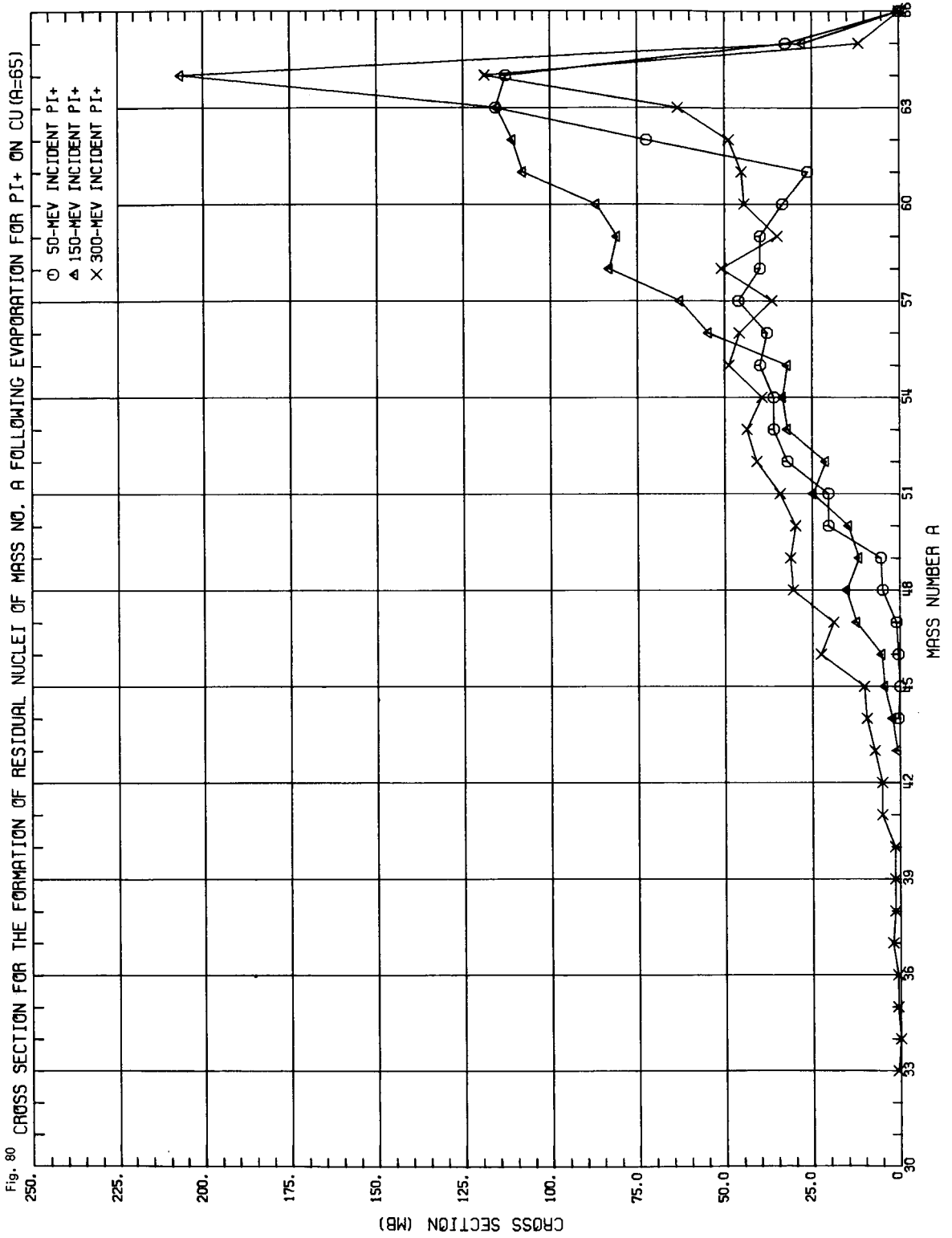
ORNL DWG 67-5608



ORNL DWG 67-5609

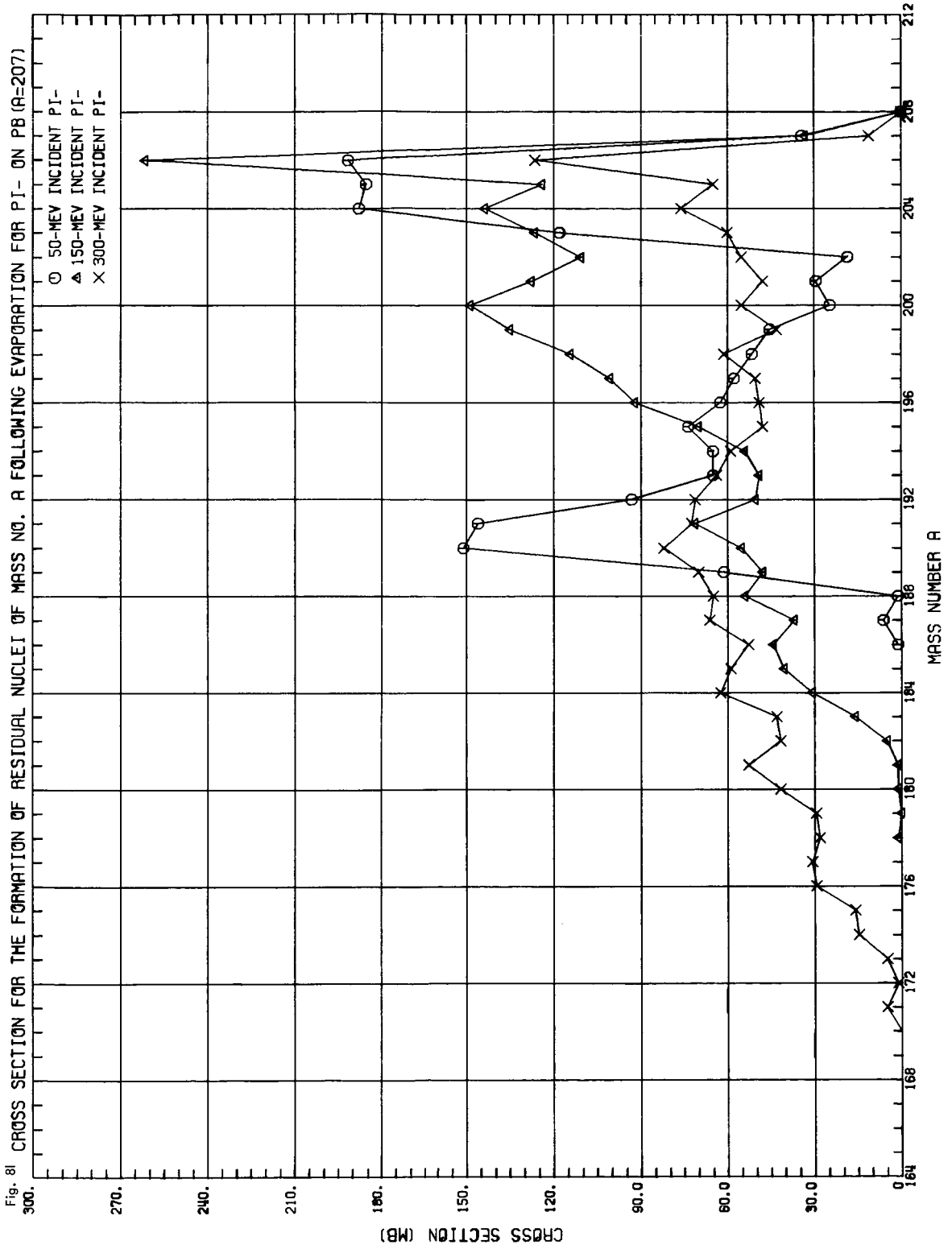


ORNL DWG 67-5610





ORNL DWG 67-5611



ORNL DWG 67-5612

